UNIVERSITÀ DEGLI STUDI DI TRIESTE

XXI. CICLO DEL DOTTORATO DI RICERCA IN

BIOMEDICINA MOLECOLARE

Complement component C1q and hyaluronic acid act as novel "signaling complex" in malignant pleural mesothelioma microenvironment to promote cancer progression

DOTTORANDA
ROMANA VIDERGAR

COORDINATORE
PROF. GERMANA MERONI

SUPERVISORE DI TESI
PROF. ROBERTA BULLA

CO-SUPERVISORE DI TESI
DR. PAOLA ZACCHI

CO-SUPERVISORE DI TESI
DR. CHIARA AGOSTINIS

ANNO ACCADEMICO 2017/2018

This dissertation is dedicated to my uncle Tone, who is my biggest support in my life.

Moje doktorsko delo posvečam stricu Tonetu, v zahvalo za vso podporo in vspodbudo v mojem življenju.

TABLE OF CONTENTS

AKNOWLEDGEMENT

Firstly, I would like to thank my supervisior Prof. Roberta Bulla, for accepting me in her research group, for her continuous support during my PhD study, for her patience and motivation to support me whenever I needed. My life in Trieste would not be possible without her support. I was blessed with so many sweet memories from the lab and her family which helped me to survive and grow up here alone and made one of my biggest wish come true.

My sincerest gratitude goes to my advisory committee members, Dr. Uday Kishore and Prof. Angela Gismondi, for their critical reading of the Thesis and their suggestions which help me to widen my research from various perspectives.

Special thanks goes to Dr. Paola Zacchi, for professional guidance and support she gave me while writing the thesis. Her positive personal attitude changed my point of view on research and affected my life forever.

Special thanks to Dr. Chiara Agostinis, who introduced me in research and laboratory life in Trieste since from the beginning. Having the support of a cell isolating "guru" by my side always made things easier.

I would like to thank Andrea Balduit for her support in the final period of my PhD study and for her help to conclude the project of my research topic; I would like to thank Alessandro Mangogna for his generous help with *in silico* analysis and all others bioinformatic issues.

A special thanks go to Dr. Fleur Bossi, Leonardo Amadio and all former lab members, they were always available for any kind of advices and discussions. I wish to thank Michaela Grandolfo for her kind help on confocal microscopy.

Posebna zahvala gre mojemu strcu Tonetu, za vse kar je naredil zame v življenju. Vedno mi je bil v največjo oporo tekom mojega šolanja in kasneje študija. Njegova vspodbuda in neomajna vera vame, sta mi pomagali premagati ovire in probleme na moji poti do cilja.

A special thanks go to my friend Neža, for all frienship and professional advices, which made my PhD period much easier.

Last but not least, I would like to thank to my mother Mojca and father Srečo and all my friends for their continuous support during this intense period of my life.

ABBREVIATIONS

β1	Integrin, beta 1
Akt	Protein kinase A
BRCA1	BRCA1, DNA repair associated
BSA	Bovine Serum Albumin
C	Complement
C1	C component 1
C1q	C component 1, subunit q
C1r	C component 1, subunit r
C1s	C component 1, subunit s
C3	C component 3
C3a	C component 3, fragment a
C3b	C component 3, fragment b
C4	C component 4
C4BP	C4b-binding protein
C5a	C component 5, fragment a
C5b	C component 5, fragment b
C6	C component 6
C7	C component 7
C8	C component 8
C9	C component 9
C5b-9	Terminal Complement Complex
cC1q	Collagen-like domain of C1q
cC1qR	Receptor for the collagen-like domain of C1q
CD	Cluster of Differentiation
CD44	CD44 molecule (HA receptor)
CD45	Tyrosine phosphatase, leukocyte
CD68	Cluster of Differentiation 68, markers of monocyte lineage
CDK	Cyclin dependent kinase
CDKN2A	Cyclin dependent kinase inhibitor 2A
Cy3	Cyanine3
DAPI	4',6-diamidino-2-phenylindole
DCs	Dendritic Cells
DNA	Deoxyribonucleic acid
MPM	Malignan pleural mesothelioma
ECM	Extracellular Matrix

EGF	Epidermal Growth Factor
EGFR	Epidermal Growth Factor Receptor
ELISA	Enzyme-linked immunosorbent assay
EMT	Epithelial–Mesenchymal Transition
ERK	Extracellular signal-Regulated Kinase
Fas	TNF receptor superfamily, member 6)
FGF	Fibroblast Growth Factor
FH	Factor H
FITC	Fluorescein isothiocyanate
FN	Fibronectin 1
GAGs	Glycosaminoglycans
gC1q	Globular “head” domain of C1q
gC1qR	Receptor for the globular heads of C1q
GFP	Green fluorescent protein
GlcUA	UDP-glucuronic acid
GlcNAc	UDP-N-acetylglucosamine
GPI	Glycophosphatidy
HA	Hyaluronic acid
HABP	Hyaluronan-Binding Protein
HARE	Hyaluranan receptor for endocytosis
HAS1	Hyaluronan synthase 1
HAS2	Hyaluronan synthase 2
HAS3	Hyalronan synthase 3
HMGB1	High-mobility group box 1 protein
HESF	Human endothelial serum free medium
HMW-HA	High molecular weight hyaluronic acid
HYAL1	Hyaluronidase 1
HYAL2	Hyaluronidase 2
HYAL3	Hyaluronidase 3
IHC	Immunohistochemistry
IARC	International Agency for Research on Cancer
Ig	Immunoglobulin
IL	Interleukin
INFγ	Interferon-γ
JNK	c-Jun N-terminal kinase
Ki-67	Proliferation-related Ki-67 antigen

LMW-HA	Low molecular weight hyaluronic acid
lncRNA	Long non-coding RNAs
LYVE-1	Lymphatic Vessel Endothelial Hyaluronan Receptor 1
MAC	Membrane Attack Complex
MAC-IP	Membrane Attack Complex-inhibitory protein
MAPK	Mitogen-activated protein kinases
MAPK	Mitogen-activated protein kinase
MBL	Mannose-Binding Lectin
MCP-1	Membrane Cofactor Protein1
MDSCs	Myeloid-Derived Suppressor Cells
MES	Cancer mesothelioma cells
Merlin	Moesin-ezrin-radixin-like protein
miRNA	MicroRNA
MHC	Major Histocompatibility Complex
MIP-2	Major intrinsic protein of lens fiber
MM	Malignant mesothelioma
MMPs	Matrix metalloproteinases
MPM	Malignant pleural mesothelioma
MΦ	Macrophages
mTOR	Mechanistic target of rapamycin kinase
NaN_3	Sodium azide
ncRNA	Non-coding RNA
NF2	Neurofibromatosis type 2
NF-κB	Nuclear factor kappa-light-chain-enhancer of activated B cells
NK	Natural Killer
OD	Optical density
p38	p38 mitogen-activated protein kinases
PBS	Phosphate Buffered Saline
PGs	Proteoglycans
PH-20/Spam1	Hyaluronidase PH-20 (protein), SPAM1 (gene)
PI3K	Phosphatidylinositol 3-Kinase
pNPP	p-Nitrophenyl Phosphate
RAGE	The receptor of advanced glycation end products

RNS	Reactive nitrogen species
ROS	Reactive oxygen species
RTKs	Receptor tyrosine kinases
SDS/PAGE	Sodium Dodecyl Sulphate – PolyAcrylamide Gel Electrophoresis
STAT3	Signal Transducer and Activator of Transcription 3
YAP	Yes-associated protein
TAMs	Tumour-Associated Macrophages
TGFβ	Transforming Growth Factorβ
TNFα	Tumour Necrosis Factor α
VEGF	Vascular Endothelial Growth Factor
TLR	Toll-like receptor

SUMMARY

Malignant pleural mesothelioma (MPM) is a rare form of cancer that develops from cells of the pleural mesothelium and is most commonly associated with exposure to asbestos. Like all form of cancer, mesothelioma (MES) cells acquire the ability to proliferate in an uncontrolled manner, invading the surrounding tissue and spreading to distant organs. It has been widely recognized that tumour growth not only depends on genetic abnormalities accumulating in cancer cells, but also on the local microenvironment which can provide a permissive niche for their survival, growth and migration.

Hyaluronic acid (HA), a member of the glycosaminoglycans (GAGs) family, is an abundant and ubiquitous component of the ECM which plays a fundamental role in cancer progression. The apparent structural simplicity of HA masks a very complex signalling behaviour that varies according to its size: high molecular weight HA (HMW-HA) keeps the structural integrity of tissues while low molecular weight HA (LMW-HA) stimulates cell proliferation, migration and sprout formation. HA is highly expressed in MPM and it has been shown to enhance the aggressiveness and spreading of MES cells into adjacent, non-cancerous, stromal tissues, even though the molecular mechanisms involved are still poorly understood.

Another key component of the tumour microenvironment, that has received increasing attention, is represented by the complement system, a well-known arm of the innate immunity which participates in the immune surveillance and homeostasis. In particular C1q, the first component of the classical pathway, has emerged to exert a wide range of immune-modulatory functions that are independent from complement activation. We were able indeed to demonstrate that C1q enhances adhesion, proliferation and migration of murine melanoma cells *in vitro*, rendering it an active player in tumor growth.

Based on these findings we decided to investigate the contribution of C1q on MPM progression. Immunohistochemistry performed on human bioptic speciments revealed that C1q is abundantly present in all MPM histotypes analysed. C1q seemed to be associated with monocytoid cells but also with tumour cell membrane and small vessels, suggesting that it might exert a proangiogenic activity. We also unveiled that C1q is able to interact with several extracellular matrix components, being HA the strongest interaction partner. Taking into account that HA is abundantly expressed in MPM, as C1q, these findings raised the

possibility that C1q bound to HA would function as a novel "signalling complex" able to promote the development and progression of MPM. Several lines of evidence support this scenario. Firstly, the pro-adhesive properties of C1q on MES cells were clearly enhanced by C1q bound to HA as compared to HA or C1q alone. Secondly, MES proliferation also resulted increased by C1q bound to HA. These phenotypes were associated with alteration of the phosphorylation status of components of the MAP3Ks and the mTOR signalling cascades thus suggesting that C1q-HA complex is able to sustain tumour growth by enhancing several cancer-related signaling pathways.

Since the effects mediated by C1q-HA are different from that observed for HA or C1q alone, these considerations prompted us to hypothesise that C1q deposited in the ECM can considerably modify the signalling properties of the tumour microenvironment. This could be additionally affected by another C1q-HA dependent mechanism, which is expected to impact the HA homeostasis. The expression of all the enzymes involved in the HA synthesis (HAS1, 2 and 3) and degradation (hyaluronidase (Hyal) 1, 2 and 3) were analyzed by quantitative RT-PCR. At the same time, bioinformatics analyses (Oncomine dataset and Kaplan-Meier plotter platforms) unveiled that HYAL2 and HAS3 overexpression is correlated with worst prognosis. Whereas HAS3 mRNA appeared to be downregulated upon C1q-HA interaction, we confirmed the bioinformatics data for HYAL2, whose mRNA and protein content resulted both increased. LMW-HA has been proven to play a crucial role in tumorigenesis by affecting cell proliferation and motility and by exhibiting pro-inflammatory and pro-angiogenic effects. In addition LMW-HA has been shown to activate the production of reactive oxygen species (ROS), powerful signalling molecules involved in tumour initiation, promotion and progression. We also provided evidence that C1q can contribute to ROS production only in the presence of LMW-HA. On the basis of these findings we can propose the following model: C1q-HA interaction, by enhancing HA degradation via HYAL2, feeds LMW-HA deposition in the tumour microenvironment which, in turn, favours ROS production and further HA degradation.

In conclusion, we identified C1q-HA interplay as a novel signalling complex able to act through multiple pathways to sustain tumour growth, in particular by affecting HA metabolism and by stimulating signal transduction cascades already known to promote MPM progression.

INTRODUCTION

Chapter 1. Malignant pleural mesothelioma

1. 1 Molecular Mechanisms of Asbestos-Related Carcinogenesis

Malignant pleural mesothelioma (MPM) is a rare and aggressive form of cancer that develops from cells of the pleural mesothelium and is most commonly associated with exposure to asbestos. It is characterized by a long and remarkably variable latency period between exposure and disease presentation (13–70 years). The life expectancy for mesothelioma patients is poor since effective treatment options are very limited. Up to 10,000 asbestos-related mesothelioma cases occur annually in the populations of Western Europe, Scandinavia, North America, Japan and Australia (Nurminen et al., 2003).

The mesothelial cells of the pleura that lines the lungs are the most frequent site of mesothelioma development and indeed MPM accounts for 70–80% of all cases. However, other serosal membranes, such as the peritoneum (peritoneal mesothelioma (PeM); ~25% of cases), as well as the pericardium and the tunica vaginalis, are also affected. Histologically, MPM can be classified into three different variants: (i) epithelioid, (ii) sarcomatoid, and (iii) mixed/biphasic. The lack of sensitive and specific disease subtype-specific markers continues to hamper the diagnosis of malignant mesothelioma, even though immunohistochemical (IHC) markers have been improved in recent years. Therefore, when abnormal mesothelial proliferations are identified by IHC in serosal membranes, it is difficult to distinguish benign from malignant growths. Currently, diagnosis relies heavily on morphology, where malignant growths are characterized by deep stromal invasion with dense cells and complex growth patterns (Husain et al., 2013, Galateau-Salle et al., 2016, Sage et al., 2018).

The International Agency for Research on Cancer (IARC) concluded in 1977 and 1987 that asbestos fibers qualify as a human carcinogen. At the beginning asbestos-related risks have mainly been deduced from cases occurring in mine workers and their close relatives (de Klerk and Reid, 2017). Nowadays, a significant proportion of the newly diagnosed cases of malignant mesothelioma are the result of other professional occupations, as well as environmental exposure (Goldberg and Luce, 2009). Together, these data indicate that the current and future burden of mesothelioma is largely underestimated.

It was suggested that fibers can translocate into the pleural cavity either directly through the lung parenchyma, and this mechanism may require decades, or along lymphatic/blood

circulation (Miserocchi et al., 2008). Macrophages can also play a role in fiber translocation when they undergo phagocytosis of the fibers and drain into the lymph nodes. When fibers reach the pleural cavity, they are carried in the pleural fluid that is then channeled out into the lymphatic system through the small openings (called the "stomata") on the parietal pleura. Fibers that are long enough fail to get through the stomata and they accumulate around the openings, causing persistent mesothelial injury which accounts for the initiation of mesothelioma (Boutin et al., 1996).

Asbestos fibers can cause genetic damage either directly or indirectly. Indirect genotoxicity involves the generation of free radicals and reactive oxygen species (ROS) (Kamp et al., 1992). The majority of asbestos types contains iron, in particular chrysotile fibers, which are able to induce hemolysis and release of iron (Harington et al., 1971). Iron can act as a catalyst through Fenton reaction to generate hydroxyl radicals, which then damage DNA or other biomolecules. Another source of ROS are the macrophages, which are recruited to sites of asbestos deposition. The term "frustrated phagocytosis" has been designated to describe the phenomenon in which the macrophages fail to consume long fibers and die with a concomitant massive release of ROS (Donaldson et al., 2010).

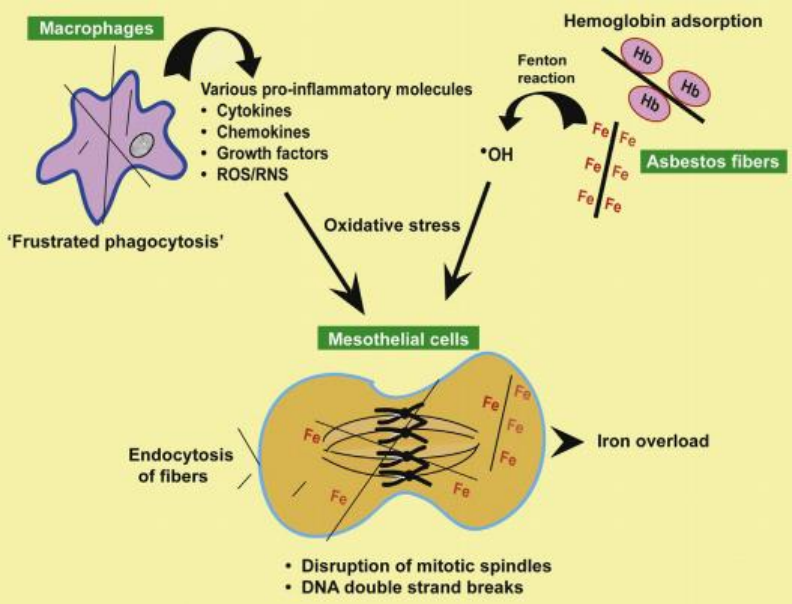

Figure 1: Mechanisms of asbestos-induced mesothelial carcinogenesis. Asbestos fibers can directly induce oxidative stress via the catalysis of Fenton reaction by iron on the surface or iron in the hemoglobins (Hb) adsorbed onto the fiber's surface. ROS/RNS can also be produced by macrophages which fail to consume long fibers ("frustrated phagocytosis"), along with a plethora of proinflammatory molecules. Mesothelial cells take up asbestos fibers, and the endocytosed fibers can disrupt mitotic spindles or cause DNA double-strand breaks, leading to chromosomal aberrations. Iron on the endocytosed fibers and its deposition contribute further to oxidative stress in mesothelial cells (decribed in (Chew and Toyokuni, 2015)).

Asbestos can also cause genetic damage directly. Mesothelial cells take up asbestos fibers which, in turn, can cause DNA double-strand breaks (Jiang et al., 2008) or mechanical disruption of the mitotic spindle during cell division, resulting in chromosomal abnormalities such as aneuploidy (MacCorkle et al., 2006).

1.2 Asbestos-induced genomic alterations

MPM is caused by a series of genetic changes and alterations, but only a few of them are well known and decribed. Studies in animals and humans have shown extensive chromosomal rearrangements and losses: in particular, chromosome 22 is affected, together with chromosomes 1p, 3p, 6q and 9p (Kaufman and Pass, 2008). The most frequently altered genes on these loci are important tumour suppressor genes, such as Neurofibromatosis type 2 (NF2) gene (22q12), p16 and p14 (both located in the CDKN2A locus at 9p21) and BRCA1-associated protein 1 (3p21) (data available on website http://www.ncbi.nlm.nih.gov/gene).

1.2.1 $p16^{INK4A}$ and $p14^{ARF}$

An important target genetic segment altered in MPM is the CDKN2A locus which contains the tumour suppressor genes $p16^{INK4A}$ and $p14^{ARF}$ (Stone et al., 1995). The role of p16 is to prevent phosphorylation of pRB by binding CDK4/675, which in turn impedes the cell to undergo G1/S phases. Furthermore, p14 is the alternative splice variant, which is involved in MDM2 sequestration or degradation as well as in pRB and p53 stabilisation, leading to the overall effect of cell cycle arrest in G1 and G2/M phases (Stott, 1998). The consequences of homozygous deletion of $p16^{INK4a}$/$p14^{ARF}$ are cells cycle progression and inhibition of apoptosis, see on **Figure 2** (Chew and Toyokuni, 2015).

1.2.2 Neurofibromatosis type 2 (NF2) gene

Another genomic alteration frequently found in malignant mesothelioma (MM) is the inactivation of the tumor suppressor gene known as neurofibromatosis type 2 (NF2), that encodes a product known as moesin-ezrin-radixin-like protein (Merlin), a membrane-cytoskeleton scaffolding protein, linking actin filaments to cell membrane or membrane proteoglycans (McClatchey and Giovannini, 2005). In MM, nearly 50% of cases harbor NF2 inactivation, which occurs mainly through homozygous deletion, nonsense mutation, or missense mutation (Bianchi et al., 1995). A downstream molecular target regulated by Merlin, Yes-associated protein (YAP), has been shown to mediate survival and proliferation in MM cells (Yokoyama et al., 2008).

1.2.3 BRCA1

The BRCA1-associated protein 1 (BAP1) gene product is a deubiquitinase, that translocates to the nucleus and interacts with the BRCA1 protein. Recently it was discovered that BRCA1 is also frequently inactivated in MM (Bott et al., 2011). It is a nuclear tumour suppressor that exerts a central role in the regulation of the cell cycle checkpoint and DNA repair such as double-strand breaks and interstrand crosslinks (Huen et al., 2010), which occur frequently in iron-catalyzed oxidative DNA damage (Toyokuni and Sagripanti, 1992).

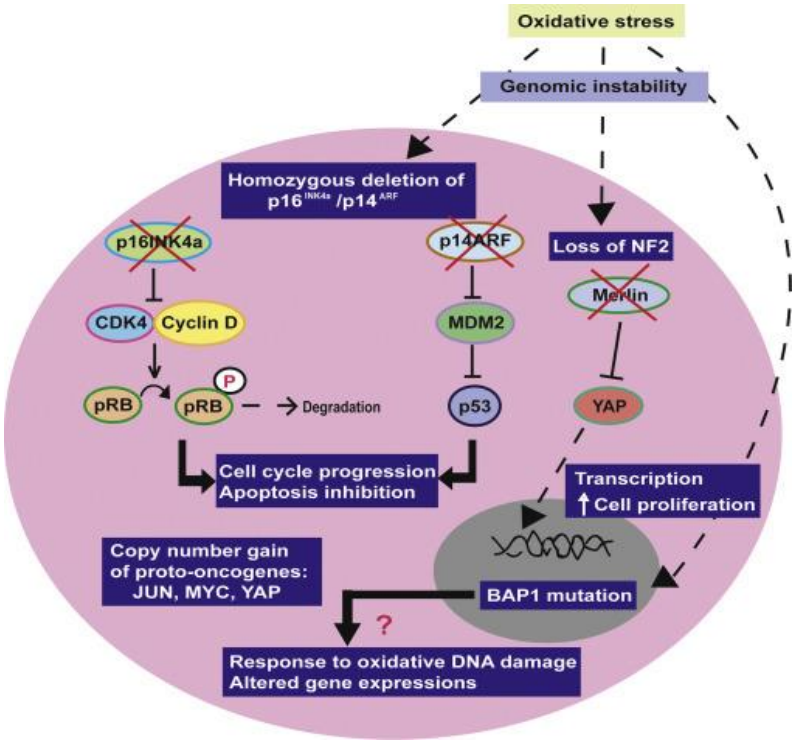

Figure 2: Genomic alterations observed in MM cells. Homozygous deletion of $p16^{INK4a}/p14^{ARF}$ leads to the inactivation of other two important tumour suppressor genes, pRB and p53. NF2 loss results in the absence of its protein product, Merlin, that normally inhibits its downstream molecule, YAP. Merlin deficiency results in YAP translocation into the nucleus, where it acts as transcription co-activator and promotes cell proliferation. BAP1 is part of a multiprotein complex that is involved in DNA damage response and regulation of gene transcription. The exact functional consequence of BAP1 mutation in MM remains to be clarified (decribed in (Chew and Toyokuni, 2015)).

1.3 Asbestos-induced cellular signaling pathways

Activation of intracellular signalling might occur as a result of direct interaction between asbestos fibers and cell surface receptors. It has been shown that the generation of a massive amount of ROS and RNS following asbestos exposure both *in vitro* and *in vivo* can serve as an important mediator in the initiation of cellular signalling events (Heintz et al., 2010). Asbestos fibers are able to trigger intracellular signalling cascades that lead to the activation

of transcription factors, followed by increased expression of target genes.

Asbestos fibers are able to trigger mitogen activated protein kinase (MAPK) pathway, which consists of several distinct members such as ERK1/2, JNK, and p38 kinases. The major MAPK pathway member induced by asbestos fibers is ERK1/2. Phosphorylation and activation of ERK1/2 was suggested to be closely associated with cellular proliferation that is responsible for the development of MM (Zanella et al., 1996). Two key redox-sensitive transcription factors frequently activated in mesothelial cells exposed to asbestos fibers are AP-1 and NF-κB. Treatment of rat pleural mesothelial cells with crocidolite asbestos has been shown to enhance the expression of JUN and FOS, the main components of the AP-1 transcription complex (Heintz et al., 1993). Asbestos-induced activation of NF-κB has been shown in many different cell types and it is closely associated with inflammatory responses (Brown et al., 1999). NF-κB activation is central to the elaborated expression of various pro-inflammatory cytokines and chemokines by cells exposed to asbestos fibers such as TNF-α, IL-6, MCP-1, IL-8 and MIP-2 (Yang et al., 2006). Asbestos exposure has also been associated with overexpression and activation of receptor tyrosine kinases (RTKs) such as EGFR and c-MET (Jagadeeswaran et al., 2006). Deletion or mutation of the tumour suppressor NF2 occur frequently in MM. NF2 encodes for Merlin, a key component of the Hippo signalling pathway. In the absence of Merlin expression, YAP, a downstream target of Merlin in the Hippo signalling pathway, becomes activated. YAP translocates into the nucleus where it acts as a transcription co-activator and it is be able to promote mesothelial growth (Yokoyama et al., 2008). Furthermore, enhanced secretion of connective tissue growth factor (CTGF) in serum has emerged to promote mesothelioma tumorigenicity *via* a vicious autocrine loop involving the activation of the β-catenin signalling pathway (Jiang et al., 2014). Phagocytosis of asbestos fibers by macrophages results in generation of ROS by NADPH oxidase which then triggers the activation of NALP3 inflammasomes and subsequent secretion of mature IL1β (Dostert et al., 2008). A key mediator of inflammation in MM, HMGB1 (high-mobility group box 1 protein), is also involved in NALP3 inflammasome activation and acts in an autocrine manner to promote the growth, motility, and survival of MM cells (Jube et al., 2012). HMGB1 is normally localized in the cell nucleus but, upon exposure to stimuli such as asbestos fibers, it is released into the extracellular space where it binds to receptors such as RAGE (the receptor of advanced glycation end products) or TLR (toll-like receptor), leading to the production of TNF-α and IL-1β, which are important for the malignant transformation of mesothelial cells (Qi et al., 2013).

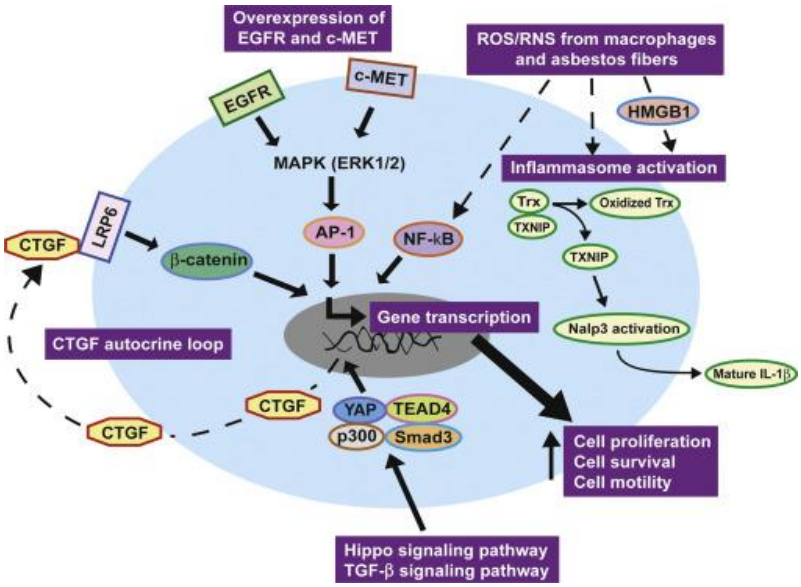

Figure 3. Cellular signalling pathways activated in MM cells in association with those stimulated in mesothelial cells following asbestos exposure. Overexpression of receptor tyrosine kinases such as EGFR and c-MET results in the activation of the MAPK pathway. AP-1 and NF-κB are redox-sensitive transcription factors that can be activated by the oxidative stress caused by asbestos exposure. Merlin deficiency leads to the dysregulated Hippo signalling pathway, which cross talks with the TGF-β signalling pathway to activate transcription of CTGF (an important mediator of MM cell growth) through YAP–TEAD4–Smad3–p300 complex formation. Secreted CTGF creates an autocrine loop and regulates its own expression via the activation of the β-catenin pathway. ROS also mediate the activation of the NALP3 inflammasome at least partially through HMGB1, resulting in mature IL-1β secretion, which contributes to an asbestos-related inflammatory response (decribed in (Chew and Toyokuni, 2015).

1.4 Expression of miRNA in MM

The advent of the next generation sequencing has unveiled roles for RNA transcripts that do not encode proteins in the regulation of gene expression; these species are termed non-coding RNAs (ncRNAs). Categorized on the basis of size—small ncRNAs (<200 nt) and long ncRNAs (>200 nt) — these transcripts have emerged as key regulators of critical processes, such as the cell cycle, proliferation, and tumorigenesis (Huarte, 2015).

1.4.1 miRNA

Perhaps the most well-studied species of the non-coding transcriptome are microRNAs (miRNAs), small (18–22 nt) transcripts. These transcripts have emerged as a group of important regulators of gene expression and they are involved in various pathological conditions, including cancer. miRNAs have recently been shown to be involved in cellular stress responses, such as DNA damage, oxidative stress, and other environmental changes (Leung and Sharp, 2010). Expression of miRNA-126 was shown to be downregulated in patients with MM, where it inhibits tumour growth by metabolic shift. In addition, miRNA-

126 can affect mitochondrial energy metabolism by reducing mitochondrial respiration and upregulating glycolysis-induced energy in an insulin receptor substrate-1 (IRS1)-dependent manner (Tomasetti et al., 2014). Also, miRNA-126 can be used as a serum diagnostic marker in combination with another reported MM biomarker, such as soluble mesothelin-related peptides (SMRPs), to predict the risk of an asbestos-exposed population to develop MM (Santarelli et al., 2011). Moreover, miRNA expression profile can be used to differentiate the three different histopathologic subtypes of MM (epithelioid, sarcomatoid, and biphasic). A lower expression of miRNA-17-5p and miRNA-30c correlates significantly with a better survival of the sarcomatoid MM patients (Busacca et al., 2010).

1.4.2 Long non-coding RNAs

Long non-coding RNAs (lncRNAs) can exert their regulatory effects on DNA, RNA and protein levels, and tissue-specific expression patterns have been observed, thus they can be considered important diagnostic and prognostic markers. Characterizing the landscape of lncRNA deregulation in MM has the potential to reveal novel insights into mechanisms of MM-associated gene regulation as well as novel therapeutic intervention points (Quinn et al., 2015).

1.5 MPM treatment

A big progression for the treatment of the patients with MPM has been made over the past decade, with the development of novel treatments, including new chemotherapeutic and immunotherapeutic regimens as well as new surgical techniques. Disease-directed treatment options available for the management of MPM include systemic therapy, surgery, and radiation therapy. Surgery is an important treatment modality that may, in selected cases, most optimally allow for prolonged survival, but only a minority of patients are medically operable and technically resectable (Ettinger et al., 2012). Chemotherapy is recommended for non-operable MPM and as a part of multimodal therapy for operable MPM. At the moment the most widely used chemotherapeutic drugs are represented by pemetrexed, cisplatin, carboplatin, gemcitabine, vinorelbine, bevacizumab and/or combinations of them (Raynaud et al., 2015). Like chemotherapy, radiation for MPM may be administered either pre- or postoperatively. In recent years, radiation is increasingly being incorporated into both lung-removing and lung-sparing multimodal therapy protocols (Rosenzweig, 2017). Most patients with MPM are diagnosed at advanced stages. Determining the histologic subtype is very important to guide therapeutic options and to inform prognosis. The three major histologic

subtypes of MPM are epithelioid, sarcomatoid, and biphasic, in which both epithelioid and sarcomatoid characteristics are present. Epithelioid histology is the most common and is associated with a better prognosis and a higher response to treatment when compared to sarcomatoid and biphasic histologies (Tsao et al., 2009). The resistance of MPM to conventional treatment and the poor clinical outcome have prompted basic research to better understanding the MPM biology with the aim to identify new possible molecular targets.

Chapter 2. Extracellular matrix – Hyaluronic acid

1. Tumor microenvironment

It is widely recognized that the local microenvironment plays an important and active role in cancer development providing favorable conditions for the seeding of cancer cells in a protective niche that allows the growth and expansion of the tumour mass. Tumour microenvironment is composed by a variety of cell populations, such as immune cells of all types, blood and lymphatics vessels and fibroblasts embedded into the extracellular matrix (ECM) (Yuan et al., 2016). This latter is build-up by a complex meshwork of macromolecules secreted by different cell types, made up of both proteins and proteoglycans (PGs) with covalently attached sugar chains, glycosaminoglycans (GAGs). The ECM, besides providing the structural support of the organ, is instrumental in modulating cell functions such as proliferation, cytoskeletal organization, differentiation and receptor signalling. Beyond direct interaction with cellular signalling receptors, the network of macromolecules also functions as a reservoir for growth factors or signallling molecules, thus influencing cellular behavior indirectly (Lorusso and Rüegg, 2008).

1.1 Hyaluronic acid (HA)

One of the main component of the ECM, which plays a pivotal role during embryogenesis, inflammation and cancer, is the carbohydrate - hyaluronic acid or hyaluronan (HA), a negatively charged, unbranched polymer composed of repeated disaccharides of glucuronic acid and N-acetylglucosamine (Salwowska et al., 2016). It was first discovered in 1934 by Karl Meyer and John Palmer, as a component of the vitreus body of cows' eyes and it was named HA from hyalos (the Greek word for 'glass') and the uronic sugar found in the substance (Meyer and Palmer, 1934).

1.1.1 Chemical structure of HA

As described above HA is a high molecular weight glycosaminoglycan composed of repeating disaccharide units of N-acetylglucosamine and glucuronic acid [(1→3)-β-dGlcNAc-(1→4)-β-d-GlcA-] (Weissmann and Meyer, 1954). This relatively simple structure is conserved throughout all mammals, suggesting that HA is a biomolecule of considerable importance (Chen and Abatangelo, 1999). In the body, HA occurs in the salt form and is found in high concentrations in several soft connective tissues, including skin, umbilical cord, synovial fluid, and vitreous humor. Significant amounts of HA are also found in lung, kidney, brain, and muscle tissues (Necas et al., 2008).

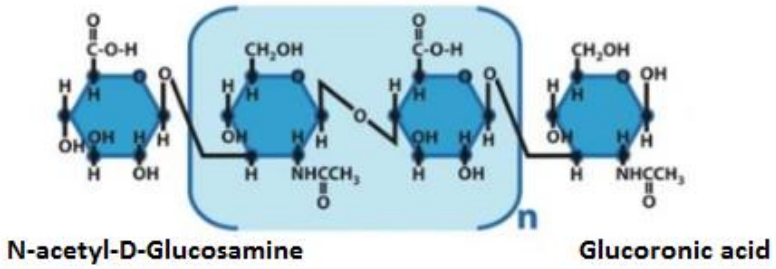

Figure 4. Structure of hyaluronic acid. Biochemical structure of hyaluronic acid disaccharide "building block" consisting of N-acetyl-Dglucosamine and glucoronic acid (figure adapted from Adamia et al., 2013).

Under physiological conditions, the backbone of a hyaluronan molecule is stiffened by a combination of the chemical structure of the disaccharide, internal hydrogen bonds, and interactions with the solvent. Solutions of HA are exceedingly lubricious and very hydrophilic. In solution, hyaluronan polymer chain takes on the form of an expanded, random coil. These chains entangle with each other at very low concentrations, which may contribute to the unusual rheological properties. At higher concentrations, solutions have an extremely high but shear-dependent viscosity. A 1% solution is like jelly, but when it is put under pressure it moves easily and can be administered through a small-bore needle. It has therefore been called a "pseudo-plastic" material. The extraordinary rheological properties of hyaluronan solutions make them ideal as lubricants. There is evidence that hyaluronan separates most tissue surfaces that slide along each other. The extremely lubricious properties of hyaluronan, meanwhile, have been shown to reduce post-operative adhesion formation following abdominal and orthopedic surgery. As mentioned, the polymer in solution assumes a stiffened helical configuration, which can be attributed to hydrogen bonding between the

hydroxyl groups along the chain. As a result, a coil structure is formed that traps approximately 1.000 times its weight in water (Necas et al., 2008).

1.1.2 Function of HA

HA is primarily located in the extracellular and pericellular matrix, but it has also been found intracellularly (Fraser et al., 1997). The biological functions of HA include maintenance of the elastoviscosity of liquid connective tissues such as joint synovial and eye vitreous fluid, control of tissue hydration and water transport, supramolecular assembly of proteoglycans in the ECM (Hascall et al., 2004, Dechert et al., 2006). HA has been proposed to be functionally important in processes such as embryogenesis, angiogenesis, cell growth and migration, wound healing, and the formation of high-molecular-mass aggregates with various proteoglycan (Laurent and Fraser, 1992). HA plays very important roles also in malignancy; it functions as a template for the assembly of pericellular macromolecules, it interacts directly with cell surface receptors that transduce intracellular signals, and it promotes anchorage-independent growth and invasiveness (Toole, 2002). One of the most notable diagnostic features of MPM is massive pleural effusion containing high levels of hyaluronic acid, even though the biological correlation between HA and mesothelioma progression is still poorly understood (Lesley et al., 1992). The apparent structural simplicity of HA masks a very complex signalling behaviour that varies according to its size (Cyphert et al., 2015). While high molecular weight HA (over 1 million Da) keeps the structural integrity of tissues, medium- or low- molecular weight HA stimulates cell proliferation, migration and sprout formation, all processes responsible for tumour growth and progression (Dicker et al., 2014).

1.2 Biosynthesis of HA

In mammals HA is naturally synthesized by a class of integral membrane proteins called hyaluronan synthases (HASes), of which vertebrates possess three different variants or isoforms: HAS1, HAS2, and HAS3 (Lee and Spicer, 2000).

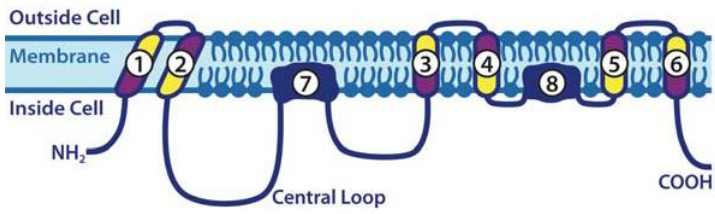

Figure 5. Structure of mammalian HAS. The mammalian HASs are comprised of seven membrane-spanning regions and a large cytoplasmic (the figure is from (Adamia et al., 2013)).

These enzymes are comprised of seven membrane-spanning regions and a large cytoplasmic loop and they synthesize HA predominantly at the inner face of the plasma membrane (Weigel et al., 1997). This means that the growing HA molecule is extruded into the extracellular space via the membrane-spanning domains of the HA synthases as the polymer grows (Philipson et al., 1985).

HAS enzymes polymerize nucleotide sugars, UDP-glucuronic acid (GlcUA) and UDP-N-acetylglucosamine (GlcNAc) sequentially to the reducing end of the growing HA molecule (Weigel et al., 1997). HA lacks a protein backbone which makes this molecule unique compared to the other GAGs and thus only the presence of nucleotide sugars is required to synthesize a new HA chain. Although the three isoforms of HAS are very similar (55-71% amino acid sequence identity), they produce HA of different sizes and are different in catalytic activity (Itano et al., 1999). HAS1 and HAS2 produce HMW-HA (~ from 2 x 10^5 to 2 x 10^6 Da), being HAS2 catalytically more active than HAS1. HAS3 appears to have the highest rate of synthesis but produces LMW HA (~1 x 10^5 Da). Variation in the molecular weight of HA may be required to regulate the diverse biological roles within an organism (Törrönen et al., 2014).

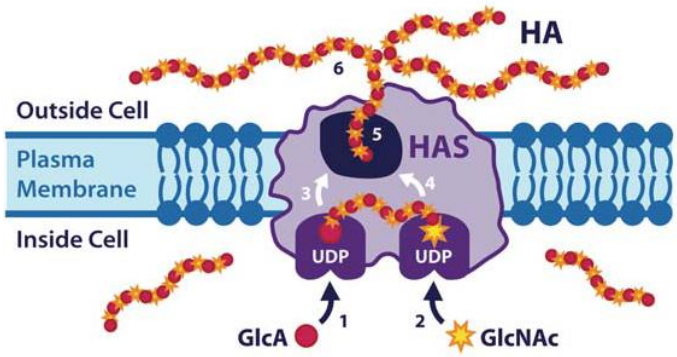

Figure 6. Translocation system of HA in the cells. 1., 2. UDP-GlcA (uridine diphospho-glucose) and UDP-GlcNAc (uridine diphospho-N-acetylglucosamine) binding to the HAS protein; 3., 4. GlcA and GlcNac transfer by HAS transferase activity. 5. Newly synthesized HA binding to HAS protein and, 6. HA translocation through the membrane into the ECM (adapted from (Adamia et al., 2013)).

1.3 Degradation of HA

In the human genome there are six known genes coding for hyaluronidase-like sequences, all of which show an high degree of homology. They include Hyal-1, Hyal-2, Hyal-3, Hyal-4, and PH-20/Spam1, as well as a pseudogene, Phyal1, that is transcribed, but not translated, in humans. They possess a unique tissue distribution, and except for PH-20, are widely

expressed. The first three human Hyals (Hyal-1, -2, and -3) are clustered on chromosome 3p21.3 and the latter are similarly clustered on chromosome 7q31.3. Human Hyal-1 and Hyal-2 are the two major hyaluronidases engaged in HA degradation in somatic tissues. Hyal-2 degrades high molecular weight HA to an approximately 20 kDa product (which corresponds to about 50 disaccharide units), whereas Hyal-1 can degrade high molecular weight HA to small oligomers, primarily to tetrasaccharides. Human Hyal-1 is an acid-active (pH = 3.8) enzyme while Hyal -2 seems to have a broader pH optimum (collected in review Stern and Jedrzejas, 2006).

1.3.1 Hyaluronidase-1 (HYAL-1)

HYAL-1 is an acid-active enzyme that cleaves HA to tetrasaccharides by hydrolyzing the β1-4 glycosidic bond between GlcUA and GlcNAc (Frost et al., 1997). Most highly expressed HYAL-1 mRNA is in the liver, kidney, spleen, and bone marrow, where HA degradation maintains highest levels (Shuttleworth et al., 2002). HYAL-1 is synthesized as a 52 kDa protein that is primarily secreted out of the cell and re-internalized by endocytosis where it undergoes proteolytic cleavage and transforms into 48 kDa mature protein (Puissant et al., 2014). HYAL-1 deficiency causes abundant HA accumulation in the lysosomes of macrophages and fibroblasts of joint tissues, resulting in mucopolysaccharidosis (MPS) IX, which is primarily characterized by an arthritis-like phenotype involving multiple joints (Triggs-Raine et al., 1999). In addition, a mouse model of HYAL-1 deficiency also exhibited a similar phenotype, with pathological manifestations limited to the joints (Martin et al., 2008).

1.3.2 Hyaluronidase-2 (HYAL-2)

HYAL-2 genes are composed of six exons encoding an mRNA that can be translated into a 473 amino acid protein (Strobl et al., 1998). The corresponding polypeptide is predicted to have an amino-terminal 20 residue endoplasmic reticulum signal sequence that directs the protein into the lumen of the RER where it undergoes glycosylation and glycosylphosphatidylinositol (GPI) anchor addition (Andre et al., 2011; Rai et al., 2001). Expression of HYAL2 mRNA was reported in adult and embryonic human and mouse tissues (Strobl et al., 1998). Northern blot (with human) and Western blot (with mouse) analyses performed on several tissues have shown that HYAL-2 has a broad mRNA expression pattern (heart, skeletal muscle, colon, spleen, kidney, liver, placenta, and lung) (Lepperdinger et al., 1998), except the adult brain, where HYAL-2 enzyme is absent (Strobl et al., 1998). The

intracellular localization of HYAL-2 has been controversial. It was initially proposed that HYAL-2 is localized in the lysosomal compartment but since a green fluorescent protein (GFP)-tag Hyal2 was used in these studies, it turned out that the GFP-tag attached to the C-terminus of the protein prevented GPI addition to HYAL-2 (Lepperdinger et al., 1998). Further studies clearly indicated the presence of HYAL-2 at the cell surface as a GPI anchored protein (Chow et al., 2006; Rai et al., 2001). Moreover, HYAL-2 was found intracellularly in the mitochondria of L929 fibroblasts (Chang, 2002) and in the nucleus of blood vessels (de la Motte et al., 2009). More recently it has been demonstrated that endogenous mouse HYAL2 is expressed at the plasma membrane of many cell types, but it can be found intracellularly only in some cell types (Chowdhury et al., 2016). Also the optimal pH for HYAL-2 enzymatic activity has been controversial. At the beginning it was suggested that HYAL-2 is catalytically active at both neutral and acidic pH (Lepperdinger et al., 1998). Subsequently it was reported that neither acidic nor neutral pH were suitable to allow detection of HYAL-2 dependent HA turnover (Rai et al., 2001). More recent studies are indicating CD44, a key HA receptor, as the co-factor required to activate HYAL-2 catalytic activity (Harada and Takahashi, 2007).

1.3.3 Proposed mechanism for HA degradation

The current hypothesis to describe HA degradation is that HMW-HA is anchored to the cell surface through CD44, HA receptor for endocytosis (HARE, also known as stabilin-2), or LYVE-1 HA receptors, and HYAL2, and they are localized in the lipid rafts on the cell membrane (Harada and Takahashi, 2007; Triggs-Raine, 2015).

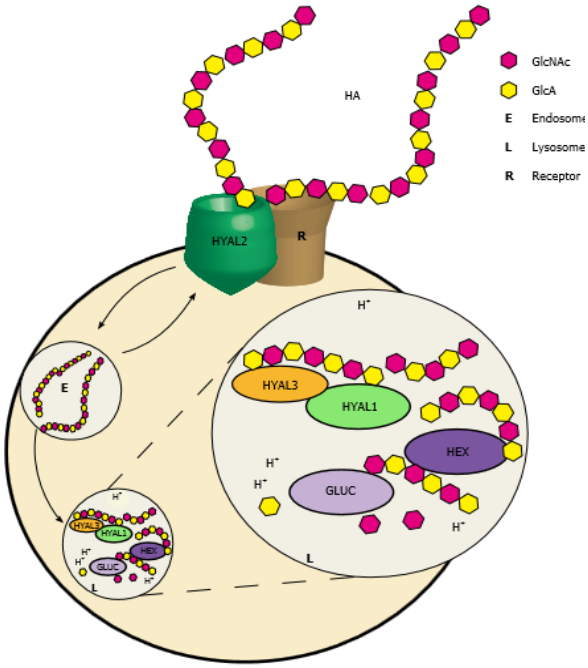

Figure 7. Proposed model for hyaluronan degradation. Hyaluronan (HA) bound to cell- or matrix-associated receptors such as CD44, HARE, or LYVE-1 is proposed to be hydrolyzed to intermediate-sized fragments by the GPI-linked HYAL2. The fragments are then internalized by receptor-mediated endocytosis and transported to lysosomes. In lysosomes, HYAL1 cleaves the intermediate-sized HA fragments to smaller fragments. These fragments become substrates for the sequential action of the two exoglycosidases family enzymes, β-glucuronidase (Gluc) and β-N-acetylhexosaminidase (Hex) which hydrolyze terminal GlcA and GlcNAc. The role of HYAL3 is still unclear (figure described and taken from Triggs-Raine, 2015).

The acidic environment necessary for HYAL2 activity is provided by Na^+/H^+ Exchanger (NHE2), facilitating the generation of HA polymers of approximately 20 kDa (or 50 disaccharide units)**.** In this model, 20 kDa fragments are internalized and transported first to endosomes and then to lysosomes, where lysosomal HYAL1, together with two lysosomal β-exoglycosidases, called β-glucuronidase and β-N-acetyl-glucosaminidase, further degrades the HA into tetrasaccharide units (Triggs-Raine, 2015).

1.4. HA and extracellular matrix

HA is responsible for various important organizational functions such as cell growth, differentiation, and migration (Paiva et al., 2005; Tsepilov and Beloded, 2015). To stabilize the integrity of ECM hyaluronan-binding proteins play an important role; they are cell receptors specific for glycosaminoglycans, in this case HA, and are often called hyaladherins. Many of these proteins have already been described, and they are characterized by a variety of functions, including tissue affiliation, cellular localization, specificity, affinity, and other properties, which are continuously being elucidated (Toole, 1997). It was reported that HA strongly interacts with two well-known and extensively characterized hyaladherins, namely CD44 (Aruffo et al., 1990) and Receptor for Hyaluronan-Mediated Motility (RHAMM) (Hardwick et al., 1992).

CD44 is a multifunctional cell surface glycoprotein expressed on most cell types (Karjalainen et al., 2000). Extensive alternative splicing of nine variable exons and different combinational insertions result in many distinct CD44 splice variants. The standart CD44 is the shortest and also the most abundantly expressed isoform; the other variants are expressed in a cell-specific manner and in the pathophysiology of many disorders. CD44 has several important physiological functions in cell–cell and cell–matrix interactions including proliferation, adhesion, migration, hematopoiesis, and lymphocyte activation, homing, and extravasation (Mattheolabakis et al., 2015; Ponta et al., 2003). This variability in cellular activity seems to rely on the differential expression of the different CD44 splice variants, but also is due to post-translation modifications such as N- and O-glycosylation, and binding by a variety of ligands. The diversity of isoform expression, post-translational modifications, abundance and spatial distribution of CD44 are likely to be critical for the regulation of signalling events, in particular because high molecular weight hyaluronic acid (HMW-HA) can bind multivalently to CD44 (Mattheolabakis et al., 2015; Misra et al., 2015; Ponta et al., 2003).

RHAMM, an acidic and coiled-coil protein designated as CD168, has been found on cell surfaces, as well as in the cytosol and nucleus. RHAMM lacks a transmembrane domain but is GPI-anchored to the cell membrane, where it can interact with CD44 and participate in many cell functions, including cell motility, wound healing, and modification of signal transduction signalling cascades. RHAMM contains no signal peptide and is thought to be transported, via unconventional transport mechanisms, to the cell surface, where it associates with the cell surface via docking with HA synthase, and like CD44, it transduces signals that influence cell motility (Misra et al., 2015; Toole, 1997).

1.5. Hyaluronic acid and cancerogenesis

A progressive tumour is something more complex than a set of clones of mutant cells, it is indeed a complicated three dimensional heterogeneous formation sustained by a complex network of intercellular interactions established among tumour cells, normal cells and the tumour microenvironment. For invasion and metastasis, the ECM must be degraded and this degradation is usually associated to changes in its intercellular signal transduction potential. In fact, HA and the products of its degradation catalysed by hyaluronidases, act as signals promoting angiogenesis, which guarantees the appropriate supply of nutrients to the actively dividing cells (Tsepilov and Beloded, 2015). Numerous data have been provided regarding

the direct participation of HA in the development of the tumour. For instance, enhanced HA synthesis was shown to promote penetration and spreading of transformed keratinocytes into epithelial tissues (Toole et al., 2002). Some tumours influence the surrounding cells to upregulate their HA biosynthesis, whereas in the context of carcinomas it was shown that high levels of HA are directly produced by malignant cells themselves (Auvinen et al., 2000; Ropponen et al., 1998). Upregulated levels of HA and hyaluronidase activity are considered of diagnostic significance for malignant change and carcinogenesis. High amount of HA in tumor stroma and peritumoral space suggests unfavorable prognosis of breast cancer (Auvinen et al., 2000) and ovarian cancer (Anttila et al., 2000). In patients affected by mesothelioma, high amount of HA has been detected in pleural effusions and serum (Afify et al., 2005; Törrönen et al., 2016). The presence of HA and its receptor CD44 have been shown to facilitate neoplastic cell motility and invasion. The diagnostic relevance of HA and CD44 is so high that both molecules have the potential to be used as biomarkers in this kind of tumour (Cortes-Dericks and Schmid, 2017).

Chapter 3. Complement system

1. Complement system

Complement system (C) is a well-known arm of innate immunity, providing an early warning signal and fast response upon encountering a foreign antigen, although recent findings have revealed that C orchestrates many other immunological and inflammatory processes, thus contributing to the maintenance of the homeostasis of different organs and tissues (Walport, 2001). It consists of nearly 50 fluid-phase and membrane proteins, which can be zymogens (enzymes becoming active upon complement activation), effectors, receptors, or control proteins. The role of C system is to control the adaptive immunity and to enhance the humoral immunity. It participates also in removal of apoptotic cells, regulation of the coagulation system, maturation of synapses, angiogenesis, mobilization of hematopoietic stem-progenitor cells, regeneration of tissue and lipid metabolism. C acts like a bridge between innate and adaptive immunity helping to regulate B- and T-cell responses. Apart from these, C is implicated in several processes including regulation of neuronal networks development, tissue regeneration and angiogenesis (reviewed by Pio et al., 2014; Ricklin et al., 2010; Sim et al., 2016).

1.1 Pathways of complement activation

There are three well-established mechanisms leading to C activation, named classical, lectin and alternative pathways (Nonaka, 2014; Walport, 2001).

All three C pathways converge on activating the central component C3 but target recognition and activation mechanisms are different. The first component of the **classical pathway** is the C1 complex, which is composed of a C1q macromolecular complex associated with C1r and C1s, two serine protease proenzymes (Kojouharova et al., 2010). Activation of the classical pathway is initiated upon binding of C1q either to antibodies of the (Ig)G or IgM families or endogenous ligands such as dying cells (Nauta et al., 2002), extracellular matrix proteins (Sjöberg et al., 2009), pentraxins (McGrath et al., 2006), amyloid deposits (Ying et al., 1993), prions (Mitchell et al., 2007) and DNA (Ying et al., 1993). Binding of C1q activates C1s and C1r. C1s cleaves C4 into two fragments: C4b, which binds to the cell surface through a thioester bond, and C4a which diffuses away. Next, C2 binds to C4b and becomes a target for C1s. The cleavage of C2 generates two fragments: C2a and C2b. This latest fragment remains bound to C4b, forming the C4bC2b complex known as C3 convertase. Furthermore, C2b acts as a serine protease and cleaves C3 to C3b and C3a. C3b binds covalently to the cell membrane through a thioester bond and joins to the C3 convertase and forms the classical pathway C5 convertase (C4bC2bC3b) (Pangburn and Rawal, 2002). Analogous to the classical pathway is the lectin pathway which is initated by the binding of mannose-binding lectin (MBL) and H-, L- or M-ficolins (Thiel, 2007) to molecular patterns (e.g. sugars) found on pathogens, leading to mannan-associated serine protease (MASP)-2 activation and subsequent cleavage of C4 and C2, and generation of C4bC2a, the C3-convertase (Matsushita et al., 2000). The alternative pathway is initiated by spontaneous low-level hydrolysis of C3 - C3(H_2O) (Pangburn et al., 1981), which can bind to factor B. Factor B is cleaved by factor D to form the initial alternative pathway C3 convertase complex (C3(H_2O)Bb) (Bexborn et al., 2008), which begins to convert C3 into C3b and C3a (reviewed by Alawieh and Tomlinson, 2016; Nonaka, 2014).

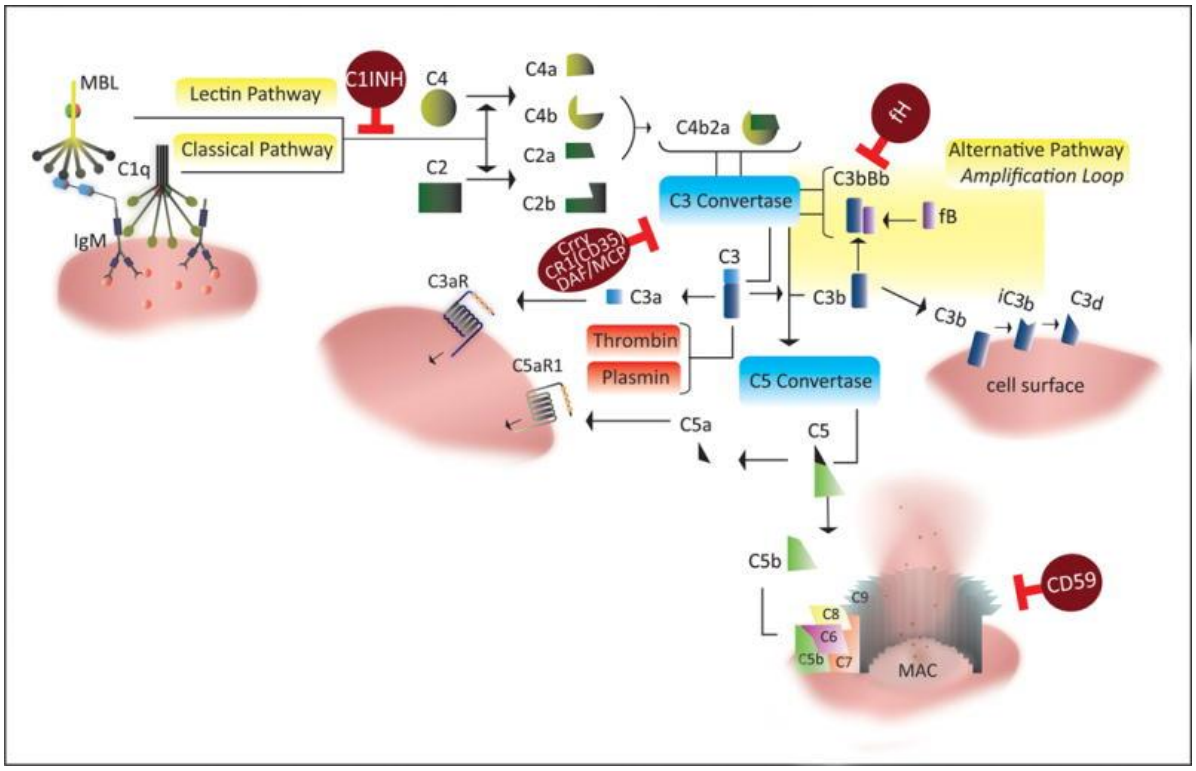

Figure 8. **Overview of the complement system and complement regulators.** Complement system is activated by one of three pathways. The first one is the classical pathway, via C1q binding to Fc-domains of antigen-bound antibodies or directly to apoptotic/stressed cells. The second is the lectin pathway, via binding of MBL to sugar moieties on pathogenic surfaces and glycosylated proteins, and, the third one is the alternative pathway, through spontaneous hydrolysis of serum complement C3 ("tick-over") with the involvement of factors B and D. C3 convertase is formed by the cleavage of C4 and C2 to constitute C4b2a (classical and alternative pathway) and the alternative pathway C3 convertase is formed by association of C3b with factor B and subsequent cleavage of factor B by factor D forming C3bBb. C3 cleavage leads to the production of C3b and C3a. Deposited C3b can further amplify C3 cleavage by recruitment of the alternative pathway, and additionally serves as an opsonin that is subsequently processed into iC3b and C3d. C3b can also associate with C3 convertase (C4b2a or C3bBb), forming a C5 convertase that cleaves C5 into C5b and C5a. C3a and C5a are anaphylatoxins and signal through G-protein coupled receptors. C5b deposits on cell surfaces and recruits downstream complement proteins C6-C9 leading to the formation of membrane attack complex (MAC). Uncontrolled complement activation is prevented by several complement regulators, which serve as a checkpoints at different points in the complement pathway (Figure and text adapted from Alawieh and Tomlinson, 2016).

C3b is either rapidly inactivated or can bind to complement-activating surfaces and associate with factor B. Factor B in complex with C3b, can be cleaved by factor D, forming the predominant alternative pathway C3 convertase (C3bBb). The stability of this convertase is enhanced by the binding of properdin. The fragment Bb on the C3 convertase cleaves more C3 and initiates an amplification loop, generating more C3b that can create new alternative C3 convertases and the C5 convertase (C3bBbC3b) (Hourcade, 2008).

1.2 Complement system in cancers

Inflammation caused by complement system has been recognized as a pathogenic factor for many chronic inflammatory diseases, such as rheumatoid arthritis, glomerulonephritis,

atherosclerosis, asthma and multiple sclerosis. Absence, alteration or overactivity of several complement proteins have been associated with the development of infectious or autoimmune diseases (Rutkowski et al., 2010).

However, two important reasons justify the study of the role of complement activation in cancer progression and the effect of its manipulation in cancer therapy. First, the complement system is an important component of the inflammatory response, which is involved in various stages of tumorigenesis and cancer progression (Coussens and Werb, 2002); second, C activation regulates adaptive immune response (Carroll and Isenman, 2012) having therefore the possibility to regulate T cell response against tumours. From this dualism, a theory arose according to which the recognition of cancer cells by complement elements creates a selective pressure, that leads to the expansion of new tumour populations able to control complement activation and to exploit intermediate activation products (Pio et al., 2014). Recently the protective role of C in cancer has been discussed focusing on the beneficial effect of C-fixing antibodies that are activators of the classical pathway and are able to inhibit tumour progression as a result of MAC-mediated cancer apoptosis and C-mediated inflammation (Macor et al., 2018).

1.3. Complement in immune surveillance against tumours

The C system is one of the immune actors present in the tumour microenvironment which plays an important role in the control of tumour growth. C activation made by antigen initiates an inflammatory reaction and the opsonization of the target cell, which can have, in some cases, killing effect. This is the common role C may have on the control of tumour growth (Pio et al., 2014). Genetic and epigenetic alterations connected with tumour growth dramatically change the morphology and the composition of the cell membrane. Very important, for the progression of epithelial cells from a normal to a malignant phenotype, is an increase in the metabolism of membrane phospholipids (Costello and Franklin, 2005; Griffin and Kauppinen, 2007). Furtermore, altered glycosylation is considered as a hallmark of cancer cells (Hakomori, 2002). Lung cancer cell lines were shown to deposit C5 and generate C5a more efficiently than bronchial epithelial cells. An increased level of C5a was also found in the plasma samples of patients with non-small-cell lung cancer (Corrales et al., 2012). Deposition of C3b, C3c and C4 C components was detected in primary lung tumours (Gmiński et al., 1992; Niehans et al., 1996). Elevated levels of C3a and soluble C5b-9 are present in the intraperitoneal ascitic fluid of patients with ovarian cancer (Bjørge et al., 2005).

In brain tumours, higher C hemolytic activity and C3 levels have been observed in serum samples from children with neuroblastoma (Carli et al., 1979). Some of the first evidences for the activation of the classical pathway of the C have been described in patients with chronic lymphatic leukemia (Füst et al., 1987), papillary thyroid carcinoma (Lucas et al., 1996), follicular lymphoma, and mucosa-associated lymphoid tissue lymphoma (Bu et al., 2007). Activation of lectin pathway was increased in patients with colorectal cancer compared to healthy patients (Ytting et al., 2004). Moreover, the alternative pathway of C activation by malignant transformed cells has been found to be activated in lymphoblastoid cell lines (Budzko et al., 1976) and patients with multiple myeloma (Kraut and Sagone, 1981). Apart from the traditional pathways of C activation, cancer cells may have the capacity to activate C by an extrinsic mechanism. This was proved in lung cancer cell lines, characterized by the ability to produce C5a in the absence of an exogenous supply of serum, which represents the main source of C components (Corrales et al., 2012). Also human mast cell lines (HMC-1) are able to produce anaphylatoxins by soluble and membrane-bound serine proteases independently from complement activation (Amara et al., 2008). The exact trigger for C activation upon these transformations is still not fully understood, although activation through immune complexes, antibody binding or direct C1q binding to necrotic and apoptotic cellular components are all possibilities. The relative contribution of each activation pathway has not been clarified yet, but increasingly data suggest an influence of all three pathways (Pio et al., 2014).

1.4 Complement activation can promote tumor growth

The role of C in the tagging and elimination of tumour cells represents a very interesting issue addressed by many researchers, since it was demonstrated that mice deficient in C3 or C5aR show decreased tumour growth when compared to wild-type mice (Corrales et al., 2012; Markiewski et al., 2008). C can assist the escape of tumour cells from immunosurveillance, promote angiogenesis, activate mitogenic signalling pathways, contribute to cellular proliferation and resistance to apoptosis, and participate in tumour cell invasion and migration (Rutkowski et al., 2010) (Figure 9).

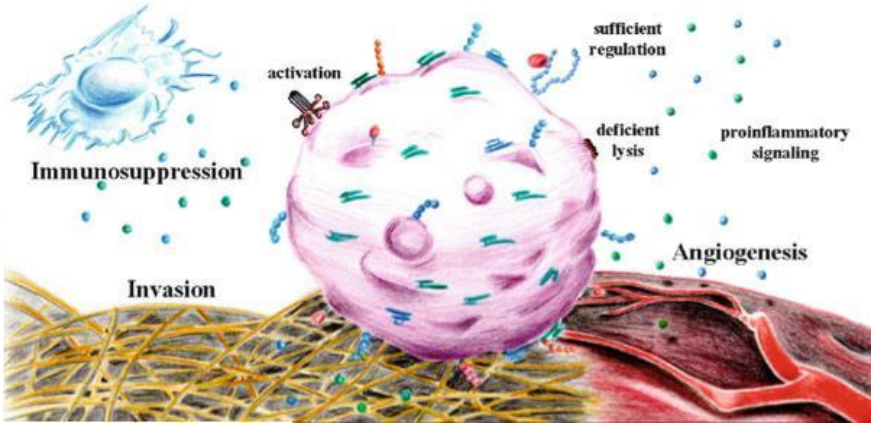

Figure 9. Tumor promoting role of C proteins in the tumor microenvironment. The contribution of C to the antibody-mediated cancer cell killing remains controversial (Pio et al., 2014)

1.4.1 Complement and immunosupression

Immunosuppression is orchestrated by lymphoid and myeloid cells, recruited and activated in the tumour microenvironment, including regulatory T cells, tumour-associated macrophages (TAMs), regulatory dendritic cells and myeloid-derived suppressor cells (MDSCs) (Zou, 2005). The most important points in tumor-derived immunosuppressive mechanisms are: first, downregulation (or loss) of major histocompatibility complex class I molecules, second, tumor-associated antigens and third, the secretion of immunosuppressive factors such as vascular endothelial growth factor (VEGF), TGF-β, IL-10, reactive oxygen species (ROS) and prostaglandins (Kim et al., 2006). Many recent studies showed that C activation can suppress immune response. Anaphylatoxin C5a has dose dependent effect on differentiation of regulatory T cells (Gunn et al., 2012), as well as on recruitment and activation of MDSCs into tumours. The role of C5a in the immunosuppressive function of MDSCs was confirmed *ex vivo* when isolated MDSCs from C5aR-deficient mice were unable to inhibit T-cell proliferation (Markiewski et al., 2008). Moreover, the blockade of C5a signalling downregulated the expression of key immunosuppressive molecules in a lung cancer mouse model (Corrales et al., 2012). All these studies suggest that anaphylatoxin molecule C5a can suppress the T-cell-mediated antitumour response via promoting an immunosuppressive microenvironment and recruiting regulatory T cells, as well as MDSCs into the tumour (Pio et al., 2014).

1.4.2 Complement and angiogenesis

The creation of new vessels from pre-existing ones, called angiogenesis or neovascularization, is a key mechanism of tumour progression and it is directly related to the tumour

aggressiveness (Carmeliet, 2003). Complement-activated factors can have pro- or anti-angiogenic role on neovascularization in some disease, such as cancers. Girardi and colleagues demonstrated an upregulation of anti-angiogenic factor in monocytes after C activation in an antibody-independent model of spontaneous miscarriage and intrauterine growth restriction (Girardi et al., 2006). In contrast, the presence of anaphylatoxins C3a and C5a activates angiogenesis in age-related macular degeneration (Nozaki et al., 2006) through the induction of VEGF expression and thereby promoting the generation of new vessels in retinal pigmented epithelium cells. In addition, C3 and MAC are deposited in the eyes of animals with laser-induced choroidal neovascularization, concomitant with an increase of the angiogenic factors VEGF, TGF-β2, and basic fibroblast growth factor (Bora et al., 2005). Moreover, a genetic C3 deficiency in a mouse model of epithelial ovarian cancer enhanced tumour vascularization by altering the function of endothelial cells (Nunez-Cruz et al., 2012). However, these studies suggest that C activation may be important in the promotion of angiogenesis particularly during the early steps of tumor progression, which was confirmed by *in vitro* studies using endothelial cells where C5a stimulates chemotaxis and tube formation in human umbilical endothelial cells (Schraufstatter et al., 2002) and human microvascular endothelial cells (Nunez-Cruz et al., 2012). Endothelial cell are able to respond to C5a by activating the expression of genes that participate in endothelial adhesion, migration, and angiogenesis (Albrecht et al., 2004).

1.4.3 Complement and tumor cell proliferation, migration and metastasis

Invasion and metastasis are the processes in which the C system is actively involved by different mechanisms. Activation of C system releases both anaphylatoxins C3a and C5a which decrease expression of E- cadherin and induce epithelial mesenchymal transition (EMT), the key process in cancer cell invasion and metastasis (Tang et al., 2009). Cancer cells are able to migrate *via* degradation of ECM promoted by C proteins (Rutkowski et al., 2010). Very important proteins is metastatic process are matrix metalloproteinases (MMPs). When C system is once activated, C5a signalling through C5aR promotes the release of matrix metalloproteinases (MMP), in particular MMP-9 is released by macrophages (Gonzalez et al., 2011; Pio et al., 2014). Overexpression of MMP-1 protected murine melanoma cells from the damaging effects of C and promoted the formation of lung metastasis *in vivo* (Rozanov et al., 2006). In melanoma cells, overexpression of procathepsin-L switched their phenotype from non-metastatic to highly metastatic (Frade et al., 1998).The role of proteases in this processes

is inactivating C proteins and protecting tumour cells from complement attack (Pio et al., 2014).

2. C1q: the first component of the complement system

C1q is a versatile molecule of the innate immunity that serves as a initiation subcomponent of the classical pathway of the C activation. The versatility of potent pattern recognition molecule has fuelled its functional flexibility (Nayak et al., 2012). C1q is a 460-kDa macromolecule made up of 3 distinct polypeptide chains, A (34 kDa), B (32 kDa) and C (27 kDa), arranged to form 6 triple helical strands with three peptide chains–A, B, and C–forming a single strand (Brodsky-Doyle et al., 1976; Knobel et al., 1975). Chains A, B and C are the product of three distinct genes clustering in the same orientation, and in the order A–C–B in ratio 1:1:1 on the short arm of chromosome 1p (Sellar et al., 1991). Each of the three polypeptide chains is composed of a short N-terminal region followed by a collagen-like region (CLR) and a C-terminal globular region, also called the gC1q domain (Sellar et al., 1991) and in turn has its own ligand specificity capable of recognizing different molecular patters (Kishore et al., 2004). The two C1q domains can independently interact with a multiplicity of biological structures including pathogen-associated and cell associated molecules. In addition, it is the gC1q domain itself that defines the versatility of the C1q molecule and defines the interaction between C1q and its self, non-self and altered-self ligands (reviewed by Ghebrehiwet et al., 2017; Nayak et al., 2012). Similar than other C components, also C1q is synthesized by resident and recruited cells including fibroblasts, endothelial cells, tissue specific cells, and macrophages (Agostinis et al., 2017a; Lubbers et al., 2017) and is released in the tumour microenvironment.

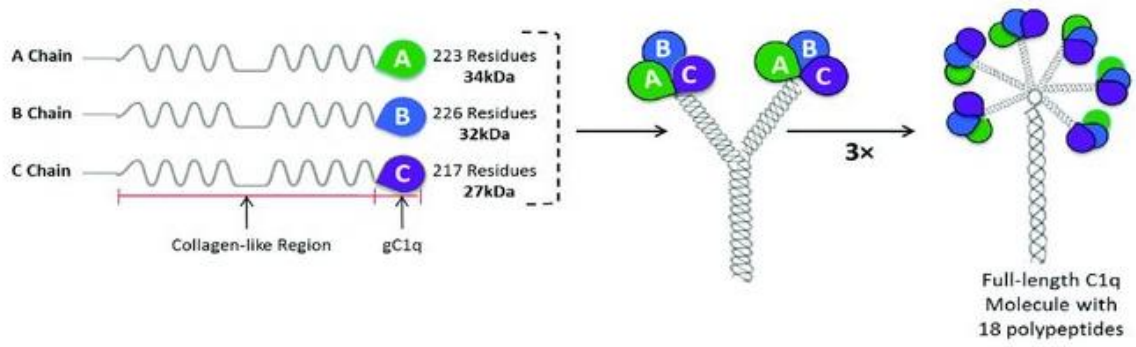

Figure 10. Structural organization of intact C1q. C1q is a charge pattern recognition protein with MW 460 kDa composed by homologous polypeptide chains, 18 in total (6A, 6B and 6C chains) linked with a collagen-like region (N-terminal) and a globular head domain (gC1q). (The figure adapted by (Pondman et al., 2017).

2.1 Classical role of C1q

C activation is one of the most important factors causing inflammation in pathologies such as autoimmune and neurodegenerative diseases, as well as atherosclerosis. Charge pattern molecule C1q recognises and binds self and non-self ligands directly by gC1q domain or adaptor molecules, such as IgG/IgM and C-reactive protein (CRP). In addition, C1q has ability to bind IgG and IgM *via* ionic bonds and activate classical C pathway through the binding of the gC1q domain to aggregated IgG or IgM on immune complexes (Ghebrehiwet et al., 2018; Kishore et al., 2004; Nayak et al., 2010a). Apart from the binding to IgG and C activation C1q is involved in different cell processes such as apoptosis and coagulation. C1q binds to the apoptotic cells and surface blebs on apoptotic cells. This binding is able to activate C system and leads to the removal of the apoptotic cells which is crucial in maintaining normal homeostasis (Nauta et al., 2002). Inability to remove apoptotic cells resullts to their accumulation, contributes to cronic inflammation and developes C1q-defiency disorder, such as systemic lupus erythematosus (SLE) (Nayak et al., 2012). Furthermore, C1q has an effect on cells function through its autocrine and paracrine functions (Ghebrehiwet et al., 2017). Binding between C1q and C-Reactive protein (CRP), a strong activator of the classical C pathway and an important clinical marker of inflammation particularly in cardio-vascular diseases and cancer (Danesh et al., 2004), induces subsequent C activation and leads to inflammation following tissue damage, such as atherosclerosis (Biró et al., 2007; Nayak et al., 2012). Classical pathway can be activated on the surface of endothelial cells by C1q which is leading to inflammation and causes endothelial cell damage (Yin et al., 2007). Moreover, C1q recognises deposited low density lipoprotein (LDL) on atherosclerotic lesions and activates C which leads to inflammation (Biró et al., 2007).

C activation that follows binding of C1q invariably leads to inflammation but in some cases the inflammation can be also protective for the organism as it leads to host defence against pathogens. When C1q binds to outer membrane proteins of Gram-negative bacteria leads to C susceptibility of the harmful pathogen (Roumenina et al., 2008). Moreover, also some human astrovirus exist with special coat proteins that bind to C1q and inhibit the C activation to avoid the host immune response (Hair et al., 2010). As well as low molecular mass heparin,

C1q is able to inhibit C activation in pregnancy and thus hence pregnancy loss (Oberkersch et al., 2010).

2.2 Alternative role of C1q

Even though C1q is a complement initiating molecule, it is also engaged in an array of processes that are completely independent from C activation (Kishore et al., 2016; Kouser et al., 2015). C independent functions modulated via C1q are very important for the central nervous system (CNS) by microglia activation. These phagocytic cells are known to synthesise C1q and their activation is dependent on extrinsic C1q; they attempt to phagocyte the opsonised targets, such as apoptotic neurons and amyloid peptides (Fraser et al., 2010). Recently, C1q has been shown to be expressed locally in the microenvironment of a range of human malignant tumours, where it can promote cancer cell adhesion, migration, and proliferation, without involving complement activation (Agostinis et al., 2017b; Bulla et al., 2016). C1q has been shown to be present in the ascitic fluid formed during ovarian cancers where it can affect tumour cells; this was demonstrated by exogenous treatment with C1q, that *via* its globular domain induced apoptosis in an ovarian cancer cell line SKOV3 through TNF-α induced apoptosis pathway involving upregulation of Bax and Fas (Kaur et al., 2016). In addition, C1q is able to downregulate the production of the pro-inflammatory cytokines IL-1a, IL-1b, IL-6 and TNF-α and has a neuroprotective role upon activating microglial cells in order to ingest apoptotic neurons and by suppressing pro-inflammatory cytokine production in CNS. Opposite from that, C1q can have also neurodegenerative role in CNS by tiggering C activation (Bonifati and Kishore, 2007). Defective local production of C1q may be involved in pregnancy disorders, such as pre-eclampsia. Agostinis et al. for the first time demonstrated a novel role of C1q in physiological and pathological pregnancies (Agostinis et al., 2017a). In extracellular matrix, C1q binds to various matrix proteins, such as decorin, biglycan, lumican, laminin and fibronectin and hampers activation of C system (Krumdieck et al., 1992). Binding of C1q to these proteins, probably *via* CLR domain, has been implied in deposition and retention of immune complexes in the basement membrane (Sjöberg et al., 2009). C1q has a very important role, which is not connected with C activation also during the early phase of placental development, promoting trophoblasts cell migration and tissue remodelling. Fetal cytothrophoblasts express C1q on their surface as a bridge toward the maternal decidua. C1q can interact with components of the decidua extracellular matrix, thus allowing adhesion and invasion of trophoblasts (Agostinis et al., 2010). The angiogenic activity of C1q was supported by its ability to induce new vessel formation in *in vitro* and *in vivo* models of

wound healing. C1q is selectively localized on the vessel endothelium and in the stroma of wound healing in the absence of C4 and C3 and acts as a unique angiogenic factor (Bossi et al., 2014). On endothelial cells C1q promotes spreading and adhesion via cC1qR and gC1qR, abundandly present on human dermal endothelial cells. cC1qR and gC1qR in association with adhesion molecules, particularly β_1 integrins, transduce signals into endothelial cells, thus promoting their adhesion and spreading to C1q-coated cell surfaces (Feng et al., 2002). Apoptotic cell clearance is mediated by C1q in a complement-dependent and complement-independent manner. C1q is able to maintain the tissue homeostasis by recognizing blebs or other molecules exposed on the surface of apoptotic cells. cC1qR on macrophages binds to the collagen region of bound C1q and signals for the uptake and phagocytosis of apoptotic cells through association with CD9 (Ogden et al., 2001). C1q can inhibit platelets adhesion and aggregation by binding to different C1q receptors expressed on the platelet surface and to adsorbed IgGs. Platelets activation is the triggering event of the coagulation cascade (Nayak et al., 2010b). Further researches into the ligand binding capacity of C1q can lead to a better understanding of the process of inflammation along with many more other cellular processes including apoptosis and cell adhesion (Nayak et al., 2012).

RATIONALE AND AIMS OF THE STUDY

Malignant pleural mesothelioma is a rare and aggressive cancer that develops in the pleura, a thin layer of tissue surrounding the lungs. It is mainly induced by long-term exposure to asbestos, a naturally occurring silicate mineral, and its incidence and associated mortality rate are increasing in most countries. Like all form of cancer, mesothelioma (MES) cells acquire the ability to proliferate in an uncontrolled manner, invading the surrounding tissue and spreading to distant organs. It has been widely recognized that the local microenvironment is actively involved in the process of carcinogenesis since it can provide a permissive niche for tumour cells survival, growth and migration.

Hyaluronic acid (HA), a member of the glycosaminoglycan family, is an abundant and ubiquitous component of the ECM which has emerged to play a fundamental role in cancer progression. Interestingly, HA is highly expressed in MPM where it enhances the aggressiveness and spreading of MES cells into adjacent, non-cancerous and stromal tissues. Elevated levels of HA can be detected in pleural effusions and serum of the patients affected by such devastating disease.

Another key component of the tumour microenvironment, that has received increasing attention, is represented by the complement system, a well-known arm of the innate immunity which participates in the immune surveillance and homeostasis. In particular C1q, the first component of the classical pathway, has emerged to act in the tumour microenvironment as a cancer promoting factor, independently of C activation. We recently unveiled that C1q is able to interact with several extracellular matrix components, being HA the strongest interaction partner. Taking into account that HA is abundantly expressed in MPM, as C1q, these findings raised the possibility that C1q bound to HA would function as a novel “signalling complex” able to promote the development and progression of MPM.

Here we present novel data showing that C1q bound to HA is able to affect HA homeostasis. In particular signalling events initiated by C1q bound to HA on mesothelioma cells are capable to modify the expression of enzymes responsible for the synthesis and degradation of HA in the tumour microenvironment. We also provided evidence that C1q can contribute to ROS production only in the presence of LMW-HA. Based on these findings we can propose the following model: C1q-HA interaction, by enhancing HA degradation via Hyal2, feeds LMW-HA deposition in the tumour microenvironment which, in turn, favours ROS production and further HA degradation.

MATERIALS AND METHODS

Cell isolation and culture

MES cells were isolated from pleural biopsy specimens. The tissue was finely minced with a cutter, incubated with a digestion solution composed by 0.5% trypsin (Sigma-Aldrich, Milan, Italy) and 50 μg/ml DNase I (Roche, Milan, Italy) in Hanks' Balanced Salt solution with $Ca^{2+}Mg^{2+}$ 0.5mM (Sigma-Aldrich) overnight at 4◦C. Next, the enzymatic solution was changed with collagenase type 1 (3 mg/ml) (Worthington Biochemical Corporation, DBA) diluted in Medium 199 with Hank's salts (Euroclone Spa, Milan, Italy) for 30 min at 37°C. The digestion was blocked with 10% fetal bovine serum (FBS, GIBCO, Life Technology) and the cell suspension was filtered through a 100 μm pore filter (BD Biosciences, Italy).

The cells were seeded in a 12.5 cm^2 flasks and cultured using Human Endothelial serum free medium (HESF, Life Technologies), 10% heat-inactivated FBS supplemented with EGF (5 ng/ml), basic FGF (10 ng/ml) and Pennicillin-Streptomicin (Sigma-Aldrich). Fresh medium was replaced every 2-3 days.

Antibodies

The following antibodies were used: anti-HYAL2 rabbit polyclonal antibody (Proteintech, 15115-1-AP), anti-HAS3 rabbit polyclonal antibody (Proteintech, 15609-1-AP), anti-M6P-R mouse monoclonal (Abcam, #2733), anti-Vimentin mouse monoclonal (Santa Cruz), anti-Calnexin mouse monoclonal antibody (Abcam, #31290), anti-EEA1 mouse monoclonal antibody (Abcam, #70521), anti-gC1qR mouse monoclonal antibody (74.5.2 clone, Merck Millipore), anti-LAMP1 mouse monoclonal antibody (Santa Cruz, H4A3 clone), biotinylated anti-goat IgG antibody, streptavidin Alexa Fluor 488 conjugated, anti-mouse IgG Cyn3 conjugated and anti-rabbit IgG FITC conjugated secondary antibodies were from Sigma-Aldrich.

Coating conditions

Sterile 6-well plates (Corning) or glass round coverslips of 15 mm diameter (Menzel-Glaser) were incubated ON at 4°C with high molecular weight HA (MW 1.5 MDa, kind gift from Ivan Donati) at a concentration of 50 μg/mL in bicarbonate buffer, pH 9.6. The day after, the plate was washed 1-time with dPBS and then incubated ON at 4°C with C1q (Sigma) at a concentration of 25 μg/mL in dPBS + BSA 0.5 % (Sigma), 0.7 mM $CaCl_2$ and 0.7 mM

$MgCl_2$. After ON incubation, the wells were washed again with dPBS, before seeding the cells.

Flow cytometry

Mesothelioma cells ($5x10^5$) were fixed (or used live cells) with the fixation reagent FIX&PERM kit for 15 min at RT in the darkness and incubated with primary antibodies as listed above for 1 h at 4ºC. Antibodies directed against intracellular antigens were diluted in permeabilization reagent of the FIX&PERM kit, while antibodies for cell surface antigens were diluted in PBS with 1% BSA. Incubation with secondary antibodies anti-mouse-FITC F(ab)' (1:50) or anti-rabbit-FITC (1:300) was performed for 30 min on 4ºC. Cells were resuspended in 1% paraformaldehyde, then the fluorescence was acquired with the FACScalibur (BD Bioscience), and data processed using the software CellQuest.

Adhesion assay

1×10^5 MES cells, labelled with the fluorescent dye FAST DiI (Molecular Probes, Invitrogen), were re-suspended in Human Endothelial serum free medium (Life Technologies) containing 0.5% BSA (Sigma), pre-incubated with 10µM of Everolimus (#S1120 Selleckchem) ihibitor for 45 min at RT and then added to a 96-well plate (wells were coated as described above) for 35 min at 37°C in 5% v/v CO_2 incubator. For untreated cells, cells without pre-incubation with Everolimus were used. The unbound cells were removed and the adherent cells were lysed with 10mM Tris-HCl, pH 7.4 + 0.1% SDS. The plate was read with Infinite200 (absorbance 544 nm, emission 590 nm) (TECAN) and referred to a calibration curve established with an increasing number of labelled cells.

Red Blood Cells Exclusion Assay

Different MES populations were seeded on a sterile 96 well plate (Corning). Cells were kept in culture for three days in Human Endothelial serum free medium (HESF), 10 % FBS, supplemented with 5 ng/mL of epidermal growth factor (EGF, Sigma), 10 ng/mL basic fibroblast growth factor (bFGF, Immunological Sciences), 1 % penicillin-streptomycin (Sigma-Aldrich), pH 7.6.

Medium was then removed and replaced by 0.16 % fixed erythrocytes (Institut de Biotechnologies Jacques Bay) diluted into dPBS, 0.5 % BSA, 0.7 mM $CaCl_2$ and 0.7 mM

$MgCl_2$. Red blood cells were then allowed to settle down, for 20 min at 37°C in 5% v/v CO_2 incubator.

As a negative control some wells were treated with hyaluronidase (Sigma, 500 units/mL in HESFM and 10 % FBS, pH 4.4), for 30 min at 37°C in 5% v/v CO_2 incubator. Hyaluronidase was diluted as 1 mg/mL in 0.02 M phosphate buffer (77 mM sodium chloride, 0.01% BSA, pH 7). After 30 min, medium was removed and replaced by 0.16 % fixed erythrocytes suspension. Red blood cells were then allowed to settle down, for 20 min at 37°C. Images were acquired by phase-contrast optical microscope, original magnification 200X with Canon Power Shot A640 Camera.

Alcian Blue Staining

MES were fixed with cold methanol for 10 min, washed two times with dPBS and stained with alcian blue dissolved in 3% acetic acid, pH 2.5, for 30 min at RT. After washing in dPBS, images were acquired by the fluorescence microscope Leica DM 3000 using the Leica DFC320 camera.

MTT Cell viability assay

Metabolic activity of Rapamycin inhibitor, Everolimus, was determined using MTT (3-[4,5-dimethylthiazol-2-yl]-2,5- diphenyltetrazolium bromide) reagent. MES cells were seeded onto 96-well cell plates (Corning) and treated with 10 nM, 100 nM, 1 μM and 10 μM Everolimus for 72 h at at 37°C in 5% v/v CO_2 incubator . After treatment MTT (Sigma-Aldrich, USA) at a final concentration of 0.5 mg/ml was added respectively. Upon 6 h incubation, when MTT was used, the formed formazan crystals were dissolved in DMSO and the optical density (OD) measured at 570 nm with a spectrofluorimeter (Titertek Multiskan ELISA reader). Cell viability was calculated as a ratio of the mean OD value of treated vs. untreated cells.

Epithelial/Mesothelial mesenchymal transition

24-well plates were coated as it was described in Coating conditions. MES cells were seeded onto different matrices (C1q, HA, C1q-bound HA) at the concentration of 1×10^5 cells/well, ON at 37°C in 5% v/v CO_2 incubator in HESF medium, containing 0.5% BSA. No treated cells were used as a control sample. Cells were washed once with cold dPBS and lysed with 400 μl RNA Lysis Buffer (EuroGOLD). mRNA isolation, reverse transcription and RT-qPCR analysis were performed as previously described.

Samples preparation for qPCR

Different MES populations were used for this assay. After preparing the plate with the matrix of C1q (25 µg/mL), HA (50 µg/mL) and HA + C1q the cells were seeded at a concentration of 9×10^5 cells/well and then collected after 3h, 6h or ON of incubation at 37°C in 5% v/v CO_2 incubator. No treated cells were used as a control sample. The cell pellet was washed 1-time with cold dPBS and centrifuged at 250 x g for 7 min. After centrifugation, cell pellet was resuspended into RNA Lysis Buffer (EuroGOLD) and stored at -80°C.

RNA isolation and retrotranscription

RNA was isolated from cell lysates using EuroGOLD Total RNA kit (EuroClone) following manifacturer instructions. Elution of RNA was performed by adding sterile RNAse-free dH_2O (50µl) directly into the binding matrix of the column, and collection was performed upon centrifugation at 5.000 x g for 1 min on a fresh tube. RNase inhibitors (1:15) were added. After isolation, RNA was stored at -80°C.

Isolated total RNA was retrotranscribed to cDNA. Reaction mix is composed of:

- 1 µl reverse transcriptase (Bioline)
- 4 µl SuperScript Mix 5X (Bioline)
- 4 µl isolated RNA
- 11 µl sterile water

Retrotranscription reaction was carried on for 1 h at 42°C, followed by 10 min incubation at 70°C to inactivate the enzyme. cDNA was stored at -20°C.

qPCR

Quantitative real-time PCR (qPCR) was performed to assess the relative mRNA expression levels of the genes under investigation. The Reaction mix was composed of the following reagents:

- 5 µl iQ SYBR Green Supermix 2X (Applied Biosystem – Life Technology)
- 0.5 mM Primer Forward (see Table 1)
- 0.5 mM Primer Forward (see Table 1)
- 1.0 µl cDNA
- 3.0 µl sterile water

The reaction was carried on with the Rotor-Gene 6000 (Corbett, Explera), setting the cycling conditions as followed:

- Denaturation: 60 seconds at 95°C
- Annealing: 30 seconds at the primer Tm
- Amplification: 60 seconds at 72°C
- 45 cycles

In order to verify the specificity of the obtained PCR products, a final melting curve was performed increasing temperature from 50°C to 90°C at a rate of 0.5°C/10sec.

Gene	Tm	Sense	Sequence	Accession number
HAS1	60	Forward Reverse	GGAATAACCTCTTGCAGCAGTTC TCATCCCCAAAAG	NM_001523.3
HAS2	58	Forward Reverse	TCGCAACACGTAACGCAAT ACTTCTCTTTTTCCACCCCATTT	NM_005328.2
HAS3	60	Forward Reverse	CGCAGCAACTTCCATGAGG AGTCGCACACCTGGATGTAGT	NM_005329.2
HYAL1	59	Forward Reverse	CGATATGGCCCAAGGCTTTAG ACCACATCGAAGACACTGACAT	NM_153282.2
HYAL2	60	Forward Reverse	GGCCCCACCGTTACATTGG ATTCTGGTTCACAAAACCCTCAT	NM_003773.4
HYAL3	59	Forward Reverse	CTGTGCTGTGGAATGTACCCT GTCATGTTCTGACCGTGAAAATG	NM_003549.3
TBP	60	Forward Reverse	GAGCCAAGAGTGAAGAACAGTC GCTCCCCACCATATTCTGAATCT	NM_003194.4
E-cadherin	60	Forward Reverse	AAG TGT CCG AGG ACT TTG GCG TGG CAG CCA GTT GGC AGT GTC TCT CCA	NM_004360.3
N-cadherin	60	Forward Reverse	CATCACAGTGGCAGCTGGACTTG GGCCGTGGCTGTGTTTGAAAGG	NM_001792.4
SNAIL	60	Forward Reverse	TCC GAC CCC AAT CGG AAG CCT CCA GGA CAG AGT CCC AGA TGA	NM_005985.3
LEF-1	60	Forward Reverse	CGAATGTCGTTGCTGAGTGT GCTGTCTTTCTTTCCGTGCT	NM_016269.4
β-catenin	60	Forward Reverse	TCC AGC GTG GAC AAT GGC TAC AGC CGC TTT TCT GTC TGG TTC	NM_001904.3

Table 1. Primers used for qPCR analysis.

Western blot

Samples preparation: Different MES populations were used for this assay. Cells were seeded at a concentration of 1×10^6 cells/well on pre-coated (as described in Section Coating conditions) 6-well plates and incubated ON at 37°C in 5% v/v CO_2 incubator. No treated cells were used as control samples. The cells were washed and collected with a scraper in cold dPBS and centrifuged at 250 xg for 7 min. The cell pellet was resuspended into 100 µL of ice cold 1 mM Cell Lysis Buffer (Cell Signaling Technology) supplemented with protease inhibitors (1:100), incubated 10 min on ice and centrifuged at 16.000 x g for 10 min. The lysates were stored at -80°C.

Before using, lysates were supplemented with 2X Laemmli loading buffer (0.004 % of bromophenol blue, 10 % 2-mercaptoethanol, 20 % glycerol, 14 % sodium dodecyl sulfate (SDS, Sigma-Aldrich) and 0.125 M Tris-HCl). The samples were boiled at 95°C for 5 min and then centrifuged at 16.000 xg for 5 min.

Protein quantification: Bradford assay for protein quantification was performed into a not-sterile 96 well plate (Corning). Standard curve was prepared using 2 mg/mL BSA. Different dilutions of the samples in triplicate were measured (4X, 8X and 20X). Bradford reagent (Sigma) was added to each diluted samples and the plate was measured at 595 nm immediately and after 5 min, using a PowerWaveX spectrophotometer (BioTek).

Electrophoresis: Mini-PROTEAN Tetra Cell System (BIORAD) was used. Samples were run on 10% poly-acrylamide (Sigma-Aldrich) gels. Usually 10-15 µg of total protein were loaded on each lane. Amersham ECL rainbow molecular weight markers enabled simpler identification of proteins on SDS-polyacrylamide gels (RPN800E). Buffer tank and Mini-PROTEAN Tetra Electrode Assemblay were filled with 1X running buffer (25 mM Tris HCl, 200 mM glycine, 0.1 % SDS). Electrophoresis power supply Consort EV243 (Wolf Laboratories) was set to 100 V and 25 mA.

To transfer the proteins from the gel onto a 0.2 µm nitrocellulose membrane (GE Healthcare) Trans-blot Turbo Transfer System (BIORAD) was used. Ponceau S staining (Sigma) was performed to check equal loading of gels. The membrane was then rinsed in a distilled water until the background was clean. The membrane was blocked in 5 % skim milk in TBS-T (0.1 M Tris and 1.5 M NaCl, pH 7.6, supplemented with 0.1 % Tween (Sigma)), for 1 h at room temperature (RT). After blocking the membrane was incubated with the primary antibody anti-HYAL2 (1:500) in blocking buffer, ON at 4°C on an orbital shaker.

Next day, the membrane was washed 3-times in TBS-T and further incubated with anti-rabbit IgG peroxidase conjugated secondary antibody (Sigma, A0545), diluted into blocking buffer (1:2000), for 1 h at RT on orbital shaker.

β-actin detection was used as internal loading control. To this aim the nitrocellulose membrane was incubated with anti-β-actin HRP-conjugated antibody (1:2000), for 30 min at RT.

Development: Membrane was developed using the ECL Blotting Reagents (GE Healthcare, RPN2109). ImageJ sofware was used to quantify protein bands from Western blot films.

Immunofluorescence for the intracellular localization of HYAL2

Cells were seeded on glass coverslips of 15 mm diameter (Menzel-Glaser) and allowed to grow to 70 % confluency. Before use, coverslips were incubated with xylene for 1 h, washed 2-times with acetone for 5 min and incubated with acetone for 2-3 h and after incubated with ≥ 99.8 % ethanol for additional 2-3 h.

Coverslips were washed with dPBS/0.05 % Tween to remove the medium. Cells were fixed with 3 % paraformaldehyde (Sigma-Aldrich) for 15 min in the darkness and washed two times with dPBS/0.05 % Tween. The cells were then permeabilized with 0.1 % Triton X-100 (Sigma-Aldrich) diluted in HEPES buffered saline (HBS, composed by 139 mM NaCl, 2.5 mM KCl, 10 mM HEPES, 10 mM D-glucose, 2 mM $CaCl_2$ and 1.3 mM $MgCl_2$) for 5 min at RT. Blocking of unspecific binding sites was performed with dPBS-BSA 2% for 30 min at RT. Cells on coverslipes were incubated with anti-HYAL2 rabbit polyclonal antibody (1:50) diluted in HBS/5 % goat serum for 1 h at RT. To enhance the detection of HYAL2, MES were incubated first with biotinylated goat anti-rabbit antibody (1:100) in dilution buffer for 30 min at RT, followed by Streptavidin-Alexa Fluor 488 conjugated (1:500) for additional 30 min at RT. The nuclei were stained with DAPI (Sigma-Aldrich, 1:500) for 5 min. Coverslipes were washed two-times with washing buffer and distilled water and mounted on fluorescence mounting medium (Dako).

Colocalization with intracellular components: Coverslips were incubated with the following primary antibodies: anti-LAMP1 (1:50), anti-EEA1 (1:200), anti-gC1q receptor (1:100) and anti-Calnexin (1:1000) for 1 h at RT. Secondary antibodies used were: anti-mouse Cy3 conjugated. Nuclei were stained with DAPI (1:500) for 5 min. After placing on a glass slide with fluorescence mounting medium (Dako) upside down, images were acquired by the confocal microscope (Nikon Eclipse Ti2, Microscopy Facility of the International School for Advanced Studies-SISSA, Trieste, Italy).

Immunofluorescence detection of HA

MES cells, seeded on coverslips, were fixed in 2% paraformaldehyde (PFA) for 20 min on RT. After fixation cells were washed three times for 2 min. We permebilized the cell membranes and blocked the unspecific binding site with dPBS containing 1% BSA, 0,1% Triton X and 50 mM Glycine for 30 min at RT. After incubation cells were washed 3-times for 2 min. Cells were incubated with 5µg/ml Hyaluronic acid binding protein (HABP, Merck Millipore) and α-Vimentin (Santa Cruz, 1:40) diluted in dPBS with 3% BSA ON on 4ºC. α-Vimentin Ab was included to detect the morphology of the cells. The day after, coverslipes with the cells were washed 3-times with dPBS for 2 min and incubated with secondary antibodies Streptavidin Cyn3 (1:100) and α-rabbit FITC (1:300) for 30 min on RT. After 3-times washing steps for 2 min each, coverslipes were mounted and analysed under confocal microscope (Nikon Eclipse Ti2).

Surface Biotinylation Assay

MES cells were seeded on HA or C1q-bound HA at a concentration of 1×10^6 cells/well and incubated ON at 37°C in an air/CO_2 incubator. No treated cells were used as a control sample. After, cells were placed on ice, washed 3-times with ice-cold dPBS containing 1 mM $MgCl_2$ and 0.1 mM $CaCl_2$ to remove any contaminating protein. After, cells were incubated with EZ-Link™-Sulfo-NHS-Biotin (1 mg/mL) for 30 min on ice, on an orbital shaker. Cells were washed 3-times with ice-cold dPBS to remove excess of biotin, and quenching was performed upon incubation with 0.1 M glycine in dPBS shaking. Cells were then collected with a cell scraper, washed 3-times with dPBS and cell pellets were resuspended into lysis buffer (10 mM Tris-HCl, 1 % NP-40, 150 mM NaCl, 0.1% protease inhibitors, pH 7.4), kept on ice for 20 min and then centrifuged at 16.000 x g for 10 min at 4°C. Lysates were incubated with High Capacity Streptavidin Agarose Resin (50 % slurry, 0.02 % sodium azide; Thermo Scientific) for 2 h at 4°C, rotating. The Agarose Resin was washed 3-times in lysis buffer supplemented with 0.1 % protease inhibitors. After the last washing step, the solution was carefully removed and the precipitated biotinylated proteins were eluted in 20 µL Laemmli buffer. Samples were stored on -80°C or used immediately for Western Blot analysis.

Uptake of exogenous Fluoresceine-labeled HA by MES

MES cells were seeded on coverslips and allowed to grow for 72 h. Fluorescein-labelled hyaluronic acid (FA-HA, Sigma) at concentration 10 µg/ml was added directly into the culture medium and MES were allowed to internalized it during ON incubation at 37°C in 5 % v/v CO_2 incubator. Next day cells were fixed in 1 % PFA, for 20 min at RT in the darkness and washed 3-times with dPBS. For permeabilization, quenching and blocking we incubated them in dPBS containing 1 % BSA, 0,1 % Triton X-100 and 50 mM glycine for 30 min at RT. Other 3 washing steps were followed by incubation in a humidity chamber with 5 µg/mL of HABP diluted in dPBS with 3 % BSA for 1 h at RT. After 3 washing steps, MES were incubated with streptavidin Alexa Flour 594 (1:150) for 30 min at RT in darkness. DAPI was used for stained the nuclei. After 3-times washing steps, coverslipes were mounted and analysed under confocal microscope (Nikon Eclipse Ti2).

Measurement of total H_2O_2 production

Hydrogen peroxide production was measured using AmpliFlu Red (Sigma) reagent. MES cells were seeded on 96-well plate to reach 90% confluence. To assess total H_2O_2, cell medium was changed with dPBS + 2%BSA + 0,7 mM $MgCl_2$ and 0.7 mM $CaCl_2$ containing 40 µM Amplex Red reagent, 1 µg/ml HRP, 5 µg/ml SOD and 100 µM NaN_3 in a final volume of 100 µl. After 5 min of preincubation with C1q (25 µg/ml), HMW HA (50 µg/ml), LMW HA (200 µg/ml) or LMW HA+C1q the readings were taken at 576 nm with Infinite200 (TECAN).

Statistic analysis

Data were analyzed using Two-way ANOVA, Tukey–Kramer test, and unpaired two-tailed Student's *t*-test or one-way ANOVA with Bonferroni corrections. Results were represented as mean ± SEM. Non-parametric data were assessed by Mann–Whitney *U* tests and the results were expressed as median and interquartile range. p values < 0.05 were considered significant. All statistical analyses were performed using Prism 6 software (GraphPad Software Inc., La Jolla, CA, USA

RESULTS – Paper inserted (1st part)

frontiers in Immunology

ORIGINAL RESEARCH
published: 20 November 2017
doi: 10.3389/fimmu.2017.01559

Complement Protein C1q Binds to Hyaluronic Acid in the Malignant Pleural Mesothelioma Microenvironment and Promotes Tumor Growth

*Chiara Agostinis[1], Romana Vidergar[2], Beatrice Belmonte[3], Alessandro Mangogna[2], Leonardo Amadio[1], Pietro Geri[4], Violetta Borelli[2], Fabrizio Zanconati[4], Francesco Tedesco[5], Marco Confalonieri[4], Claudio Tripodo[3], Uday Kishore[6] and Roberta Bulla[2]**

[1] Institute for Maternal and Child Health, Istituto di Ricovero e Cura a Carattere Scientifico (IRCCS) Burlo Garofolo, Trieste, Italy, [2] Department of Life Sciences, University of Trieste, Trieste, Italy, [3] Department of Human Pathology, University of Palermo, Palermo, Italy, [4] Department of Medical, Surgical and Health Science, University of Trieste, Trieste, Italy, [5] Istituto di Ricovero e Cura a Carattere Scientifico (IRCCS), Istituto Auxologico Italiano, Milan, Italy, [6] Biosciences, College of Health and Life Sciences, Brunel University London, Uxbridge, United Kingdom

OPEN ACCESS

Edited by:
Robert Braidwood Sim, University of Leicester, United Kingdom

Reviewed by:
Gunnar Houen, State Serum Institute (SSI), Denmark
Taruna Madan, National Institute for Research in Reproductive Health, India

***Correspondence:**
Roberta Bulla
rbulla@units.it

Specialty section:
This article was submitted to Molecular Innate Immunity, a section of the journal Frontiers in Immunology

Received: 24 August 2017
Accepted: 31 October 2017
Published: 20 November 2017

Citation:
Agostinis C, Vidergar R, Belmonte B, Mangogna A, Amadio L, Geri P, Borelli V, Zanconati F, Tedesco F, Confalonieri M, Tripodo C, Kishore U and Bulla R (2017) Complement Protein C1q Binds to Hyaluronic Acid in the Malignant Pleural Mesothelioma Microenvironment and Promotes Tumor Growth. Front. Immunol. 8:1559. doi: 10.3389/fimmu.2017.01559

C1q is the first recognition subcomponent of the complement classical pathway, which acts toward the clearance of pathogens and apoptotic cells. C1q is also known to modulate a range of functions of immune and non-immune cells, and has been shown to be involved in placental development and sensorial synaptic pruning. We have recently shown that C1q can promote tumor by encouraging their adhesion, migration, and proliferation in addition to angiogenesis and metastasis. In this study, we have examined the role of human C1q in the microenvironment of malignant pleural mesothelioma (MPM), a rare form of cancer commonly associated with exposure to asbestos. We found that C1q was highly expressed in all MPM histotypes, particularly in epithelioid rather than in sarcomatoid histotype. C1q avidly bound high and low molecular weight hyaluronic acid (HA) *via* its globular domain. C1q bound to HA was able to induce adhesion and proliferation of mesothelioma cells (MES) *via* enhancement of ERK1/2, SAPK/JNK, and p38 phosphorylation; however, it did not activate the complement cascade. Consistent with the modular organization of the globular domain, we demonstrated that C1q may bind to HA through ghA module, whereas it may interact with human MES through the ghC. In conclusion, C1q highly expressed in MPM binds to HA and enhances the tumor growth promoting cell adhesion and proliferation. These data can help develop novel diagnostic markers and molecular targets for MPM.

Keywords: complement system, malignant pleural mesothelioma, hyaluronic acid, mesothelioma cells, C1q, cancer

Abbreviations: MPM, malignant pleural mesothelioma; MES, mesothelioma cells; ECM, extracellular matrix; HA, hyaluronic acid; ghA, ghB and ghC: globular head region of human C1q A, B and C chain, respectively; MBP, maltose-binding protein; HMW, high molecular weight; LMW, low molecular weight.

INTRODUCTION

Malignant pleural mesothelioma (MPM) is a rare form of cancer that develops from cells of the pleural mesothelium and is most commonly associated with exposure to asbestos (1). MPM typically develops after a long latency period, which averages 30–40 years, and the average age of patients is 60 years (2). MPM is highly invasive to surrounding tissues leading to the failure of the organs underlying the serosal membranes (3). Although low in metastatic potential, metastasis in MPM are more frequent postsurgery; at the autopsy, metastatic diffusion is observed in 50% of patients (3). Microscopically, MPM shows mainly one of the three patterns: epithelioid, sarcomatoid, or biphasic (4).

MPM is an aggressive malignancy; most patients succumb within 2 years of being diagnosed (5). Treating MPM remains a challenge. There are two main treatment alternatives: palliative chemotherapy or multimodal treatment including surgical resection combined with chemotherapy or radiotherapy, or both (6). The resistance of MPM to conventional treatment and poor prognosis has renewed interest in basic research in order to understand the MPM biology fully with the aim of identifying possible new molecular therapeutic targets.

The local microenvironment, which encourages survival, growth, and invasion of cancer cells, plays a critical role in cancer development; the extracellular matrix (ECM) is an essential constituent of such microenvironment (7). Hyaluronic acid (HA), a member of the glycosaminoglycan family, is an abundant and ubiquitous component of the ECM (8). HA is a negatively charged high-molecular-weight (HMW) polysaccharide (4–800 kDa) which is made up of the repeating disaccharide (glucuronic acid and *N*-acetylglucosamine) (9). In the tumor microenvironment, HA offers a molecular 3D-scaffold for cells *via* the assembly of ECM, thus modulating stromal as well as tumor cells (10). HA, whose multiple functions are dictated by its molecular size and tissue concentration, relies on balanced biosynthetic and degradation processes. Increased HA synthesis has been associated with cancer progression and metastasis (11). In patients with MPM, large quantities of HA are found in the tumor tissue although both malignant and benign mesothelial cells have been found positive for intracytoplasmic HA (12).

The complement system also constitutes the local environment for cancer as an immune surveillance against malignant cells due to its ability to promote inflammation and causes direct cell killing (13). We focused our investigation on C1q, which is the first recognition subcomponent of the complement classical pathway. C1q is a potent link between innate and adaptive immunity by virtue of its ability to bind IgG- and IgM-containing immune complexes (14). In addition to being involved in the clearance of apoptotic cells, and thus maintenance of immune tolerance, C1q also has the ability to directly impact upon cell differentiation and proliferation, dendritic cell maturation, and synaptic pruning; functions that are not reliant on complement activation by C1q (15). Recently, involvement of C1q in pregnancy *via* its ability to modulate the endovascular (16) and interstitial invasion (17) of trophoblast cells in placenta has also been demonstrated. In addition, we have recently showed that C1q is present in several solid human tumor tissues and is involved in tumor progression (18).

The present study focused on the involvement of C1q in the proliferation and invasiveness of MPM. We found that C1q can bind to HA and acquires protumorigenic properties, leading to heightened adhesion, migration and proliferation of human mesothelioma cells (MES).

MATERIALS AND METHODS

Reagent and Antibodies

Hyaluronic acid was a kind gift from Prof. Ivan Donati, Department of Life Sciences, University of Trieste (19). C1q was either purified from fresh human serum following the procedure as described previously (20) or bought from Sigma-Aldrich (Milan, Italy). The recombinant globular head regions of the A, B, and C chains (ghA, ghB, and ghC, respectively) were expressed as fusion proteins linked to maltose-binding protein (MBP) in *Escherichia coli* BL21 and purified, as described previously (21). Poly-L-lysine, bovine serum albumin (BSA) and all reagents were from Sigma-Aldrich. The following antibodies were used: monoclonal antibody (mAb) mouse anti-human C1q was from Quidel (Quidel Corporation, San Diego, CA, USA), sheep anti-human C1q and anti-human C4 were purchased from The Binding Site (Bergamo, Italy). Mouse Monoclonal anti-C5b-9 antibody (aE11) was from AbCam. Mouse mAb anti-human von Willebrand factor (vWF), mouse mAb anti-human CD68, rabbit anti-human C1q, and goat anti-mouse-FITC F(ab)′ were purchased from Dako (Milan, Italy). Mouse mAb anti-human CD44-PE, mouse mAb anti-human CD45-PE-, or FITC-conjugated, unrelated mouse IgG1-PE- and FITC-conjugated were from Immunotools (Friesoythe, Germany). Cy3-conjugated $F(ab')_2$ goat anti-mouse IgG, and FITC-conjugated $F(ab')_2$ goat anti-rabbit IgG. Mouse mAb anti-human Mesothelin and rabbit anti-human Calretinin were from Santa Cruz Biotechnology (DBA, Milan, Italy). Mouse monoclonal anti-human Vimentin, goat anti-mouse IgG alkaline phosphatase (AP)-conjugated, anti-rabbit IgG-AP-conjugated, and anti-goat IgG-AP-conjugated were from Sigma-Aldrich.

Patients and Specimens

MPM patients who were diagnosed and followed up at the Department of Pneumology, University Hospital of Cattinara, Trieste, Italy, were enrolled for this study. None of the patients received chemotherapy or radiotherapy prior to sampling.

Patients (five male) with reported asbestos exposure underwent pleuroscopy for diagnosis of pleural effusion. All the procedures were performed under conscious sedation achieved by titration of intravenous midazolam and meperidine. Before the procedure, patients were placed in the lateral decubitus position with the pleural effusion uppermost and a bedside chest ultrasonography was used to determine the entry site. After the creation of the sterile field and injection of 2% lidocaine in the intercostal space in order to obtain local anesthesia, a 2-cm skin incision was made with a scalpel, then blunt dissection of the chest wall was performed using curved Kelly forceps down to the parietal pleural. Finally, a trocar was placed into the pleural

space and the pleuroscope (Karl Storz GmbH, Tuttlingen, Germany) was inserted to examine parietal and visceral pleura to obtain parietal pleural specimens using dedicated forceps. At the end of the procedure, pleuroscope and trocar were removed and a chest tube was inserted trough the chest wall.

Tissue samples from patients were collected after informed consent following approval of the ethical considerations by the Institutional Board of the University Hospital of Trieste, Italy.

Cell Isolation and Culture

Mesothelioma cells were isolated from pleural biopsy specimens. The tissue was finely minced with a cutter, incubated with a digestion solution composed of 0.5% trypsin (Sigma-Aldrich, Milan, Italy) and 50 µg/ml DNase I (Roche, Milan, Italy) in Hanks' Balanced Salt solution with $Ca^{2+}Mg^{2+}$ 0.5 mM (Sigma-Aldrich) overnight at 4°C. Next, the enzymatic solution was replaced with collagenase type 1 (3 mg/ml) (Worthington Biochemical Corporation, DBA) diluted in Medium 199 with Hank's salts (Euroclone Spa, Milan, Italy) for 30 min at 37°C. The digestion was blocked with 10% fetal bovine serum (FBS, GIBCO, Life Technology) and the cell suspension was filtered through a 100 µm pore filter (BD Biosciences, Italy).

The cells were seeded in a 12.5 cm^2 flask and cultured using Roswell Park Memorial Institute (RPMI) medium 1640 with GlutaMAX (Life Technologies, Milan, Italy), 45% human endothelial cells serum-free medium (HESF, Life Technologies), 10% heat-inactivated FBS supplemented with EGF (5 ng/ml), basic FGF (10 ng/ml), and penicillin–streptomycin (Sigma-Aldrich). Fresh medium was replaced every 2–3 days. MES were used at their five to eight passages for all the *in vitro* experiments.

Met5A cells were purchased from ATCC. These cells were grown in DMEM supplemented with 10% FBS and 1% antibiotic mixture (Sigma-Aldrich) and maintained at 37°C in humidified atmosphere with 5% CO_2.

Pleural Effusions

Malignant pleural effusions (MPEs) were obtained from patients who underwent thoracentesis after diagnosis of MPM in order to remove the exudative liquid filling pleural space. The surgery was performed within the Department of Pathologic Anatomy of the Hospital of Monfalcone (Gorizia, Italy). MPEs were immediately stored at 4°C for a maximum of 24 h before being processed. Approximately 1 Liter of MPE was centrifuged twice at 250 *g* for 10 min to remove the cells.

Dose-Determination of Soluble C1q

A 96-well plate (Corning Costar) was coated with sheep anti-C1q (1:6.000) diluted in carbonate/bicarbonate buffer (100 mM, pH > 9) and incubated overnight at 4°C. In order to avoid non-specific binding, the microtite wells were blocked with 2% skimmed milk (SM) in PBS and incubated for 2 h at 37°C. In the meanwhile, samples to be dose-titrated were prepared and then added to the wells in triplicate. A standard curve was prepared using a serial dilution of purified C1q (Sigma-Aldrich) from 50 to 1.56 ng/ml and the plate was incubated overnight at 4°C. Rabbit anti-human C1q (1:1,000) diluted in PBS + 0.5% SM + 0.05% Tween was incubated for 1 h at 37°C, followed by secondary probing with anti-rabbit IgG-alkaline phosphatase (AP) conjugate (1:20,000) for 30 min at 37°C. *p*-nitrophenyl phosphate (pNPP) was used as substrate, as described above, and the developed color was measured at 405 nm using the Titertek Multiskan ELISA Reader (Flow Labs).

Immunohistochemical Analysis

Tissue samples of different MPM histotypes were fixed in 10% buffered formalin and paraffin embedded. Sections of 4 µm in thickness were fixed with xylene, 100% EtOH, and 95% EtOH and then microwaved three times in Tris–HCl/EDTA pH 9.0 buffer (Dako, Milan, Italy) for 5 min and washed in Tris-buffered saline. After neutralization of the endogenous peroxidase with H_2O_2 (hydrogen peroxide) for 10 min, the sections were first incubated with PBS + 2% w/v BSA + 0.4% w/v Casein for 5 min in order to block the non-specific sites, and then probed with rabbit anti-human C1q (1:500) overnight at 4°C. The bound antibodies were revealed using the Vectastain Elite ABC horseradish peroxidase (HRP) kit (Vector Laboratories, DBA, Italy). Secondary antibodies were detected by 3-amino-9-ethylcarbazole (AEC) + high sensitivity Chromogen (Dako). The sections were counterstained with hematoxylin (Dako). Slides were examined under a Leica DM 3000 optical microscope and images were collected using a Leica DFC320 digital camera (Leica Microsystems, Wetzlar, Germany).

Alcian Blue Staining

After deparaffinizing and rehydrating, the sections were incubated with a solution of 1% Alcian blue dissolved in 3% Acetic acid, pH 2.5, for 30 min at RT. After washing in tap water for 10 min, the sections were dehydrated well in absolute alcohol and mounted. Images were acquired by the fluorescence microscope Leica DM 3000 using the Leica DFC320 camera.

Immunofluorescence Microscopy of MES

Mesothelioma cells cultured at confluence in an eight-chamber slide (BD Falcon) were fixed with FIX&PERM kit (Invitrogen, Life Technologies) for 15 min at RT. Incubation with primary antibodies (as listed earlier) was carried out for 1 h at RT. Cells were then washed and incubated with corresponding secondary antibodies (1:300) for 45 min at RT. The nuclei were stained with DAPI (Sigma-Aldrich). The glass was mounted with the Fluorescence Mounting Medium (Dako) and covered with a cover slip. Images were acquired by the fluorescence microscope Leica DM 3000 using the Leica DFC320 camera.

Flow Cytometry

Mesothelioma cells (5×10^5) were fixed with the fixation reagent FIX&PERM kit for 15 min at RT in dark and incubated with primary antibodies for 1 h at 37°C in a thermomixer (Eppendorf) at 800 rpm. Antibodies directed against intracellular antigens were diluted in permeabilization reagent of the FIX&PERM kit, while antibodies for cell surface antigens were diluted in PBS-1% w/v BSA. Incubation with secondary antibodies anti-mouse-FITC F(ab)′ (1:50) or anti-rabbit-FITC (1:300) was performed for 30 min on ice. Cells were suspended in 1% paraformaldehyde, the

fluorescence was acquired with the FACScalibur (BD Bioscience), and data processed using the software CellQuest.

Binding of C1q to MES

Mesothelioma cells were grown to confluence in 96-well tissue culture plates and incubated directly with increasing concentrations of purified human C1q or preincubated with increasing concentrations of HA, for 1 h at room temperature. Bound C1q was revealed by ELISA using mAb anti-human C1q (10 µl/ml) and alkaline-phosphatase-conjugated secondary antibodies (Sigma-Aldrich). The color, developed using pNPP (Sigma-Aldrich; 1 mg/ml) as a substrate, was read at 405 nm using a Titertek Multiskan ELISA reader (Flow Labs, Milano, Italy).

Coating Conditions

The microtiter wells were coated overnight at 4°C with HMW HA (50 µg/ml), C1q (20 µg/ml), ghA, ghB, ghC, or BSA (as a negative control; Sigma-Aldrich) diluted in 100 mM carbonate/bicarbonate buffer, pH 9.6. C1q was allowed to bind (25 µg/ml) to HA in PBS + 0.5% BSA, 0.7 mM $CaCl_2$, and 0.7 mM $MgCl_2$, overnight at 4°C.

Adhesion Assay

1×10^5 mesothelial cells or MES, labeled with the fluorescent dye FAST DiI (Molecular Probes, Invitrogen), were re-suspended in HESF (Life Technologies) containing 0.1% BSA (HESF + 0.1% BSA; Sigma), preincubated with 10 µM of ERK (#SCH772984, Selleckchem), JNK (#SP600125, SIGMA-Aldrich), or p38 (#SB203580, Selleckchem) inhibitors for 30 min at RT and then added to a 96-well plate (wells were coated as described above) for 35 min at 37°C in 5% v/v CO_2 incubator. Then, the unbound cells were removed and the adherent cells were lysed with 10 mM Tris–HCl, pH 7.4 + 0.1% v/v SDS. The plate was read *via* Infinite200 (544 nm, emission 590 nm) (TECAN) using a calibration curve generated through an increasing number of labeled cells.

Cell Proliferation

The cell proliferation assay was performed using Click-iT® Plus EdU Proliferation Kits (ThermoFisher). 5×10^3 MES were re-suspended in HESF + 0.1% BSA medium and seeded to a 96-well plate, which was earlier coated with C1q, HA or C1q + HA, as described above. Following adhesion, cells were incubated with 15 µM analog EdU nucleotide (5-ethynyl-2-deoxyuridine) for DNA incorporation during replication. Cells were then incubated for 24 h at 37°C, fixed, and set up for a marking reaction by azide Oregon-Green 488. The signal amplification step included the incubation with antibody anti-Oregon-Green conjugated with HRP that reacts with the substrate, Amplx UtraRed, and produces a bright response that beams fluorescence around red. The fluorescence was analyzed by TECAN (Tecan, Milan, Italy) in the excitation/emission range of 535/595 nm.

Apoptosis

Mesothelioma cells grown without serum, were suspended in 0.1% w/v BSA in HEFS, and 2×10^4 cells/well were seeded on precoated plates. The cells were left to adhere for 1 h at 37°C, then incubated with 500 µM of H_2O_2 for 6 h, before adding 5 µM of CellEvent™ Caspase-3/7 Green Detection Reagent (Life Technologies), a fluorogenic substrate for activated caspases 3 and 7.

Migration Assay

FAST DiI-labeled (Molecular Probes, Invitrogen, 1:100) MES (2×10^5 cells) were resuspended in 0.1% w/v BSA in HEFS and added to the upper chamber of a transwell system. The cells were allowed to migrate through HTS FluoroBlok systems with polycarbonate membranes of 8 µm pore size (Falcon) coated on the lower side, as described above. The plate was read using Infinite200, as described above.

Scratch Assay

Confluent monolayers of MES (2×10^5) were seeded in HESF + 0.1% BSA medium in 24-well plate. A scratch was placed in the middle of the well with a sterile 200 µl pipette tip. Subsequently, HA (50 µg/ml) or HA + C1q (20 µg/ml) were added to the wells. Cells incubated with 10% v/v FBS and as negative control MES were cultured in HESF/BSA (0.1%) medium without stimuli. Images were acquired by phase-contrast microscope (Leica).

Phosphorylation of ERK, SAPK/JNK, and p38 in MES

Pathway analysis was performed as per the manufacturer's instructions of the PathScan® Intracellular Signaling Array Kit (Fluorescent Readout) (#7744; Cell Signaling Technology, EuroClone, Milan, Italy). Briefly, 24 h serum-starved MES (1.8×10^6 cells) were left to adhere to HA, or HA-bound-C1q, as described above for the indicated periods of time at 37°C. Then, the cells were washed with ice-cold 1× PBS and lysed in 1× ice-cold Cell Lysis buffer containing a cocktail of protease inhibitors (Roche Diagnostics). The Array Blocking Buffer was added to each well and incubated for 15 min at RT. Subsequently, an equal amount of total lysate (0.8 mg/ml) was added to each well and incubated for 2 h at RT. After washing, the biotinylated detection antibody cocktail was added to each well and incubated for 1 h at RT. Streptavidin-conjugated DyLight 680 was added to each well and incubated for 30 min at RT. Fluorescence readout was acquired using the LI-COR Biosciences Infrared Odyssey imaging system (Millennium science) and data processed by the software Image studio 5.0.

Detection of the Interaction between Human C1q (and Its Recombinant Globular Head Modules) and HA

The microtiter wells were coated overnight at 4°C with either 50 µg/ml HA of different MWs diluted in carbonate/bicarbonate buffer (100 mM, pH 9.6). The blocking step with PBS + 1% BSA (2 h at 37°C) was followed by incubation with an increasing concentration of human C1q or the recombinant globular head modules (ghA, ghB, and ghC) of human C1q in PBS-$Ca^{2+}Mg^{2+}$ (0.7 mM) containing 0.5% BSA (PBS-CaMg-0.5% BSA) overnight at 4°C. Bound C1q was detected with sheep anti-human C1q polyclonal antibodies whereas bound ghA, ghB, and ghC were detected with mouse anti-MBP (1 h at 37°C). The binding

of anti-C1q was detected using anti-goat IgG-AP conjugate, whereas the anti-MBP binding was detected using anti-mouse IgG-AP conjugate for 30 min at 37°C. The phosphatase substrate, pNPP (Sigma-Aldrich) was dissolved in 0.1 M *glycine buffer* containing 1 mM $MgCl_2$, 1 mM $ZnCl_2$, pH 10.4 at a concentration of 1.5 mg/ml. The absorbance was measured at 405 nm with the Titertek Multiskan ELISA Reader (Flow Labs).

Evaluation of Complement Activation

Microtitre wells in a 96-well plate were coated with HA (50 µg/ml) or IgG (10 µg/ml), as described above. Non-specific binding sites were blocked with PBS-1%BSA for 1 h at 37°C, and then incubated with 20 and 50 µg/ml C1q diluted in PBS-CaMg-0.5%BSA for 1 h at 37°C. Subsequently, the wells were incubated with pooled normal human serum (1:100) as a source of complement components in PBS-CaMg-0.5%BSA and incubated for 30 min at 37°C with gentle shaking. C9 neoantigen detection was performed using the murine mAb aE11 against C9 neoantigen (kindly provided by Prof. T. E. Mollnes, Oslo, Norway) and incubated for 1 h at 37°C. The AP-conjugated anti-goat IgG (Sigma-Aldrich) or anti-mouse IgG (Sigma-Aldrich), used as secondary antibodies, were incubated 30 min at 37°C. pNPP (Sigma) was dissolved in glycine buffer at the concentration of 1.5 mg/ml. The absorbance was measured at 405 nm with the Titertek Multiskan ELISA Reader (Flow Labs).

Statistical Analysis

Data were analyzed using Two-way ANOVA, Tukey–Kramer test, and unpaired two-tailed Student's *t*-test or one-way ANOVA with Bonferroni corrections. Results were expressed as mean ± SEM. Non-parametric data were assessed by Mann–Whitney *U* tests and the results were expressed as median and interquartile range. p values < 0.05 were considered significant. All statistical analyses were performed using Prism 6 software (GraphPad Software Inc., La Jolla, CA, USA).

RESULTS

C1q Is Present in Malignant Pleural Mesothelioma Specimens

We initially looked for the presence of C1q in a panel of invasive MPM specimens, including epithelioid, biphasic, and sarcomatoid (**Figure 1A**) histotypes. As shown in **Figure 1**, a strong positivity for C1q was detected in all tumor specimen types examined, particularly in epithelioid histotype.

Within the mesothelioma microenvironment, C1q was mainly expressed by monocytoid cells suggestive of tumor-infiltrating myeloid elements (shown by arrows in the upper panels) and in the small vessels, as indicated by the black triangles of the lower panels in **Figure 1B**. C1q was also diffusely present in the tumor stroma and associated with the cell membrane of tumor cells. Immunohistochemical controls of C1q are shown in **Figure 2**. The presence of C1q was also detected in the three pleural exudate by a quantitative ELISA assay. We found out that the concentration of C1q was found to be about 76 µg/ml (±8 µg/ml), approximately two- or threefold lower than our control serum (about 200 µg/ml).

Binding of C1q to HA does not Activate the Complement Classical Pathway

Having shown that C1q is abundantly present in the mesothelioma microenvironment, we investigated the ability of C1q to interact with ECM components. We focused our attention to HA which is abundantly present in mesothelioma tissue (22). The presence of HA is clearly evident in **Figure 3**, where we show sections obtained from epithelioid and a biphasic mesothelioma tissue stained with Alcian blue.

We previously demonstrated that C1q is able to bind to a range of target ligands present in the ECM; this interaction is particularly strong with HA (17). We confirmed by ELISA the ability of C1q to bind to HA in a manner similar to IgG (**Figure 4A**). We also analyzed the binding of C1q to HA of different molecular weights (**Figure 4B**). Our results indicated that there were no statistically significant differences in C1q binding to low and high MW-HA. Furthermore, we evaluated the capability of HA-bound C1q to activate the complement classical pathway, by measuring the C4 and C9 (neoantigen) (C9 neo) deposition by ELISA. As shown in **Figures 4C,D**, only C1q bound to IgG, and not HA-bound C1q, induced complement activation, and therefore, C4 deposition and C9-neoantigen formation. In order to localize the C1q interaction with HA, we analyzed the binding of recombinant forms of individual globular head modules (ghA, ghB, and ghC) to HA. Our results indicated that the globular head of C1q A chain (ghA) bound to HA better than ghB and ghC (**Figure 4E**), suggesting a differential and modular nature of the interaction between the gC1q domains and HA.

Isolation and Characterization of Primary Tumor Cells from MPM Biopsies

Having established that C1q is present in the MPM microenvironment and that it can bind to HA, we sought to investigate the implication of its presence in MPM biology. Therefore, we isolated MES from a portion of the resected malignant pleura, obtained during diagnostic pleuroscopy, from five patients with epithelioid MPM. We compared the MES morphology with Met5A, a commercial, immortalized mesothelial cell line, commonly used as a model of healthy cells. MES had mainly an elongated and filamentous shape and were very heterogeneous and multishaped (**Figure 5A**). It is possible to notice that there are also some polygonal and more regular cells in culture, which seem to resemble the epithelial phenotype of Met5A. Generally, they had an abundant cytoplasm in which vacuoles or granules were often present, transforming themselves in signet-ring cells.

We characterized MES for the expression of typical mesothelial markers, such as mesothelin, calretinin, CK8-18, and CD44 by immunofluorescence microscopy. The cells were also positive for vimentin, a marker of mesenchymal cells (**Figure 5B**). MES were positive for the above-mentioned markers. To assess the

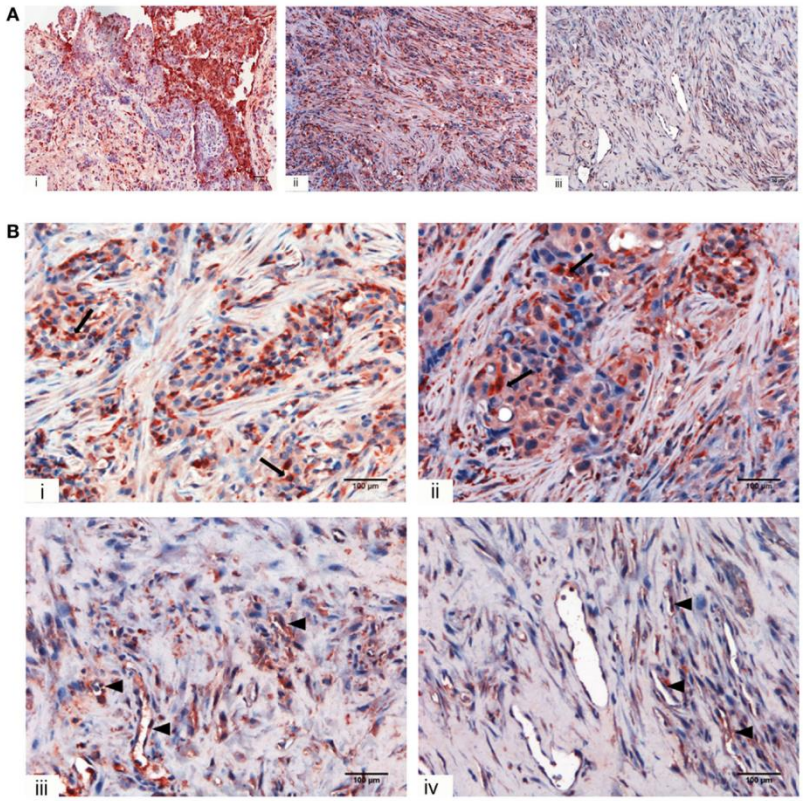

FIGURE 1 | Immunohistochemical analysis for C1q in human mesothelioma. **(A)** Representative microphotographs showing expression of C1q in different malignant pleural mesothelioma (MPM) histotypes: epithelioid (i), biphasic (ii), and desmoplastic (iii). Streptavidin–biotin–peroxidase complex system with 3-amino-9-ethylcarbazole (AEC) (red) chromogen; scale bars, 50 μm. **(B)** Representative microphotographs showing the expression of C1q in tumor-associated stroma of mesothelioma. Highlighted are monocytoid cells suggestive of tumor-infiltrating myeloid elements (arrows) and neovascular endothelial cells (arrow heads). Streptavidin–biotin–peroxidase complex system with AEC (red) chromogen; scale bars, 100 μm.

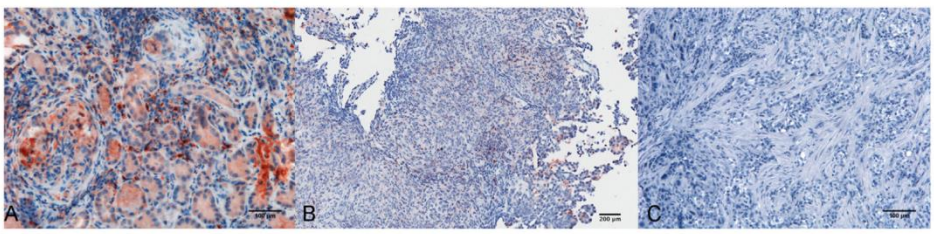

FIGURE 2 | Immunohistochemical controls for C1q. Representative microphotographs showing the immunohistochemistry controls: positive control tissue, lupus nephritis **(A)**, scale bar, 100 μm; negative control tissue, pleural benign cyst **(B)**, scale bar, 200 μm; negative control reaction, biphasic mesothelioma **(C)**, scale bars, 100 μm. Streptavidin–biotin–peroxidase complex system with 3-amino-9-ethylcarbazole (AEC) (red) chromogen.

purity of isolated primary cells, we performed immunophenotypical staining against the classical leukocyte antigen CD45 to avoid the presence of contaminating leukocytes. Furthermore, we also found that MES cells were negative for vWF, a common marker used to detect endothelial cells. Interestingly, all MES were positive for CD68, a mature macrophage marker, although they were negative for CD14. Some of these markers were also analyzed by FACS (**Figure 5C**; **Table 1**).

IHC-positive staining for C1q in MPM tissues suggested that C1q may be produced locally. In this regard, C1q expression

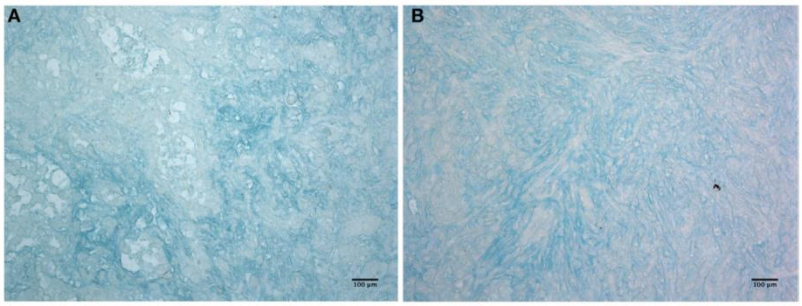

FIGURE 3 | Histochemistry of hyaluronic acid on malignant pleural mesothelioma (MPM). Alcian blue staining highlights hyaluronic acid of epithelioid **(A)** and biphasic **(B)** malignant mesothelioma sections. Scale bars, 100 µm.

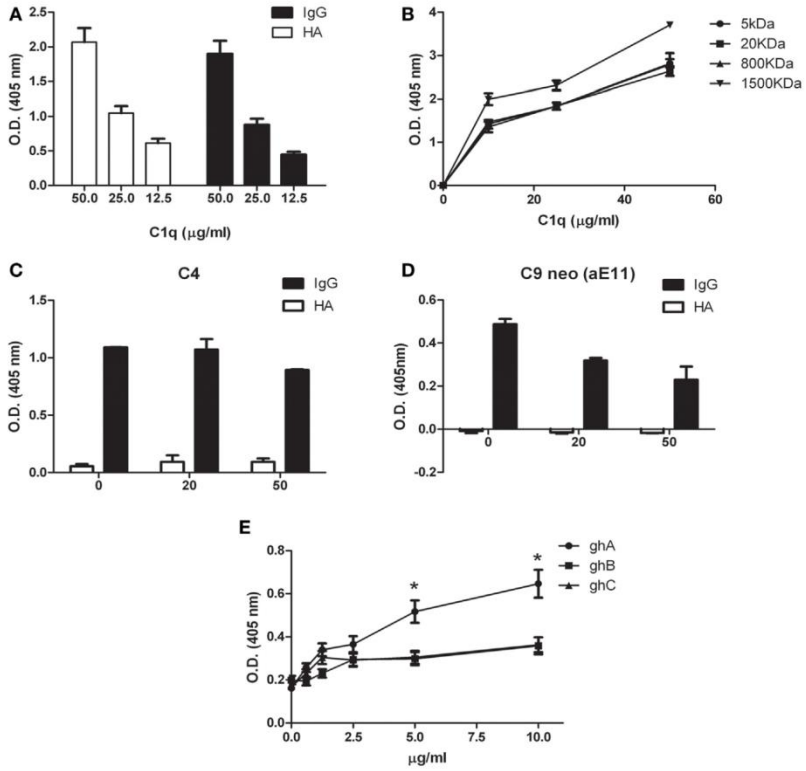

FIGURE 4 | Interaction of C1q with hyaluronic acid. **(A)** C1q interaction with high-molecular-weight (HMW) hyaluronic acid (HA) and IgG (positive control) by ELISA. Microtiter wells coated with 50 µg/ml HMW HA or 10 µg/ml IgG were incubated with an increasing concentration of C1q; HA-bound C1q was revealed with anti-C1q antibodies. C1q bound HA with an affinity similar to IgG. The data are expressed as mean of three independent experiments in triplicates ± SEM. **(B)** Binding of C1q to different MW HA. Microtiter wells coated with 50 µg/ml HMW-HA (or 5, 20, 800, or 1,500 kDa HA) were incubated with increasing concentration of C1q and bound C1q was revealed with anti-C1q antibodies. No statistically significant difference was observed between the binding of C1q to low and high MW-HA was observed. The data are expressed as mean of three independent experiments carried out in triplicates ± SEM. **(C–D)** Evaluation of the ability of C1q bound to HA to activate the classical pathway of the complement system. Microtiter wells coated with 50 µg/ml HMW HA, or 10 µg/ml IgG were incubated with 20 and 50 µg/ml C1q. Pool of normal human sera (1:100) was added as a source of complement components and the deposition of C4 **(C)** and the formation of C9-neoantigen (C9 neo) **(D)** were revealed by using specific antibodies against C4 and C9 neoantigen (mAb aE11) by ELISA. The data are expressed as mean of three independent experiments carried out in triplicates ± SEM. **(E)** Dose response curve of the binding of ghA, ghB, and ghC to HMW HA. Microtiter wells were coated with 50 µg/ml HMW HA. The wells were then incubated with increasing amounts (0–10 µg/ml) of recombinant C1q globular head modules (ghA, ghB, ghC). The binding was revealed using anti-MBP antibody. The data are expressed as mean of three independent experiments done in triplicates ± SEM.

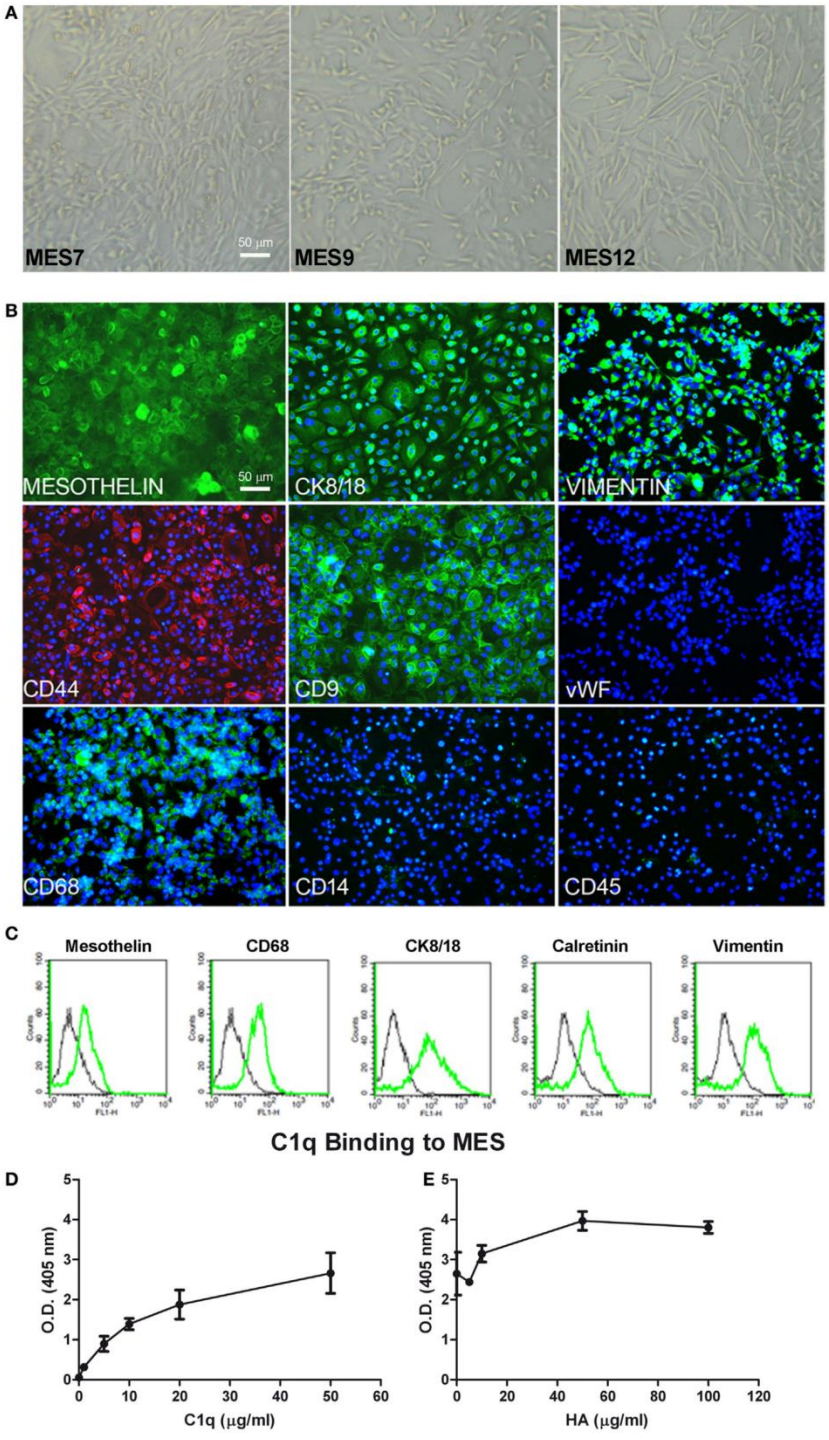

FIGURE 5 | Continued

FIGURE 5 | Continued
Characterization of mesothelioma cells (MES). **(A)** Morphological features of the three different populations of MES (MES7, MES9, and MES12) isolated from malignant pleural mesothelioma (MPM) biopsies. Images were acquired by phase-contrast microscope, Leica original magnification: 200×. **(B)** Mesothelial cells were characterized by immunofluorescence for the expression of mesothelin, CK 8/18, vimentin, CD9, CD68 (green), and CD44 (red). Mesothelioma cells were grown to confluence in eight-chamber culture slides. After fixation and permeabilization, the cells were stained with mAb anti-human mesothelin, CK 8/18, vimentin, CD9, von Willebrand factor (vWF), CD68, and CD14, followed by anti-mouse-FITC F(ab)′ secondary antibodies or mAb anti-human CD45 and mAb anti-human CD44-PE conjugate. Nuclei were stained blue by DAPI: original magnification 200×. **(C)** The expression of mesothelin, CD68, CK8/18, calretinin, and vimentin was confirmed by FACS. The expression of these markers (green lines) was compared with appropriate control antibodies (black lines). **(D)** Binding of C1q to MES**.** Tumor cells grown to confluence on 96-well tissue culture plates were incubated with increasing concentrations of purified C1q for 1 h at room temperature and the bound C1q was revealed by ELISA. **(E)** The binding of 25 μg/ml C1q to MES was detected preincubating the cells with increasing concentration of hyaluronic acid (HA). Bound C1q was revealed by ELISA as described above. The data are presented as mean ± SEM of three separate experiments.

TABLE 1 | Marker expression evaluated by FACS analysis on cells isolated from five different epithelioid mesothelioma tumors.

Marker	MES7	MES9	MES12	MES13	MES14
Mesothelin	+	+	+	+	+
Vimentin	++	++	+	+	+
CK 8/18	++	Nd	+	+	+
Calretinin	+	Nd	−	+	+
vWF	−	−	−	Nd	−
CD68	++	+	+	+	+
CD45	−	−	−	−	−
CD44	++	+	Nd	Nd	++

Data refer to cells between the third and the fifth passage in culture. ++ = positivity (>50%), + = positivity (<50%), − = negativity, Nd = not done.

was evaluated at both mRNA and protein levels in healthy (Met5A) and tumor MES. We performed qPCR for three C1q chains (*C1qA*, *C1qB*, and *C1qC*); none were positive in five different cell populations (data not shown). Interestingly, C1q was found to bind strongly to the surface of MES (**Figure 5D**) and the extent of binding increased in the presence of HA being highest at the concentration of 50 μg/ml of HA (**Figure 5E**). To investigate the role of bound C1q on complement activation, we incubated C1q-bearing cells with AB+ human serum and analyzed the cells for the presence of C4 and C9 neoantigen on their surface. We failed to detect both complement components suggesting that binding of C1q to MES is not associated with complement activation.

C1q Promotes MES Adhesion and Spreading

To evaluate the ability of C1q to interact with MES, we performed a cell adhesion assay using immobilized C1q. MES (four different populations) and Met5A cells were labeled with the fluorescent probe FAST DiI and seeded on to immobilised C1q, HA or HA-bound-C1q; BSA was used as a negative control protein. Met5A cells were able to adhere to HA, and to a less extent, to C1q or HA-bound-C1q (**Figure 6A**). In contrast, MES showed greater adherence to HA; HA-bound-C1q was able to enhance MES adhesion considerably compared to HA alone (**Figure 6B**). All four MES populations showed the same behavior on HA-bound-C1q, although MES adhesion to C1q alone varied considerably between patients' samples (**Figure 7**).

The analysis of the adherent MES by phase-contrast optical microscopy revealed that a high proportion of the cells seeded on to C1q or HA-bound-C1q were spread out, in contrast to the round morphology exhibited by those attached to HA or BSA (**Figure 6C**). In order to understand which module of the globular domain of C1q was mainly involved in MES adhesion, MES were stained with Fast DI and allowed to adhere to C1q, HA or recombinant globular heads (ghA, ghB, ghC) for 30 min. As shown in **Figure 6D**, the interaction of the cells with C1q seems to be mediated by ghC, and to a lesser extent, ghB. The cells did not seem to interact with ghA.

Since both HMW-HA and LMW-HA are present in the tumor microenvironment, we investigated the adhesion of MES to LMW-HA alone or in combination with C1q and we compared the results with the adhesion to HMW-HA with or without C1q. We did not observe any statistical difference between the MES adhesion to LMW or HMW-HA (**Figure 6E**).

C1q Promotes MPM Tumor Progression by Favoring MES Proliferation and Migration

We investigated whether C1q might contribute to tumor growth by stimulating the proliferation of MES. Thus, MES were seeded on to solid phase C1q, HA, or HA-bound-C1q and the number of proliferating cells were evaluated using the Click-iT® EdU Microplate Assay. Our results indicated that HA-bound C1q was able to enhance the proliferation rate of MES (**Figure 8A**), compared to HA or C1q alone.

C1q-induced migration of labeled MES was examined by monitoring cell migration from the upper chamber through an insert coated with C1q, or HA-bound-C1q. C1q (60%) was found to be more effective than HA (~20%), in effecting migration (**Figure 8B**). In this assay, we did not observe a synergistic effect of the double matrix (HA-bound-C1q). In fact, the percentage of the cell migration due to HA + C1q was comparable to that observed with C1q alone.

The effect of C1q on the cell migration was also analyzed using a scratch wound healing assay, monitoring the mobilization of MES toward the scratched area for 18 h. As shown in **Figure 9**, MES stimulated by C1q started to enter the scratched area and migrated farther than cells exposed to HA after 18 h.

In order to investigate whether C1q was able to protect MES from apoptosis, serum-starved MES were allowed to adhere on to the wells, coated with HA or HA-bound-C1q, and then incubated with 500 μM H_2O_2 for 6 h. Subsequently, the activation of caspases 3 and 7 was detected using a fluorogenic substrate. As shown in the graph in **Figure 8C**, the fluorogenic units of the MES on HA treated with H_2O_2 was double, compared to the untreated cells.

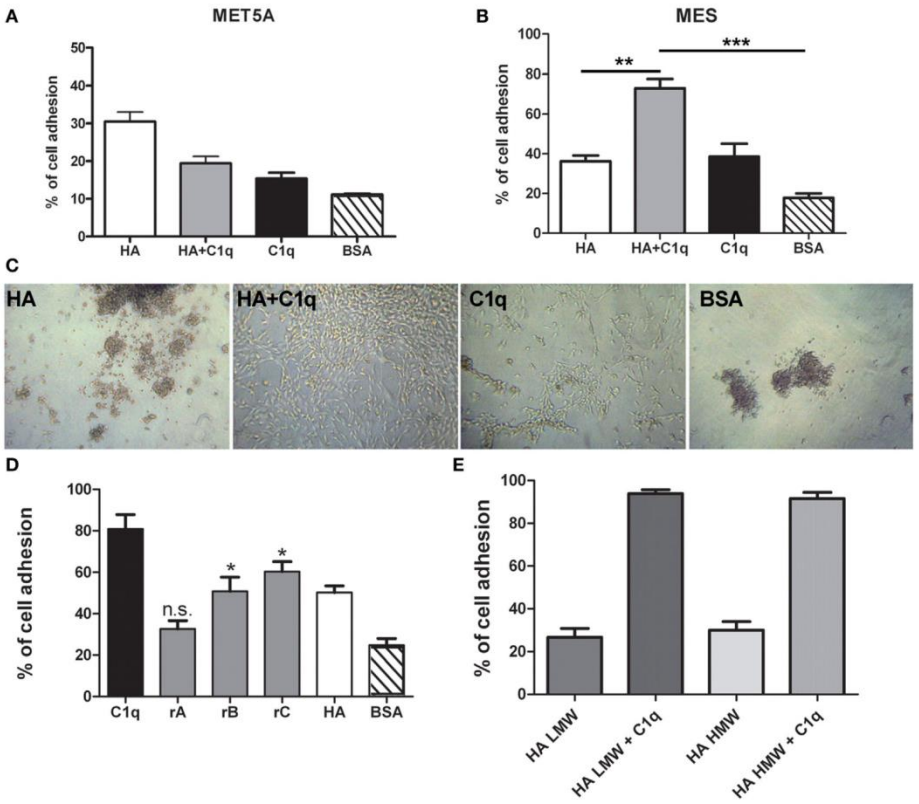

FIGURE 6 | Effect of C1q on mesothelioma cells (MES) adhesion. Mesothelial cells (Met5A) **(A)** and four different populations of MES **(B)** were labeled with the fluorescent dye FAST DiI and allowed to adhere to microtiter wells precoated with hyaluronic acid (HA), C1q, HA-bound-C1q, or bovine serum albumin (BSA). The data are expressed as mean of four independent experiments done in triplicates ± SEM. Cell adhesion was measured after 35 min. Results are expressed as percent of adhesion with reference to a standard curve established using an increasing number of labeled cells. **(C)** Morphological aspect of one representative primary cell line adhered to HA, C1q, HA-bound-C1q, or BSA. Images were acquired *via* phase-contrast microscopy, original magnification: 200×. **(D)** MES cells were labeled with the fluorescent dye FAST DiI and allowed to adhere to microtiter wells precoated with C1q, ghA, ghB, ghC, high molecular weight (HMW)-HA, or BSA. The data are expressed as mean of four independent experiments carried out in triplicates ± SEM. **(E)** MES were labeled with the fluorescent dye FAST DiI and allowed to adhere to microtiter wells precoated with HMW-HA, HMW-HA + C1q, low molecular weight (LMW)-HA, or LMW-HA + C1q. The data are expressed as mean of four independent experiments carried out in triplicates ± SEM.

Surprisingly, MES adhering to C1q or HA-bound-C1q were not protected from apoptosis induced by oxidative stress (**Figure 8C**).

C1q Enhances ERK1/2, SAPK/JNK, and p38 Phosphorylation in MES Cells

To further elucidate the mechanism of the cell activation, we analyzed the signaling pathways likely to be involved in tumor cell adhesion, migration and proliferation. We examined more specifically the activation of three members of the MAPK family, ERK1/2, SAPK/JNK, and P38 signaling molecules.

Serum-starved MES were allowed to adhere to wells coated with HA or HA-bound-C1q, for 5 or 20 min and the phosphorylation status of ERK1/2, SAPK/JNK, and P38 was evaluated by immunofluorescence using PathScan® Intracellular Signaling Array Kit (Cell Signaling Technology). As shown in **Figures 10A–C**, binding of MES to HA-bound-C1q resulted in the activation of all the signaling molecules, which was clearly seen at 20 min post stimulation for all pathways and the signal was significantly higher in the cells adhering to C1q bound to HA than in cells adherent to HA only. All three MAPK inhibitors tested in the adhesion assay proved to be effective in reducing significantly the cell adhesion to C1q bound to HA (**Figure 10D**).

DISCUSSION

C1q is expressed in the stroma and vascular endothelium of a number of human malignant tumors, including adenocarcinomas of colon, lung, breast, and pancreas. In a murine model of melanoma, C1q was found to promote cancer cell adhesion, migration and proliferation (18). Thus, as a pro-tumorigenic

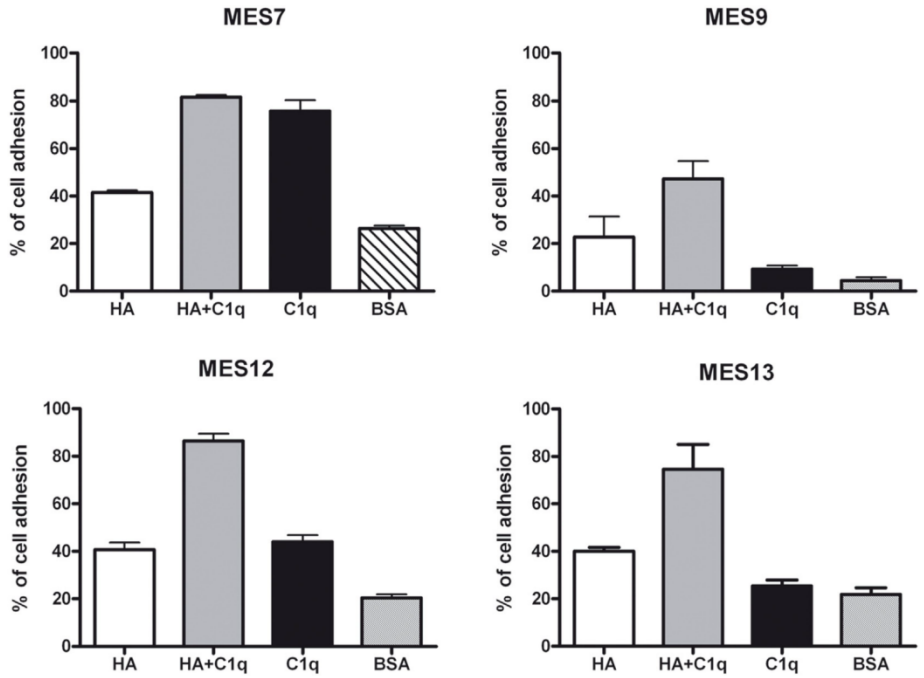

FIGURE 7 | Effects of C1q on mesothelioma cells (MES) adhesion. Four different populations of MES were labeled with the fluorescent dye FAST DiI and allowed to adhere to microtiter wells precoated with hyaluronic acid (HA), C1q, HA-bound-C1q, or bovine serum albumin (BSA). The results of each independent experiment, done in triplicates ± SEM are shown in order to highlight differential behavior of these cells. Cell adhesion was measured after 35 min. The results are expressed as percent of adhesion with reference to a standard curve established using an increasing number of labeled cells.

soluble factor, C1q can promote tumor progression by facilitating cancer cell seeding and angiogenesis. Here, we investigated the presence and the role of C1q in MPM for a number of reasons. MPM is an aggressive neoplasm with a poor prognosis, because it is resistant to chemotherapy and radiotherapy. Therefore, studying the microenvironment of this tumor can help devise novel therapeutic strategies. In this study, we particularly focused our attention on the interaction between C1q and HA and its implication on adhesion and proliferation of MPM cells. Understanding this C1q-HA interaction is of great importance given a unique expression pattern of C1q in mesothelioma tissues and a great relevance of HA in the biology of the MPM.

IHC revealed that C1q was present in all the histological variants examined and it seemed primarily associated with monocytoid cells, indicating that these cells might be the main source of C1q locally. C1q was also diffusely present in the tumor stroma and associated with the cell membrane of tumor cells mainly of the epithelioid histotype. This pattern of expression is similar to that in other solid tumors (18) and is reminiscent of its distribution in human decidua (17). There were also areas in which C1q could be found associated with small vessels, raising the possibility that C1q might exhibit a proangiogenic activity in this context, similar to that in wound healing (23).

We first investigated the interaction of purified human C1q with HA since MPM is associated with a high level of production of HA (24). HA is highly expressed in MPM because it is responsible for the lubrication of the pleural membranes and is secreted by the mesothelial cells (25). Here, we demonstrated that HA is abundantly present in MPM tissues, confirming an earlier study (22). HA has previously been shown to promote proliferation and migration of MPM cells through its interaction with hyaluronan receptor (26). We have previously shown that C1q can interact with HA (17). Here, we showed that C1q can bind to HMW-HA, and as expected, this binding does not induce complement activation. The interaction between C1 and HA has been studied in the past mainly considering its anti-complement activity (27, 28). The interaction of C1q with synovial HA in rheumatoid arthritis has been previously reported (29); however, C1q binds synovial antibodies that are covalently coupled to HA. Heated and then lyophilized HA binds C1q (and a range of complement components) better that native HA, probably *via* polyanionic charges (30). A comparable binding activity was also observed for LMW-HA, whose local accumulation can be detected in the tumor microenvironment as a consequence of enhanced synthesis and turnover of HMW-HA. Since LMW-HA, but not HMW-HA, can stimulate a number of biological processes (31, 32), it is likely that C1q can interfere with several functions

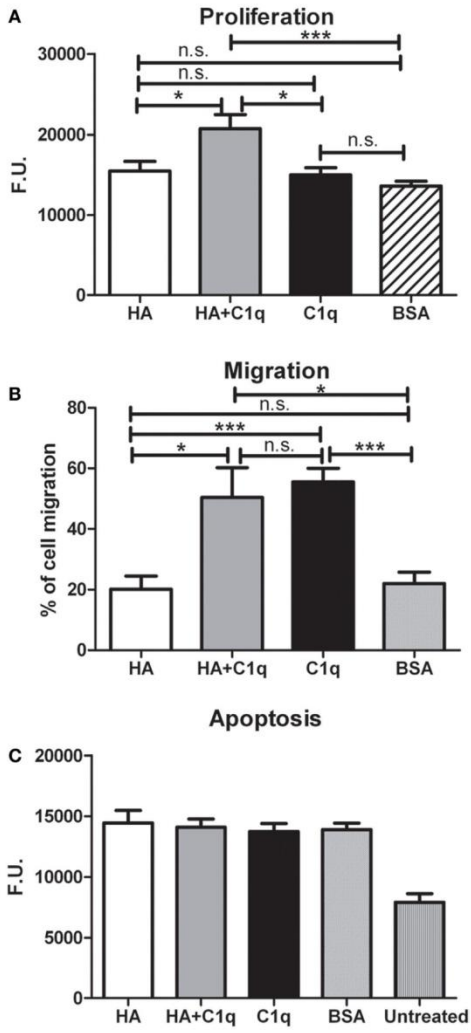

FIGURE 8 | Effects of C1q on mesothelioma cells (MES) migration, proliferation, and apoptosis. **(A–C)** The experiments of cell migration, proliferation and apoptosis were performed as detailed in Section "Materials and Methods." **(A)** MES proliferation. MES were seeded in wells precoated with hyaluronic acid (HA), C1q, HA-bound-C1q, or bovine serum albumin (BSA) and the number of proliferating cells was evaluated using the Click-iT® EdU Microplate Assay. **(B)** FAST DiI-labeled MES were allowed to migrate through a trans-well system polycarbonate membranes coated on the lower side with HA, HA-bound-C1q, C1q, or BSA. **(C)** Serum-starved MES cells were seeded in the wells precoated with HA, C1q, HA-bound-C1q, or BSA and incubated with H_2O_2. Apoptotic cells were ascertained by CellEvent™ Caspase-3/7 (Life Technologies). Data from at least five independent experiments are presented as mean ± SEM.

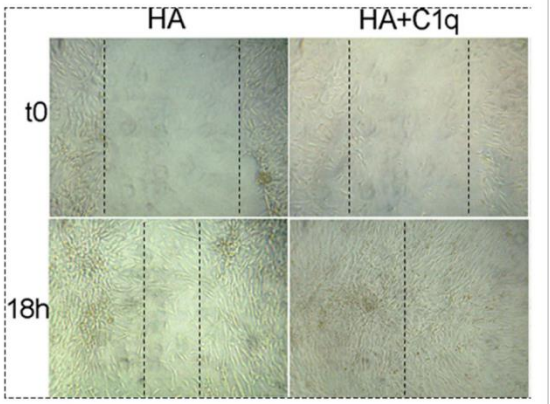

FIGURE 9 | Effects of C1q on mesothelioma cells (MES) migration. For wound healing assays MES (2×10^5) were seeded in HESF + 0.1% BSA medium in 24-well plate and grown to 90–95% confluence. A scratch was placed in the middle of the well with a sterile 200 µl pipette tip. Subsequently, hyaluronic acid (HA) (50 µg/ml) or HA + C1q (20 µg/ml) were added to the wells. The invasion was evaluated in three separate experiments performed independently. The results of a representative experiment are shown. Images were acquired by phase-contrast microscope, Leica original magnification: 200×.

mediated by HA, such as angiogenesis and inflammation. To dissect the functional contribution of each chain within the heterotrimeric globular domain of C1q, we investigated the binding properties of the recombinant ghA, ghB, and ghC modules. Our results demonstrated that the ghA module was the best binder of HA.

The proadhesive properties of C1q that we demonstrated *in vitro* for murine melanoma cells (18) were also evident for MES. In this study, we made a significant step forward since we were able to test several populations of MES isolated directly from human patients. Here, we demonstrated that the effects mediated by C1q-bound-HA were different from that observed for HA or C1q alone in terms of the number of adhering cells as well as morphology indicating that the presence of C1q can considerably modify the tumor microenvironment. The proadhesion effect of C1q seems to be restricted to the cells isolated from primary tumors while Met5A cells, which are representative of non-tumor mesothelium, adhere better to HA, compared to the adhesion on C1q-bound-HA or C1q alone. These data indicate that C1q can exert differential effects depending on the cell types and probably expression of putative receptors. Among various C1q receptors gC1qR, also called HA-binding protein-1, is an interesting molecule for its ability to bind both the gC1q domain of C1q and HA. Furthermore, CD44, the main receptor for HA, has been described as a possible docking signaling molecule for the interaction with gC1q (33). The nature and consequences of interaction between these cellular receptors and C1q-bound-HA is currently under investigation. Another interesting observation is that the adhesion of MES to C1q is predominantly mediated *via* the ghC module. Since ghA is the preferential binder to HA, the gC1q domain can act as a bridging molecule for anchoring the tumor cells to the ECM. C1q-bound-HA was able to promote the growth and the migration of MES *in vitro* confirming our previous results (18), obtained with B16/F10 murine cells and C1q bound to

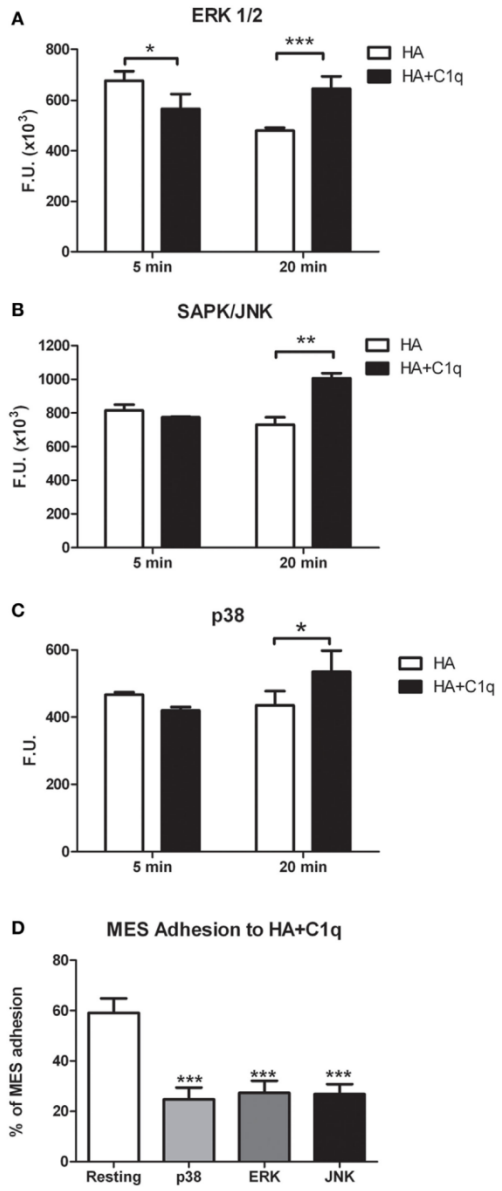

FIGURE 10 | Phosphorylation of ERK1/2, SAPK/JUNK, and p38 in mesothelioma cells (MES). **(A–C)** MES were allowed to adhere to hyaluronic acid (HA) or HA-bound-C1q and the phosphorylation status of ERK1/2, SAPK/JUNK, and p38 was evaluated using total cell lysates with PathScan Antibody Array Kit (Cell Signaling), as described in the Section "Materials and Methods." Data from at least three independent experiments are presented as mean ± SD. $^{*}p < 0.05$, $^{**}p < 0.01$, $^{***}p < 0.001$ (Student's *t*-test). **(D)** Three different populations of MES were labeled with the fluorescent dye FAST DiI, preincubated for 30 min at 37°C with P38, ERK, or JNK inhibitors and then allowed to adhere to microtiter wells precoated with HA-bound-C1q. The data are expressed as mean of three independent experiments done in triplicates ± SEM. $^{***}p < 0.001$ vs. resting.

fibronectin. The finding that C1q alone did not exert a significant proliferating effect on MES seen previously on melanoma cells may be explained by differential response of cells derived from various tumors to C1q. It is also important to emphasize that this study was carried out on primary cells, which were freshly isolated from patients.

The activation of three members of the MAPK family, ERK1/2, SAPK/JNK, and p38 in this study is also consistent with the previously reported study (17).

That C1q can act as a tumor promoting factor in MPM confirms our recent data (18). In addition, Winslow et al. have observed that the three chains of C1q were highly expressed in the stroma of breast cancers with poor prognosis (34). On the contrary, Hong et al. reported that C1q is involved in the regulation of cancer cell survival and progression sustaining the activation of the tumor suppressor *WW-domain containing oxidoreductase* (WOX1). C1q downregulation enhanced prostate hyperplasia and tumorigenesis because of the lack of WOX1 activation (35). Recently, Kaur et al. have reported that C1q, *via* its gC1q domain, induced apoptosis in an ovarian cancer cell line SKOV3 *via* TNF-α induced apoptosis pathway involving upregulation of Bax and Fas (36). These contrasting observations appear to suggest that the function of C1q in the biology of the tumor is complex and is strongly dependent on the microenvironment. Our hypothesis is that C1q can be locally produced by non-tumor cells and can interact differentially to the different ECM components present in the tumor microenvironment. The presence of C1q or C1 in soluble phase or bound to the ECM can provide different stimuli to the tumor cells present in the microenvironment.

In conclusion, C1q is abundantly present in mesothelioma tissue, interacts with HA, and interferes with adhesion, migration and proliferation of MES. The role of C1q is more complex than previously thought and is likely to be dependent on the tumor microenvironment. The availability of the recombinant globular domain of C1q may have implications for therapeutic approaches.

ETHICS STATEMENT

This study was carried out in accordance with the recommendations of governmental guidelines and approved by the CEUR (Comitato Etico Unico Regionale, FVG, Italy; number 34/2016), with written informed consent from all subjects. All subjects gave written informed consent in accordance with the Declaration of Helsinki.

AUTHOR NOTE

This work is dedicated to the memory of Bulla Gabriele and all mesothelioma patients.

AUTHOR CONTRIBUTIONS

Conception and design: RB, CA, and UK. Development of methodology: RV and LA. Acquisition of data: RV, VB, FZ, PG, and BB. Analysis and interpretation of data (e.g., statistical analysis, biostatistics, computational analysis): CT, MC, AM, and BB.

Writing, review, and/or revision of the manuscript: RB, UK, CA, and FT. Study supervision: RB and MC.

ACKNOWLEDGMENTS

We thank Ivan Donati (Department of Life Sciences, University of Trieste, Trieste, Italy) for providing of HA. The contribution of Marco Biolo (Department of Medical, Surgical and Health Sciences, University of Trieste, Trieste, Italy), Fleur Bossi (IRCCS, Burlo Garofolo, Trieste, Italy), and Alessandro Gulino (Department of Human Pathology, University of Palermo) for the immunohistochemical analysis, Gianluca Tel (Department of Medical and Biological Sciences, University of Udine, Udine, Italy) for LI-COR analysis, Damiano Rami, and Elisa Trevisan (Department of Life Sciences, University of Trieste, University of Trieste, Trieste, Italy) for the contribution for the cell characterization, are acknowledged.

FUNDING

This work was supported by grants from the Institute for Maternal and Child Health, IRCCS "Burlo Garofolo," Trieste, Italy (RC41/08, RC 01/09, RC 34/11), AIRC to CT. Fondazione Cassa di Risparmio Trieste to RB.

REFERENCES

1. Carbone M, Kanodia S, Chao A, Miller A, Wali A, Weissman D, et al. Consensus report of the 2015 Weinman International Conference on mesothelioma. *J Thorac Oncol* (2016) 11:1246–62. doi:10.1016/j.jtho.2016.04.028
2. Carbone M, Kratzke RA, Testa JR. The pathogenesis of mesothelioma. *Semin Oncol* (2002) 29:2–17. doi:10.1053/sonc.2002.30227
3. Astoul P. Pleural mesothelioma. *Curr Opin Pulm Med* (1999) 5:259–68. doi:10.1097/00063198-199907000-00015
4. Husain AN, Colby TV, Ordonez NG, Krausz T, Borczuk A, Cagle PT, et al. Guidelines for pathologic diagnosis of malignant mesothelioma: a consensus statement from the International Mesothelioma Interest Group. *Arch Pathol Lab Med* (2009) 133:1317–31. doi:10.1043/1543-2165-133.8.1317
5. Davidson B. Prognostic factors in malignant pleural mesothelioma. *Hum Pathol* (2015) 46:789–804. doi:10.1016/j.humpath.2015.02.006
6. Scherpereel A, Astoul P, Baas P, Berghmans T, Clayson H, de Vuyst P, et al. Guidelines of the European Respiratory Society and the European Society of Thoracic Surgeons for the management of malignant pleural mesothelioma. *Eur Respir J* (2009) 35:479–95. doi:10.1183/09031936.00063109
7. Lorusso G, Ruegg C. The tumor microenvironment and its contribution to tumor evolution toward metastasis. *Histochem Cell Biol* (2008) 130:1091–103. doi:10.1007/s00418-008-0530-8
8. Heldin P, Basu K, Olofsson B, Porsch H, Kozlova I, Kahata K. Deregulation of hyaluronan synthesis, degradation and binding promotes breast cancer. *J Biochem* (2013) 154:395–408. doi:10.1093/jb/mvt085
9. Itano N. Simple primary structure, complex turnover regulation and multiple roles of hyaluronan. *J Biochem* (2008) 144:131–7. doi:10.1093/jb/mvn046
10. Itano N, Zhuo L, Kimata K. Impact of the hyaluronan-rich tumor microenvironment on cancer initiation and progression. *Cancer Sci* (2008) 99:1720–5. doi:10.1111/j.1349-7006.2008.00885.x
11. Chanmee T, Ontong P, Itano N. Hyaluronan: a modulator of the tumor microenvironment. *Cancer Lett* (2016) 375:20–30. doi:10.1016/j.canlet.2016.02.031
12. Afify AM, Stern R, Michael CW. Differentiation of mesothelioma from adenocarcinoma in serous effusions: the role of hyaluronic acid and CD44 localization. *Diagn Cytopathol* (2005) 32:145–50. doi:10.1002/dc.20201
13. Ricklin D, Hajishengallis G, Yang K, Lambris JD. Complement: a key system for immune surveillance and homeostasis. *Nat Immunol* (2010) 11:785–97. doi:10.1038/ni.1923
14. Kishore U, Reid KB. C1q: structure, function, and receptors. *Immunopharmacology* (2000) 49:159–70. doi:10.1016/S0162-3109(00)80301-X
15. Kouser L, Madhukaran SP, Shastri A, Saraon A, Ferluga J, Al-Mozaini M, et al. Emerging and novel functions of complement protein C1q. *Front Immunol* (2015) 6:317. doi:10.3389/fimmu.2015.00317
16. Bulla R, Agostinis C, Bossi F, Rizzi L, Debeus A, Tripodo C, et al. Decidual endothelial cells express surface-bound C1q as a molecular bridge between endovascular trophoblast and decidual endothelium. *Mol Immunol* (2008) 45:2629–40. doi:10.1016/j.molimm.2007.12.025
17. Agostinis C, Bulla R, Tripodo C, Gismondi A, Stabile H, Bossi F, et al. An alternative role of C1q in cell migration and tissue remodeling: contribution to trophoblast invasion and placental development. *J Immunol* (2010) 185:4420–9. doi:10.4049/jimmunol.0903215
18. Bulla R, Tripodo C, Rami D, Ling GS, Agostinis C, Guarnotta C, et al. C1q acts in the tumour microenvironment as a cancer-promoting factor independently of complement activation. *Nat Commun* (2016) 7:10346. doi:10.1038/ncomms10346
19. Travan A, Fiorentino S, Grassi M, Borgogna M, Marsich E, Paoletti S, et al. Rheology of mixed alginate-hyaluronan aqueous solutions. *Int J Biol Macromol* (2015) 78:363–9. doi:10.1016/j.ijbiomac.2015.04.009
20. Stemmer F, Loos M. Purification and characterization of human, guinea pig and mouse C1q by fast protein liquid chromatography (FPLC). *J Immunol Methods* (1984) 74:9–16. doi:10.1016/0022-1759(84)90361-2
21. Kishore U, Gupta SK, Perdikoulis MV, Kojouharova MS, Urban BC, Reid KB. Modular organization of the carboxyl-terminal, globular head region of human C1q A, B, and C chains. *J Immunol* (2003) 171:812–20. doi:10.4049/jimmunol.171.2.812
22. Nakano T, Fujii J, Tamura S, Amuro Y, Nabeshima K, Horai T, et al. Glycosaminoglycan in malignant pleural mesothelioma. *Cancer* (1986) 57:106–10. doi:10.1002/1097-0142(19860101)57:1<106::AID-CNCR2820570122>3.0.CO;2-C
23. Bossi F, Tripodo C, Rizzi L, Bulla R, Agostinis C, Guarnotta C, et al. C1q as a unique player in angiogenesis with therapeutic implication in wound healing. *Proc Natl Acad Sci U S A* (2014) 111:4209–14. doi:10.1073/pnas.1311968111
24. Thylen A, Wallin J, Martensson G. Hyaluronan in serum as an indicator of progressive disease in hyaluronan-producing malignant mesothelioma. *Cancer* (1999) 86:2000–5. doi:10.1002/(SICI)1097-0142(19991115)86:10<2000::AID-CNCR17>3.0.CO;2-N
25. Wang NS. Anatomy of the pleura. *Clin Chest Med* (1998) 19:229–40. doi:10.1016/S0272-5231(05)70074-5
26. Li Y, Heldin P. Hyaluronan production increases the malignant properties of mesothelioma cells. *Br J Cancer* (2001) 85:600–7. doi:10.1054/bjoc.2001.1922
27. Chang NS, Boackle RJ. Hyaluronic acid-complement interactions – II. Role of divalent cations and gelatin. *Mol Immunol* (1985) 22:843–8. doi:10.1016/0161-5890(85)90068-9
28. Chang NS, Boackle RJ, Armand G. Hyaluronic acid-complement interactions – I. Reversible heat-induced anticomplementary activity. *Mol Immunol* (1985) 22:391–7. doi:10.1016/0161-5890(85)90123-3
29. Prehm P. Synovial hyaluronate in rheumatoid arthritis binds C1q and is covalently bound to antibodies: a model for chronicity. *Ann Rheum Dis* (1995) 54:408–12. doi:10.1136/ard.54.5.408
30. Hong Q, Kuo E, Schultz L, Boackle RJ, Chang NS. Conformationally altered hyaluronan restricts complement classical pathway activation by binding to C1q, C1r, C1s, C2, C5 and C9, and suppresses WOX1 expression in prostate DU145 cells. *Int J Mol Med* (2007) 19:173–9. doi:10.3892/ijmm.19.1.173
31. Nasreen N, Mohammed KA, Hardwick J, Van Horn RD, Sanders K, Kathuria H, et al. Low molecular weight hyaluronan induces malignant

mesothelioma cell (MMC) proliferation and haptotaxis: role of CD44 receptor in MMC proliferation and haptotaxis. *Oncol Res* (2002) 13:71–8.
32. Fuchs K, Hippe A, Schmaus A, Homey B, Sleeman JP, Orian-Rousseau V. Opposing effects of high- and low-molecular weight hyaluronan on CXCL12-induced CXCR4 signaling depend on CD44. *Cell Death Dis* (2013) 4:e819. doi:10.1038/cddis.2013.364
33. Ghebrehiwet B, Peerschke EI. cC1q-R (calreticulin) and gC1q-R/p33: ubiquitously expressed multi-ligand binding cellular proteins involved in inflammation and infection. *Mol Immunol* (2004) 41:173–83. doi:10.1016/j.molimm.2004.03.014
34. Winslow S, Leandersson K, Edsjo A, Larsson C. Prognostic stromal gene signatures in breast cancer. *Breast Cancer Res* (2015) 17:23. doi:10.1186/s13058-015-0530-2
35. Hong Q, Sze CI, Lin SR, Lee MH, He RY, Schultz L, et al. Complement C1q activates tumor suppressor WWOX to induce apoptosis in prostate cancer cells. *PLoS One* (2009) 4:e5755. doi:10.1371/journal.pone.0005755
36. Kaur A, Sultan SH, Murugaiah V, Pathan AA, Alhamlan FS, Karteris E, et al. Human C1q induces apoptosis in an ovarian cancer cell line via tumor necrosis factor pathway. *Front Immunol* (2016) 7:599. doi:10.3389/fimmu.2016.00599

Conflict of Interest Statement: The authors declare that the research was conducted in the absence of any commercial or financial relationships that could be construed as a potential conflict of interest.

Isolation and characterization of Malignant Pleural Mesothelioma cells

In our study were enrolled MPM patients followed up at the Department of Pneumology, University Hospital of Cattinara, Trieste, Italy. All these patients had clinical symptoms consistent with mesothelioma diagnosis, for instance chest pain or dyspnoea associated with pleural thickening and exsudative pleural effusion.

Biopsy	Sex	Mesotheliolma hystotype
MES7 BIO	**M**	**Not determined**
MES9 BIO	**M**	**Epithelioid**
MES11BIO	**M**	**Epithelioid**
MES12 BIO	**M**	**Not determined**
MES13 BIO	**M**	**Biphasic**
MES14 BIO	**M**	**Epithelioid**
MES19BIO	**M**	**Epithelioid**
MES22 BIO	**M**	**Biphasic**
MES23 BIO	**M**	**Epithelioid**
MES24 BIO	**M**	**Epithelioid**
MES27 BIO	**F**	**Epithelioid**
MES29 BIO	**M**	**Sarcomatoid**
MES31 BIO	**M**	**Epithelioid**
MES32 BIO	**M**	**Epithelioid**
MES36 BIO	**M**	**Epithelioid**
MES37 BIO	**M**	**Sarcomatoid**
MES39 BIO	**M**	**Epithelioid**

Table 2. Summary of primary MES cells isolated from patients.

None of them received chemotherapy or radiotherapy before the samples were taken. As previously described we were able to isolate MPM tumour cells (MES) from a portion of the resected pleura, obtained during pleuroscopy. Final diagnosis, based on pleural histology, demonstrated that most patients were affected by the most frequent epithelioid hystotype (Attanoos and Gibbs, 1997). For the second part of the study we enlarged the clinical records

of human malignant mesothelioma cells as it is described in **Table 2**. We observed that the prevailing histotype of mesothelioma tumour is epithelioid and all patients, except one female, were men.

Immunophenotypical characterization of primary cells isolated from biopsies

All tumour cells populations isolated from bioptic tissues were deeply characterized both after isolation and after some passages in order to confirm their mesothelial phenotype. Several markers were investigated, namely mesothelin, epithelial cytokeratin 8/18 (CK8/18), cell surface HA-binding glycoprotein CD44, Epithelial-Membrane Antigen (EMA), mesenchymal CD9 and vimentin. In particular, the expression of all these antigens was examined both by flow cytometry analysis and by immunofluorescence (IF) assays. All primary cultures isolated were positive for all mentioned markers.

To test the possible contamination by cells belonging to the immune system, such as leukocytes and monocytes, or cells of the vasculature, the immunophenotypical staining was extended to the following markers: CD45, a lymphocyte common antigen expressed on all leucocytes; CD14, a monocyte differentiation antigen useful for monocytes and macrophages identification; von Willebrand Factor (vWF), a common marker used for endothelial cells detection. The positivity for CD45 and CD14 as well as for vWF was lost at early passages in all primary cultures. Interestingly, all MES cells were positive for CD68, a mature macrophage marker, although they were negative for CD14. Some of these markers were also analysed by FACS (Figure 1).

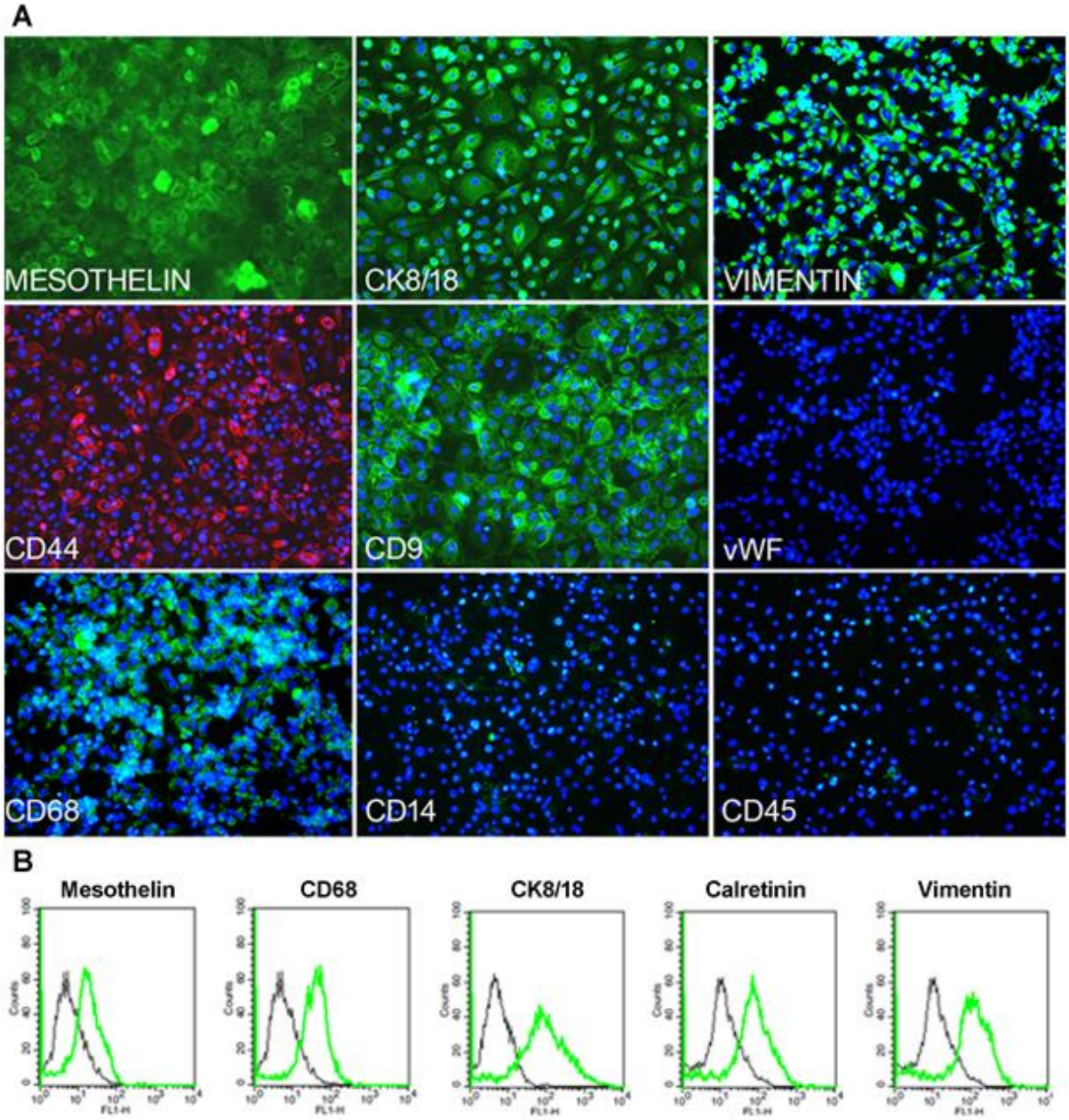

Figure 1. Characterization of MES. **(A)** Mesothelial cells were characterized by immunofluorescence for the expression of mesothelin, CK 8/18, vimentin, CD9, CD68 (green) and CD44 (red). Mesothelioma cells were grown to confluence in 8-chamber culture slides. After fixation and permeabilization, the cells were stained with mAb anti-human mesothelin, CK 8/18, vimentin, CD9, vWF, CD68, and CD14, followed by anti-mouse-FITC F(ab)' secondary antibodies or mAb anti-human CD45 and mAb anti-human CD44-PE conjugate. Nuclei were stained in blue by DAPI: original magnification 200 X. **(B)** The expression of mesothelin, CD68, CK8/18, calretinin and vimentin was confirmed by FACS. The expression of these markers (green lines) was compared with appropriate control antibodies (black lines).

C1q enhances mTOR pathway in MES cells

In the previous study we demonstrated that C1q bound to HA is able to induce adhesion and proliferation of MES cells. This phenotype emerged to rely on the activation of three members of the MAPK family, namely ERK1/2, SAPK/JNK, and p38 signalling cascades (Agostinis et al., 2017b).

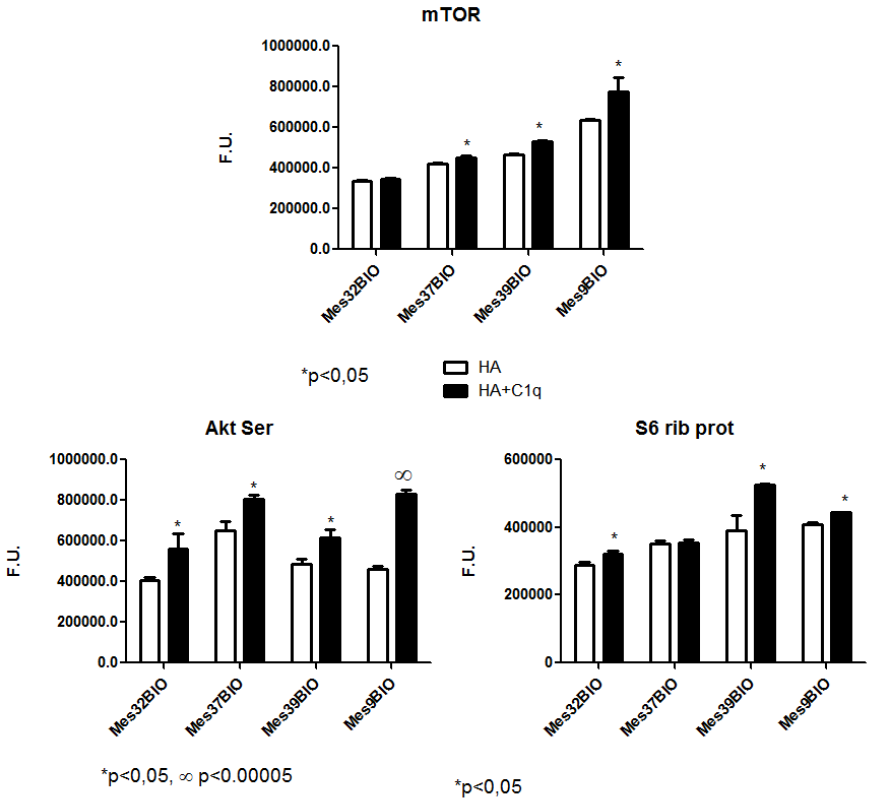

Figure 2. Phosphorylation status of mTOR, AKT and S6 in MES cells. MES were allowed to adhere to HA or C1q-bound HA and the phosphorylation status of mTOR, AKT Ser and S6 was evaluated by chemiluminescence using PathScan® Intracellular Signaling Array Kit (Cell Signaling Technology). Binding of MES to HA-bound-C1q resulted in the upregulation of mTOR, AKT and S6 signalling molecules. Data are presented as four different MES populations ± SD. *p<0.05 p<0.00005

To further elucidate the mechanism of cell activation induced by C1q-bound HA, we extended our analysis to the mTOR signalling pathway, known to play important roles in a variety of cellular processes including cell growth, cell survival, motility, transcription and cell proliferation. Since it has been demonstrated that AKT activation in MES cell lines is dependent on the coordinated activation of multiple receptor tyrosine kinases (RTKs) (Zhou et al., 2014), we aimed at better understanding the signalling properties of C1q-bound HA. To this aim serum-starved MES were allowed to adhere to wells coated with HA or C1q-bound HA for 20 min and the phosphorylation status of mTOR, AKT Ser and S6 was evaluated by read-out using the PathScan® Intracellular Signaling Array Kit (Cell Signaling Technology). As shown in **Figure 2**, the phosphorylation status of mTOR, AKT and S6 signalling

molecules, a downstream target of mTOR pathway, was significantly enhanced in MES interacting with C1q-bound HA as compared to HA alone.

The biological relevance of mTOR was then evaluated by determining its impact on cell adhesion upon mTOR inhibition using the rapamycin derivative RAD001/everolimus overnight at 10 μM concentration. Even though everolimus treatment hampered the MES adhesion irrespective of the matrix used this effect was more pronounced in the case of C1q-bound HA **(Figure 3)**.

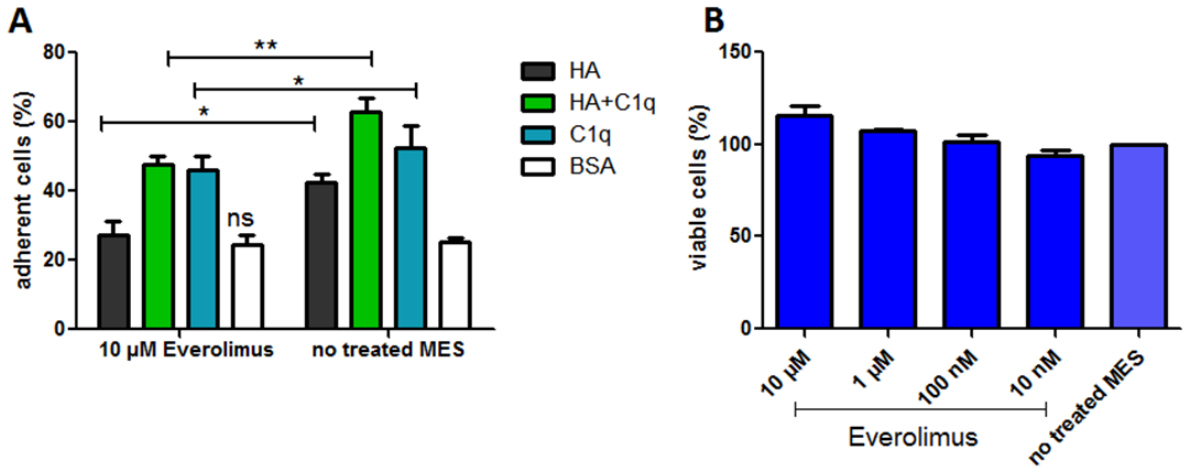

Figure 3. Effect of mTOR inhibitor RAD001/everolimus on MES adhesion and cell viability. (A) mTOR inhibitor RAD001/everolimus (10 µM) was able to reduce cell adhesion in MES cell. (B) All tested concentrations of inhibitor were not able to reduce cell viability, comparable with no treated MES cells. The data presented three different MES populations performed in triples. *p<0.05

Induction of Epithelial/Mesothelial mesenchymal transition by HA

Epithelial- or mesothelial-mesenchymal transition (EMT/MMT) is a physiopathological process by which epithelial cells lose polarization and immotility, thus acquiring mesenchymal shape and properties. EMT has a central role in both physiological and pathological processes such as cancer (Sleeman and Thiery, 2011). Typically, EMT switches gene expression from epithelial characteristic markers E-cadherin and cytokeratin to mesenchymal N-cadherin, SNAIL, Lymphoid Enhancer Binding Factor 1 (LEF-1), β-catenin and Fibronectin (FN-1). In particular EMT transition is characterized by the nuclear translocation of β-catenin (Itano and Kimata, 2008), up-regulation of Fibronectin (FN-1), downregulation of the epithelial marker E-cadherin (Li et al., 2017), up-regulation of LEF-1 which can also occur independently from β-catenin nuclear translocation (Bleckmann et al.,

2013; Kobayashi and Ozawa, 2013), upregulation of N-cadherin and SNAIL, both invasion and metastasis promoting factors (Barrallo-Gimeno, 2005).

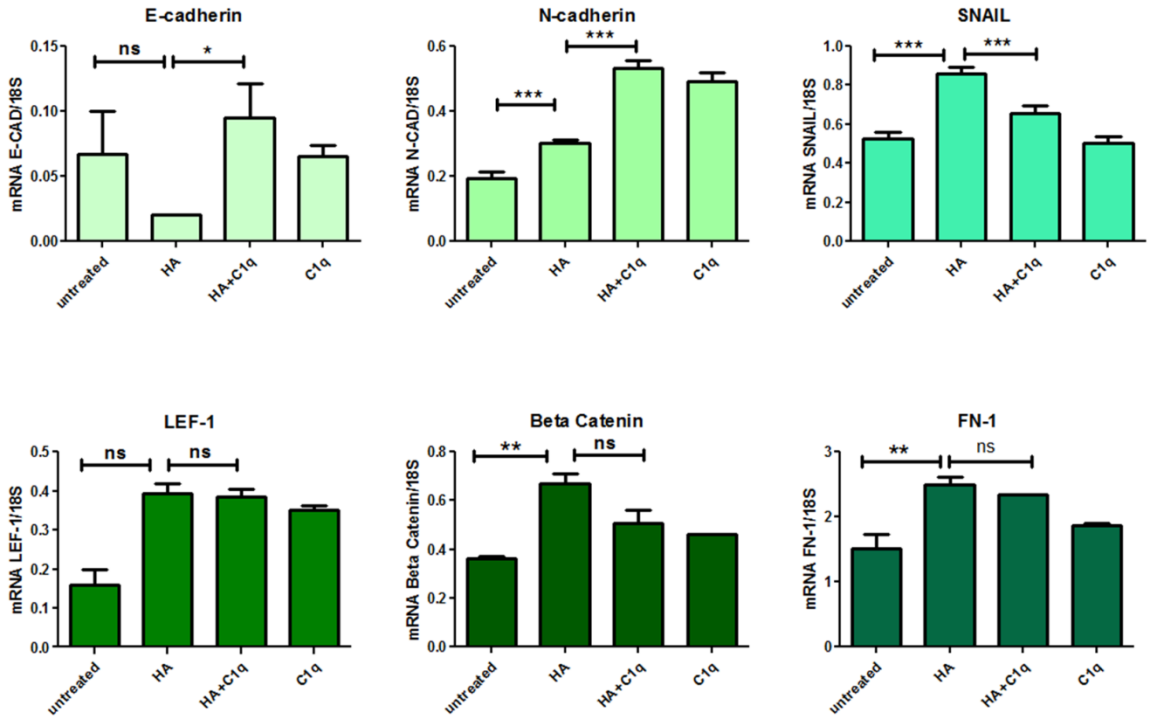

Figure 4. Effect of C1q-bound HA on EMT/MMT. MES were seeded onto high molecular weight HA, C1q or C1q-HA ON. By qPCR analysis we observed upregulated levels of epithelial marker E-cadherin and mesenchymal marker N-cadherin, but opposite than expected, downregulation of SNAIL, transcription factor for N-cadherin in samples treated with C1q-bound HA. In addition, mesenchymal markers, such as LEF-1, CTNNB, FN-1 were not affected by C1q-bound HA. The data are expressed as a mean of at least three different MES populations carried out in duplicates ± SEM.

Recent studies showed that extracellular matrix (ECM) molecules, such as HA, can promote the convertion of epithelial cells into mesenchymal cells by triggering EMT (Camenisch et al., 2000). Indeed mice lacking the expression of one of the main HA synthesizing enzymes, HAS-2, showed several cardiac and vascular abnormalities due to the lack of transformation of cardiac endothelial cells into mesenchyme (Itano and Kimata, 2008). Conversely, overexpression of recombinant HAS2 upon adenoviral infection converted normal Madin-Darby canine kidney cells and MCF-10A human mammary epithelial cells to mesenchyme as assessed by upregulation of vimentin, dispersion of cytokeratin, and loss of E-cadherin at intercellular boundaries (Zoltan-Jones et al., 2003). Morevoer, overproduction of HA in mammary carcinoma cells results in the suppression of E-cadherin expression and nuclear translocation of β-catenin (Koyama et al., 2007). The results altogether support the notion that increased HA production can be sufficient to induce EMT.

On the basis of this knowledge we wanted to test whether our freshly isolated MES cells had undergone MMT transition and whether C1q-bound HA would represent an active player in this process. To this aim MES cells were seeded on HA, C1q and C1q-HA matrixes and the expression of several EMT markers was measured by qRT-PCR after ON incubation. We observed that MES stimulated by HA downregulated the expression of the epithelial markers E-cadherin while upregulating all the other mesenchymal markers. In the presence of C1q, both E-cadherin and N-cadherin were instead upregulated, whereas the other markers appeared not to be affected, except SNAIL, which was downregulated by C1q-bound HA **(Figure 4)**.

Based on these data we can conclude that C1q, either alone or bound to HA, cannot be considered a promoting factor for EMT in MES cells.

MES cells are highly producers of HA

A common clinical feature in patients with MPM is the large amount of hyaluronan found in their pleural effusions or ascites and in their blood (Cortes-Dericks and Schmid, 2017). It has been debated whether MES cells are able to synthesise hyaluronan. Indeed several reports support the notion that HA production occurs predominantly by other cell types present in the connective tissue, such as fibroblasts, stimulated by the release of growth factor by MES cells (Klominek et al, 1989: Asplund et al, 1993).

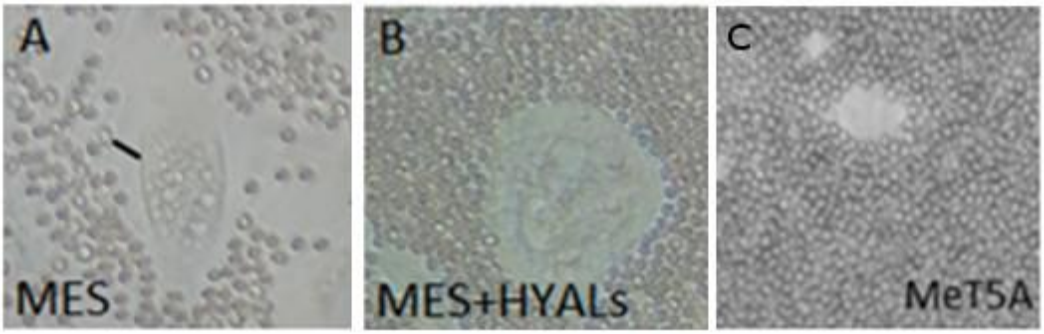

Figure 5. Red blood cell exclusion assay. MES cells demonstrating extracellular HA coat *in vitro* (A). Upon treatment with hyaluronidases hyaluronan and the exclusion space were disappeared (B). We can see no extracellular HA coat produced by MeT5A (C). In all cases the concentration of erythrocytes was the same, but on image (A), HA coat impedes erythrocytes to reach the plasma membrane. Images were acquired by phase-contrast optical microscope, original magnification 200X with Canon Power Shot A640 Camera.

If stroma initially provides a nurturing microenvironment that supports tumour cell survival, growth and invasion, aggressive tumour cells become increasingly autonomous in producing by themselves all key microenvironmental factors that facilitate their survival during their spreding and colonization of foreign microenvironments. Not only pericellular HA has

emerged to sustain activation of oncogenic, anti-apoptotic, and proinvasion/migration signal transduction pathways but also the intracellular form of HA has been identified and shown to promote cancer cell growth and malignant behavior (Evanko and Wight, 1999).

Most experimental settings used to address the relationship between HA production and the malignant phenotype of mesothelioma cells were based on transfection of non-hyaluronan producing mesothelioma cell line. Since we isolated and characterized several malignant cell populations we aimed at understanding whether they are capable of synthesising endogenous HA. To this aim MES cells were seeded at a very low density and incubated for 72 h to allow them to possibly deposit a pericellular coat. Fixed erythrocytes were allowed to settle on cell cultures and the coat was visible as an exclusion zone placed between the periphery of the cells and the erythrocytes. As shown in **Figure 5**, MES appeared to be surrounded by a halo able to keep the fixed red blood cells far away from their plasma membrane. This space could be removed upon hyaluronidase treatment indicating that HA is the main constituent of the halo which could not be detected in the non-hyaluronan producing mesothelioma cell line MeT5A (Panel C). The fact that this hyaluronidase-sensitive surface coat, as detected by exclusion of sedimenting fixed erythrocytes, is made by HA was further supported by Alcian Blue staining **(Figure 6)**.

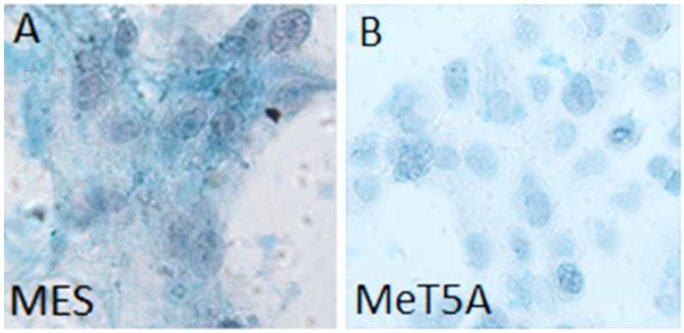

Figure 6. Alcian blue staining of hyaluronic acid on MES and MeT5A cells. MES (A)/MeT5A (B) cells were seeded on 96-well plate and hyaluronic acid was highlighted by Alcian Blue staining. Alcian blue staining was seen on the wells with MES cells and intensity decreased on the wells with MeT5A. Images were acquired by phase-contrast optical microscope, original magnification 200X with Canon Power Shot A640 Camera.

To further characterize the HA production by MES cells we took advantage of a more specific probe for hyaluronan detection, such as the HA binding protein (HABP) composed of the G1-IGD-G2 domain of aggrecan proteoglycan, as well as by the Link protein extracted from bovine cartilage (Hardingham and Adams, 1976; Hardingham and Muir, 1972).

In particular we used a biotin-labeled hyaluronic acid binding protein (HABP) and a streptavidin-Alexa488 system to visualize endogenous HA while the morphology of the cells

was given by the immunoreactivity against the intermediate filament protein vimentin. As show in **Figure 7**, while the pericellular HA coat is not detectable due to the fact that is easily lost during immunfluorescence procedure (Rilla K., personal communication) an intense hyaluronan staining filling the entire cytoplasm of MES cells was detected and clearly illustrated by the reported z-projections.

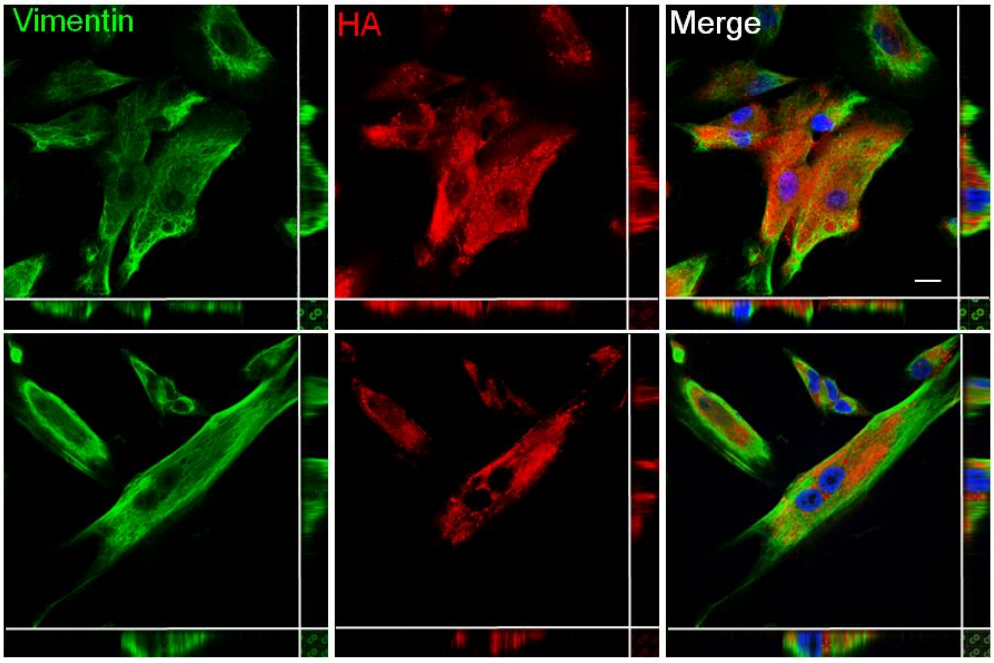

Figure 7. Immunofluorescence staining of mesothelioma cells for hyaluronic acid. For specific labelling of hyaluronic acid, MES cells were stained with biotin-labeled hyaluronic acid binding protein (HABP), while an intermediate filament protein – vimentin allowed us to identify MES cells morfology. We were able to detect only intracellular localization of HA, but not pericellulal coat, as we expected, and this was due to fixation during IF procedure. Confocal images were taken at Nikon Eclipse Ti2. Scale bar: 10μm

The intracellular HA staining appeared as round vesicular or globular structures prominently concentrated in the perinuclear region of the cells. To test whether one of the main sources for intracellular HA could derived from endocytosed extracellular HA we filled the whole cellular endocytic system by suppling overnight fluorescein-labeled hyaluronan (FA-HA) in the growth medium. The following day we fixed the cells and processed for endogenous HA visualization with HABP probe. As shown in Figure 8, we noticed that the fluorescein signal was restricted to large endosome/endosomal vesicles that did not colocalize with endogenous intracellular HA **(Figure 8)**.

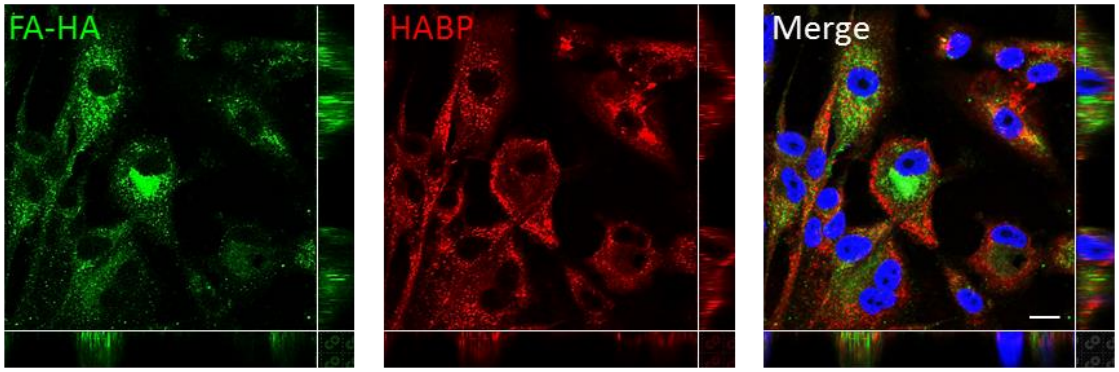

Figure 8. Hyaluronan up-take by MES cells. Fluorescein-labeled HA (FA-HA, 10 μg/mL) was added to MES cells in culture to be taken-up during ON incubation. Cells were then fixed and stained for endogenous intracellular HA (red). Confocal images were taken at Nikon Eclipse Ti2. Scale bar: 10μm

Based on these data we can exclude that HA on the cytoplasm derives from an endocytosed pool that would require to translocate from the lumen of the endosomal system to the cytosol, leading to hypothesise a cytosolic synthesis at the inner face of the plasma membrane by HASes.

RT-qPCR analysis on different MES populations

Several lines of evidence have demonstrated that aberrant HA production is able to affect the malignant behaviour of cells. Since C1q is abundantly present in all the histological mesothelioma hystotypes and it binds with high affinity HA, we hypothesised that C1q bound to HA (C1q-HA) may function as novel signalling complex able to affect the properties of the tumour microenvironment, rendering it pro-tumorigenic. It has been widely demonstrated that the molecular weight of HA represents an important determinant of HA biological activity. In fact Low Molecular Weight (LMW)-HA has been proven to play a crucial role in tumorigenesis by affecting cell proliferation and motility and by exhibiting pro-inflammatory and pro-angiogenic effects in a variety of experimental systems as compared to High Molecular Weight (HMW-HA). Since C1q is similarly able to bind both LMW-HA and HMW-HA as showed in attached paper (Agostinis et al., 2017b) we wanted to determine whether C1q-bound HA may differentially affect HA homeostasis by altering the expression level of the enzymes involved in its biosynthesis and catabolism. Biosynthesis of HA molecules is regulated by three HA synthases called HAS1, HAS2 and HAS3 (Törrönen et al., 2014), while HA degradation seems to require up to six different hyaluronidases (HYAL1, HYAL2, HYAL3, HYAL4, PH-20 and the pseudogene HYALP1) being HYAL1, HYAL2

and HYAL3 the most abundantly expressed in normal human tissues and cells (Dicker et al., 2014).

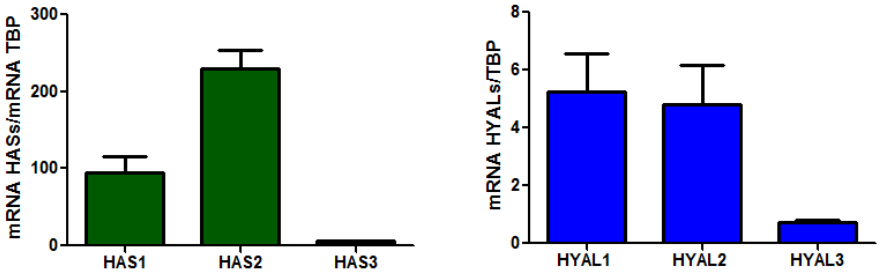

Figure 9. mRNA expression levels of hyaluronan synthases (HAS1, HAS2 and HAS3) and hyaluronidases (HYAL1, HYAL2 and HYAL3) isoforms in cultured human MES. The data are expressed as a mean of at least three to five different MES populations carried out in duplicate ± SEM.

Initial quantitative RT-PCR were performed on total mRNA, extracted from freshly isolated MES to test the basal level of expression of HAS1, HAS2 and HAS3, and HYAL1, HYAL2 and HYAL3. As shown in **Figure 9**, HAS1 and HAS2 together with HYAL1 and HYAL2 were the predominant synthases and hyaluronidases expressed, respectively, in all MES populations isolated from different patients.

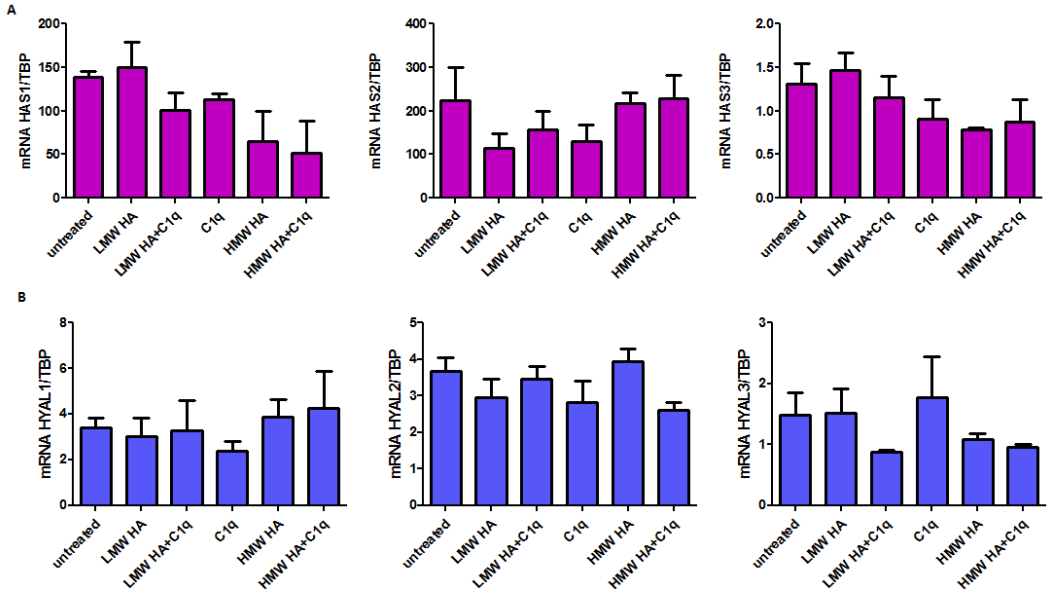

Figure 10. mRNA expression levels of HAS1, HAS2 and HAS3 isoforms and HYAL1, HYAL2 and HYAL3 following different soluble treatment of cultured human MES. We analysed the mRNA expression of all three HA synthases, HAS1, HAS2 and HAS3 (A) and all three hyaluronidases, HYAL1, HYAL2 and HYAL3 (B) on MES treated ON at 37ºC and air/CO_2 incubator with C1q (25 µg/ml), LMW HA (200 µg /ml), HMW HA (50 µg/ml), LMW HA+C1q and HMW+C1q. Untreated MES cells were included as a negative control. The presented results did not show any statistical difference between different treating conditions on mRNA expression to any of the mentioned enzymes. The data are expressed as a mean of at least three to five different MES populations carried out in duplicate ± SEM.

We proceeded then to assess the possibility that C1q together with HMW and/or LMW would affect the expression level of mRNA encoding for the enzymes responsible for HA synthesis and degradation. We initially stimulated MES cells by adding directly into the growth medium LMW HA (200 µg /ml) and HMW HA (50 µg/ml) either alone or in the presence of C1q (25 µg/ml). None of these treatments was able to produce significant changes in the expression of the genes involved in HA metabolism, in all MES populations tested (**Figure 10**). Next, MES cells were seeded on immobilized HMW-HA, C1q or C1q-bound HA and mRNA expression for all HA synthases and hyaluronidases isoforms was measured by qRT-PCR. Under these conditions it was observed that only HAS3 mRNA expression was significantly downregulated upon ON incubation of MES on C1q-HA matrix as compared to HA alone, while only HYAL2 mRNA expression was instead selectively upregulated under the same experimental conditions (**Figure 11**).

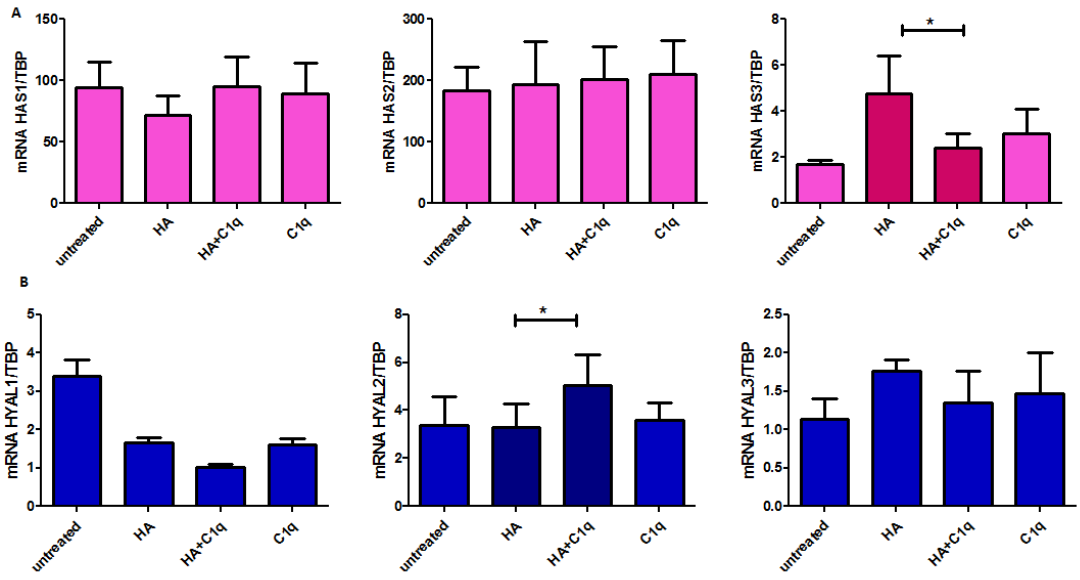

Figure 11. mRNA expression levels of HAS1, HAS2, HAS3 and HYAL1, HYAL2, HYAL3. MES were seeded onto high molecular weight HA, C1q or C1q-HA for ON at 37ºC and air/CO_2 incubator and mRNA expression of HAS1, HAS2 and HAS3 (A) and HYAL1, HYAL2 and HYAL3 (B) was analyzed. Results showed downregulation of HAS3 and upregulation of HYAL2 when cells were seeded on C1q-HA comparable to HA alone. The data are expressed as a mean of at least three to five different MES populations carried out in duplicate ± SEM.

In order not to miss possible changes in the mRNA levels that might have occurred after shorter incubation time, we measured the mRNA expression levels of HASes (**Figure 12**) and HYALs (**Figure 13**) upon 3 h, 6 h or ON plating.

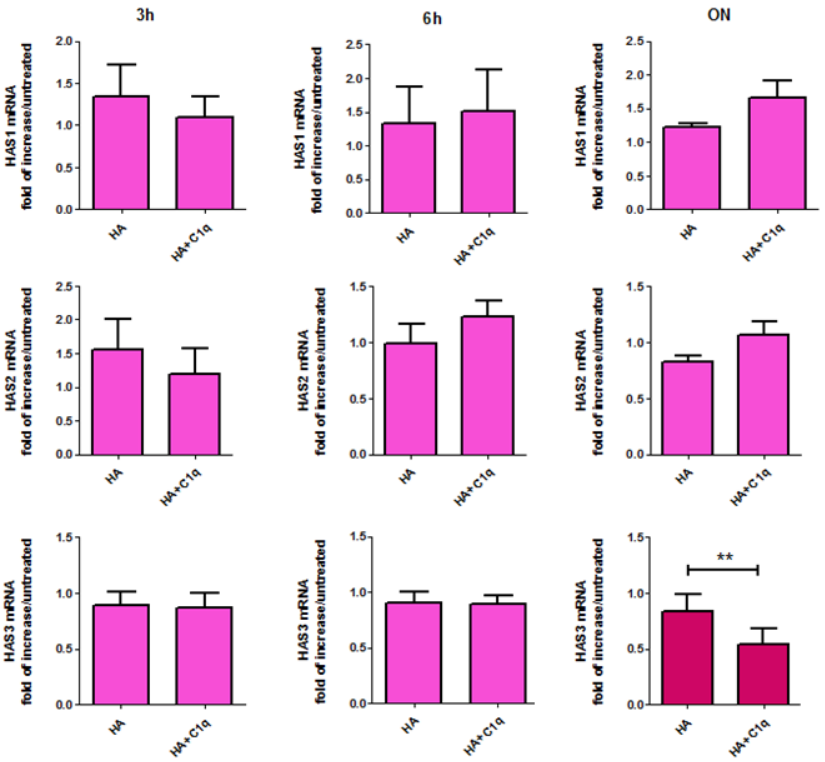

Figure 12. mRNA expression levels of HAS1, HAS2, HAS3 isoforms. MES were seeded onto high molecular weight HA or C1q-HA for 3h, 6h or ON incubation time at 37ºC and air/CO_2 incubator. Cells seeded onto C1q-HA resulted in downregulation of HAS3 mRNA comparable with the cells seeded on HA alone. The data are expressed as a mean of at least three to five different MES populations carried out in duplicate ± SEM.

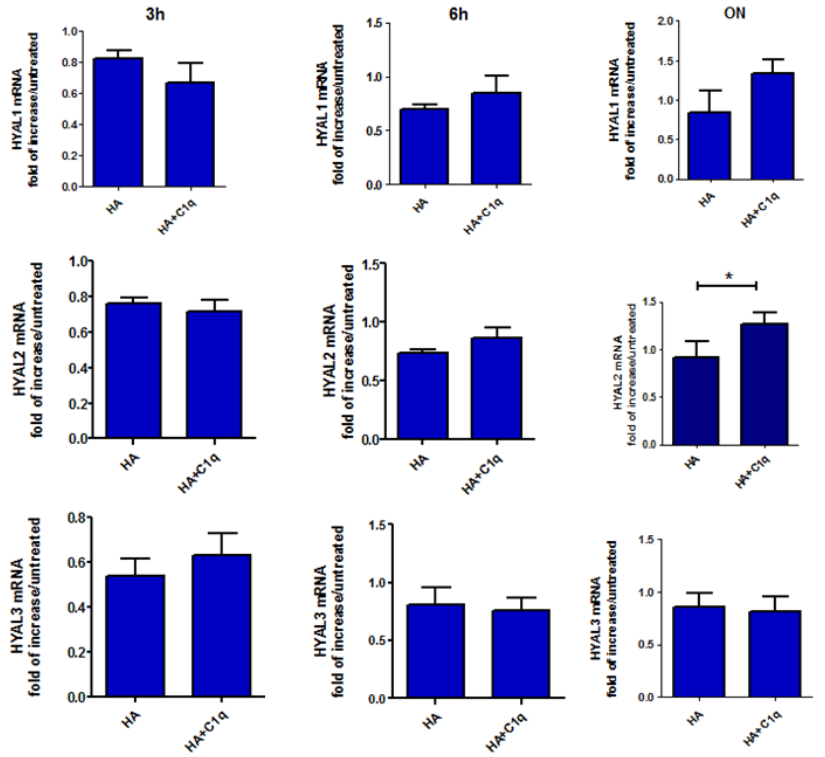

Figure 13. mRNA expression levels of HYAL1, HYAL2 and HYAL3 isoforms. MES were seeded onto HMW HA or C1q-HA for 3h, 6h or ON incubation time at 37ºC and air/CO_2 incubator. Results showed upregulation of HYAL2 mRNA level after ON incubation, respectively. The data are expressed as a mean of at least three to five different MES populations carried out in duplicate ± SEM.

The time course revealed that only in the condition of ON incubation with immobilized C1q-bound HA it was possible to appreciate alteration of the mRNA levels for HAS3 and HYAL2 thus confirming the previous findings.

Clinical significance of HAS3 and HYAL2 mRNA expression in MPM cancer

In order to investigate whether HAS3 and HYAL2 can serve as potential prognostic markers for human MPM, we compared the differences in the mRNA level of HAS3 and HYAL2 between mesothelioma cancer and healthy tissues. The data of mRNA expression for HYAL2 on mesothelioma *vs* normal tissue showed no statistical significance using the Oncomine platform (Gordon Mesothelioma dataset) (**Figure 14**) while no available results were provided for HAS3.

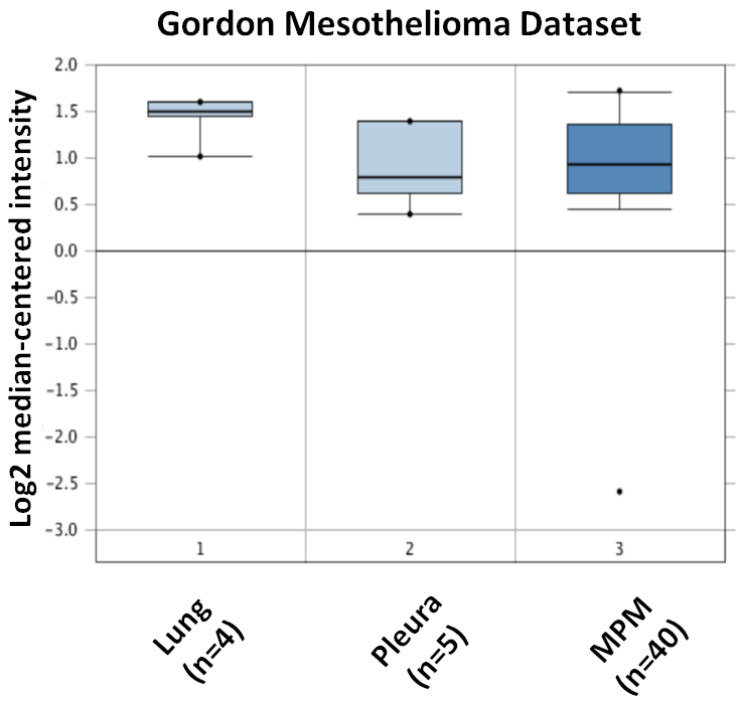

Figure 14: Pathological significance of HYAL2 expression in MPM. Gordon Mesothelioma Dataset was used for bioinformatics analysis to explore HYAL2 mRNA expression in the MPM. No significant differences in the mRNA expression of HYAL2 were observed between lung, pleura and MPM tissue.

By contrast, HAS3 and HYAL2 mRNA expressions are negatively correlated to an overall survival rate of mesothelioma affected patients ($p < 0.05$) as determined by using the PROGgeneV2 database, a survival analysis tool (**Figure 15**, (Goswami and Nakshatri, 2014) http://watson.compbio.iupui.edu/chirayu/proggene/database). Based on these datasets we observed that life expectancy in mesothelioma patients characterized by high levels of HAS3 and HYAL2 expression is lower than in patients with low expression level cancer ($p<0.05$) as illustrated in The Cancer Genome Atlas (TCGA dataset) (https://cancergenome.nih.gov).

While our HYAL2 qRT-PCR (**Figure 15A**) data are in line with the bioinformatic analysis, this is not the case for HAS3 (**Figure 15B**), giving instead an opposite outcome. Given this discrepancy and taking into account that the expression level of HAS3 is barely detectable in western immunoblotting (data not shown) we decided to focus our investigation on HYAL2 contribution to mesothelioma development/progression.

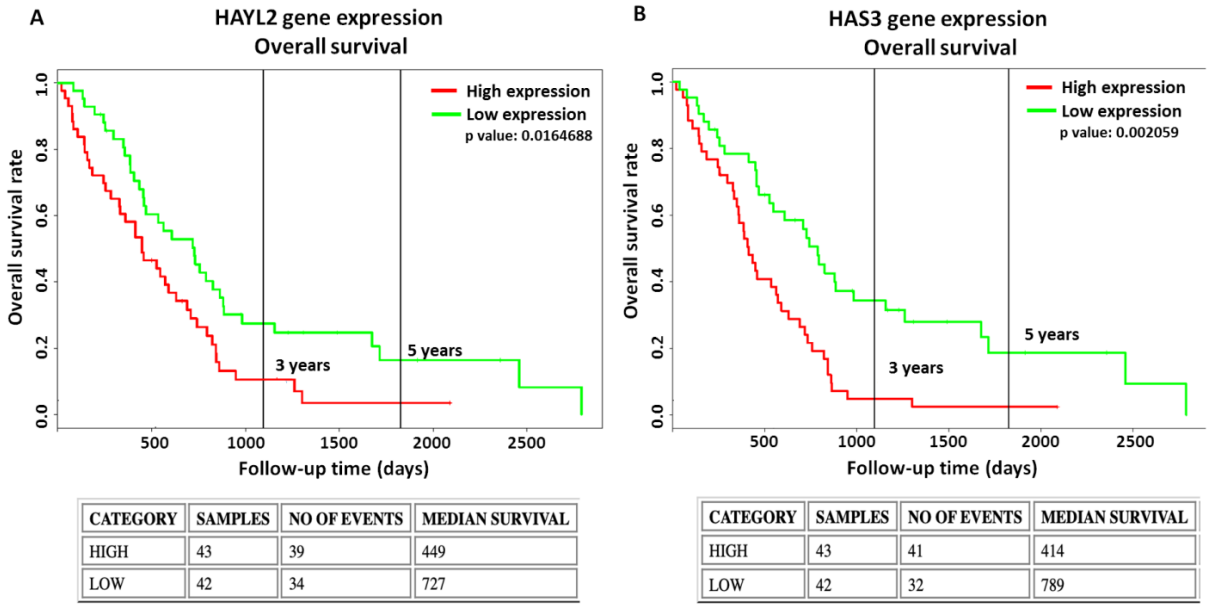

CATEGORY	SAMPLES	NO OF EVENTS	MEDIAN SURVIVAL
HIGH	43	39	449
LOW	42	34	727

CATEGORY	SAMPLES	NO OF EVENTS	MEDIAN SURVIVAL
HIGH	43	41	414
LOW	42	32	789

Figure 15: Pathological significance of HYAL2 and HAS3 expression in MPM. According to the data from PROGgeneV2 datasets for HYAL2 (A) and HAS3 (B) mRNA expression were negatively related to an overall survival rate of the patients with MPM. ($p < 0.05$). The tables underneath the graphs are reporting the number of patients tested with high and low levels of expression of the corresponding mRNA.

Up-regulation of HYAL2 expression by C1q- HA

In order to determine whether the observed increase in HYAL2 mRNA expression level, as detected in qRT-PCR, would correlate to similar changes in protein content we performed Western blot experiments on cell lysates obtained upon ON incubation of different MES cell populations grown on either HA or HA-C1q. HYAL2 GPI-anchored protein was detected using a rabbit polyclonal antibody raised against the bacterially expressed GST-HYAL2 99-448 amino acid residues, which is recognizing a band at around 55-60 kDa.

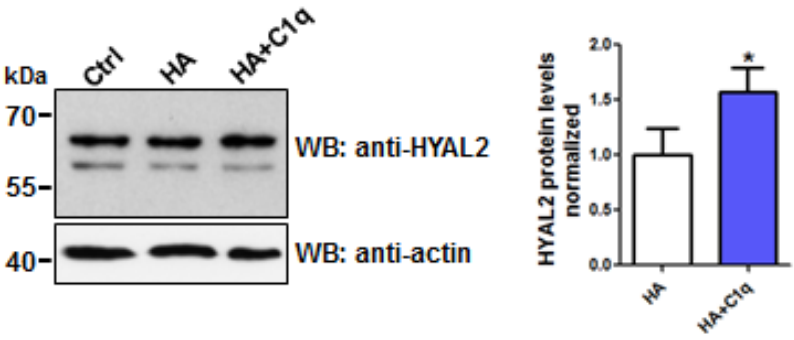

Figure 16. C1q-HA matrix upregulated HYAL2 protein level in MES cells. MES were seeded on HA and C1q-HA matrix ON. For control (Ctrl) we took untreated cells. Also on protein level we observed a significant increase of HYAL2 on the matrix with C1q-HA. The results represent three different MES populations. *p<0,05

Interestingly we found that HYAL2 accumulates upon C1q-HA interaction as compared to HA alone **(Figure 16)**, thus indicating that the upregulation detected at the mRNA level is followed by a parallel increase in the corresponding protein content.

Characterization of the intracellular distribution of HYAL2 in MES

HYAL2 together with HYAL1 have been implicated as the major players in HA catabolism in somatic tissues. Both hyaluronidases prefer acidic pH to be enzymatically active, being pH 4 the optimum for HYAL2 (Chow et al., 2006; Lepperdinger et al., 1998). This is the reason why HYAL2 was expected to be primarily present in lysosomes.

However HYAL2 is a GPI-anchored protein that can fractionate in the plasma membrane fraction where it only has weak enzymatic activity but it functions as the receptor for Jaagsiekte sheep retrovirus (Rai et al., 2001). Moreover soluble, nuclear (Hsu et al., 2009) and mitochondrial (Chang, 2002) localizations for HYAL2 were also described, underlying the complex intracellular distribution based on its cellular function. The most recent studies of endogenous mouse HYAL2 indicate that HYAL2 is expressed on the surface of many cells, but it can be found intracellularly in some cell types (Chowdhury et al., 2016).

To start understanding the cellular distribution of HYAL2 in MES, total and cell surface expression of HYAL2 was analyzed by flow cytometry. All cells under investigation expressed HYAL2, but only about 30% of them had HYAL2 present on the plasma membrane **(Figure 17)**.

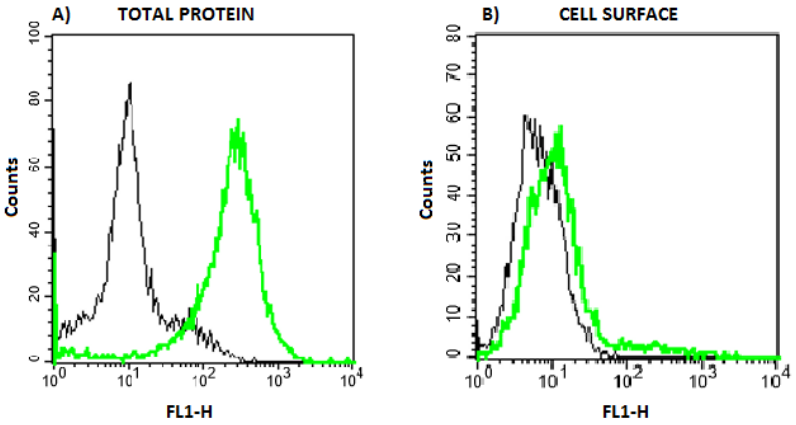

Figure 17. Characterization of MES cells for HYAL2. MES were characterized for cell surface and total (intra- and extracellular) expression of HYAL2. All cells were positive for total HYAL2, when we permebilized the cells, and only about 30% of cells expressed HYAL2 on their cell membrane. The expression of HYAL2 marker (green lines) was compared with appropriate control antibodies (black lines).

Furthermore we assessed the steady-state distribution of endogenous HYAL2 in our MES populations by performing co-immunolabelling experiments. Based on the fact that HYAL2 requires acidic pH to be functionally active we initially tested its possible distribution along the endocytic pathway.

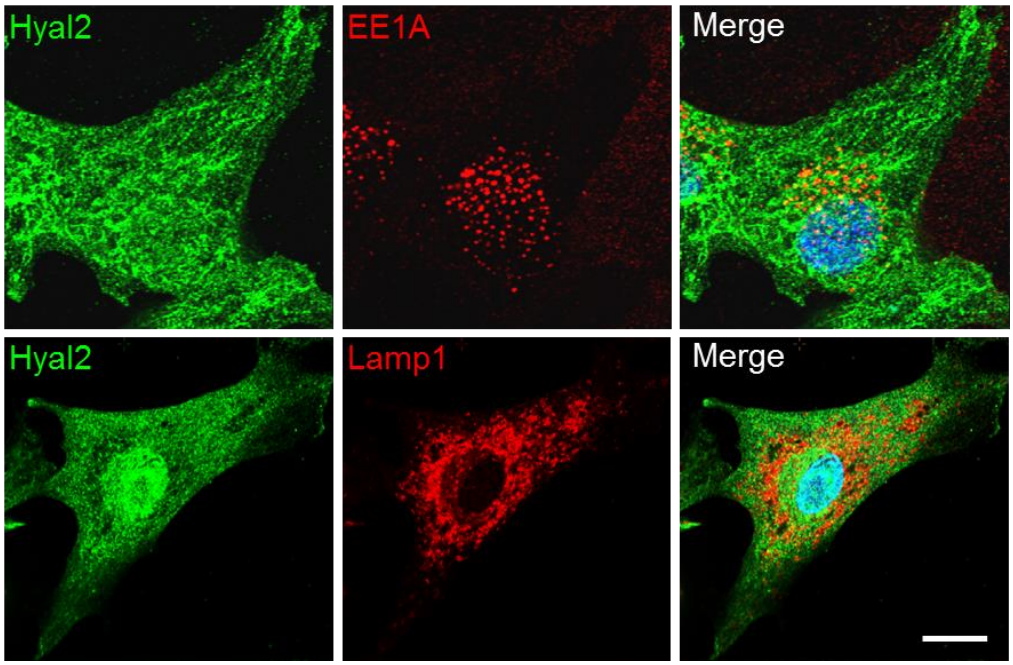

Figure 18. Confocal images of co-localization of HYAL2 with EE1A and LAMP1. MES were co-labelled with HYAL2 and EE1A, a well recognized marker of the early endosomal compartment, and Lamp1, a late endosomal/lysosomal marker. Confocal immunofluorescence microscopy failed to reveal a co-existance of HYAL2 with both proteins associated with the endocytic compartments. Scale Bar. 10 μm

MES cells were therefore co-labeled for endogenous HYAL2 together with Early Endosome Antigen 1 (EE1A), a well recognized marker of the early endosomal compartment, and

Lysosome Associated Membrane Protein 1 (Lamp1), a late endosomal/lysosomal marker. Surprisingly confocal immunofluorescence microscopy failed to reveal a co-existance of HYAL2 with proteins associated to the endocytic compartments, which were considered the optimal localization for HYAL2 activity, given their acidic lumenal pH **(Figure 18)**.

We therefore tested the HYAL2 distribution along the secretory pathway. Calnexin, which is a chaperone molecule assisting protein folding and quality control in the endoplasmic reticulum, and the Mannose 6-phosphate Receptor (M6P-R), a transmembrane glycoprotein which binds newly synthesized lysosomal hydrolases in the trans-Golgi network (TGN) and delivers them to pre-lysosomal compartments, were co-labeled with HYAL2. While the co-localization was pretty much intense with the ER resident protein Calnexin, as expected for a GPI-anchored molecule as HYAL2, this was very low, though present, in the Golgi apparatus **(Figure 19)**.

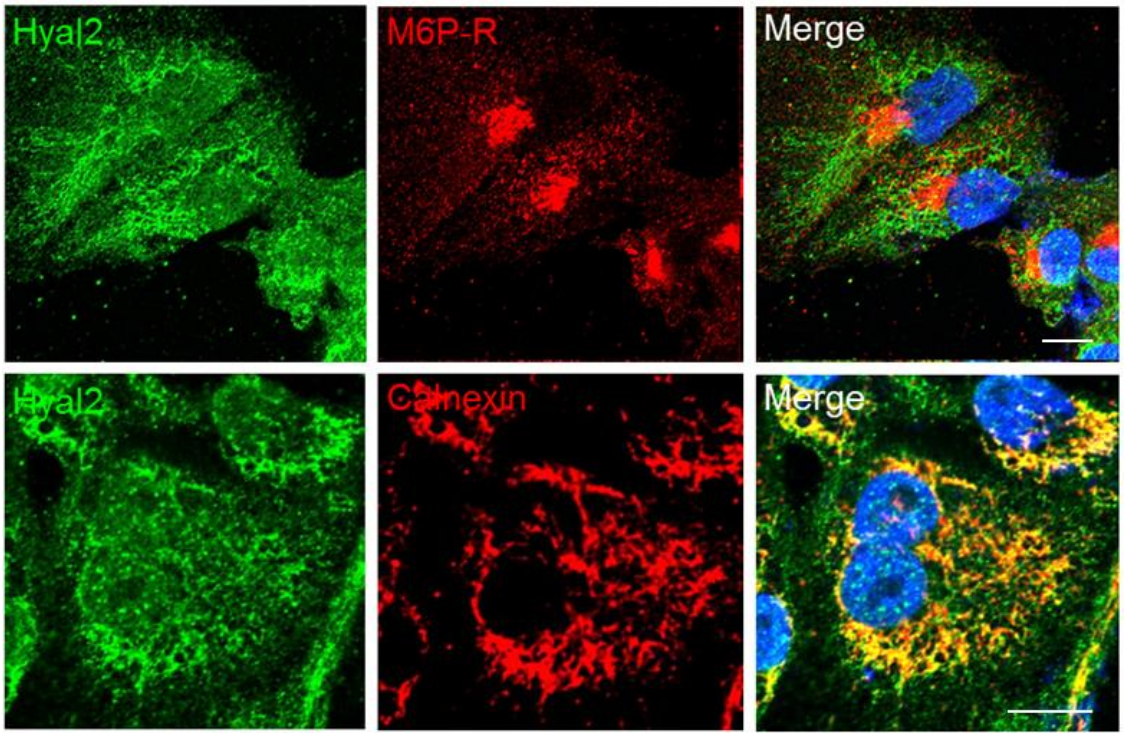

Figure 19. Confocal images of co-localization of HYAL2 with M6PR and Calnexin in MES. Co-localization was pretty much intense with the ER resident protein Calnexin but very low with M6R, marker for GA. Scale bar: 10μm.

The most striking overlap was observed when gC1q receptor was investigated in co-labeling experiments **(Figure 20)**. gC1qR/p33 is an ubiquitously expressed, highly anionic cellular protein of 33 kDA, initially identified and characterized for its ability to interact with the globular heads of the C1q complement component (Ghebrehiwet et al., 2006). Its intracellular distribution is still a puzzling issue: gC1qR seems to be predominantly localized in the

mitochondria matrix (Dedio et al., 1998; Muta et al., 1997) but it is also found in several other cellular compartments, such as the endoplasmic reticulum, the nucleus, and the cell surface, possibly associated with lipid rafts (Braun et al., 2000; Ghebrehiwet et al., 2001; Kittlesen et al., 2000). Although the biological significance of such complex multicompartmental distribution is far from being elucidated, the relevance of gC1qR as an important modulator of various ligand- mediated cellular responses, both inside and outside the cell, is increasingly recognized.

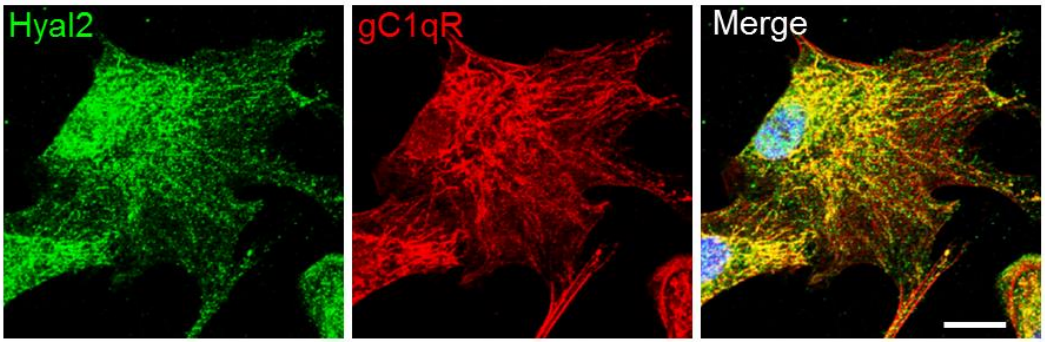

Figure 20. Confocal images of co-localization of HYAL2 and gC1q receptor. Co-localization between HYAL2 and gC1q receptor in MES cells was very strongly detectable. Scale Bar: 10 μm

C1q-HA does not alter the trafficking of HYAL2 to the cell membrane

HYAL2 has emerged as one of the genes upregulated upon C1q-bound HA MES stimulation and, based on flow cytometry assay, we observed that a small fraction of HYAL2 is exposed to the cell surface. We therefore aimed at understanding whether the amount of HYAL2 transported to, or maintained at, the plasma membrane could be affected by C1q-bound HA as compared to HA alone. To this end, MES cells were seeded onto different matrices and, after 12 h, were subjected to surface biotinylation assay. Cell surface proteins were treated with the membrane-impermeant sulfo-NHS-biotin reagent, then isolated by binding to Streptavidin beads and probed with anti-HYAL2 antibody. To check for unspecific protein binding during surface biotinylation experiments, MES not labelled with biotin were processed together with biotinylated samples. Western blot detecting the intracellular actin was included to ensure that similar amount of total lysates, biotinylated or not, were incubated with Streptavidin beads. No major differences on the total content of membrane-localized HYAL2 was observed in cells seeded on C1q-bound HA as compared to HA alone **(Figure 21)**. These results seem to exclude the involvement of C1q-bound HA in drammatically affecting HYAL2 transport and/or turnover at the plasma membrane of mesothelioma cancer cells.

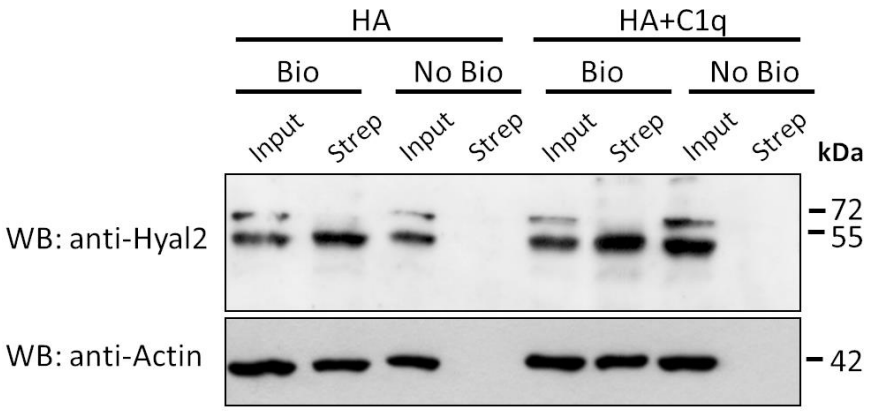

Figure 21. HYAL2 surface biotinylation assay. MES cells were seeded onto HA or HA+C1q and after 12 h of incubation on matrixes cell surface proteins were treated with the membrane-impermeant sulfo-NHS-biotin reagent, then isolated by binding to Streptavidin beads and probed with anti-HYAL2 antibody (Bio). To check for unspecific protein binding during surface biotinylation experiment, not labelled samples with biotin (No Bio) were processed together with biotinylated samples. Samples were normalized on intracellular β-actin level. No differences about the total content of membrane-localized HYAL-2 were observed between cells seeded on C1q- as compared to HA alone.

LMW-HAs are inducers of H_2O_2 production by MES

It has been extensively demonstrated that reactive oxygen species (ROS) production is triggered by pro-inflammatory LMW-HA (Grishko et al., 2009).

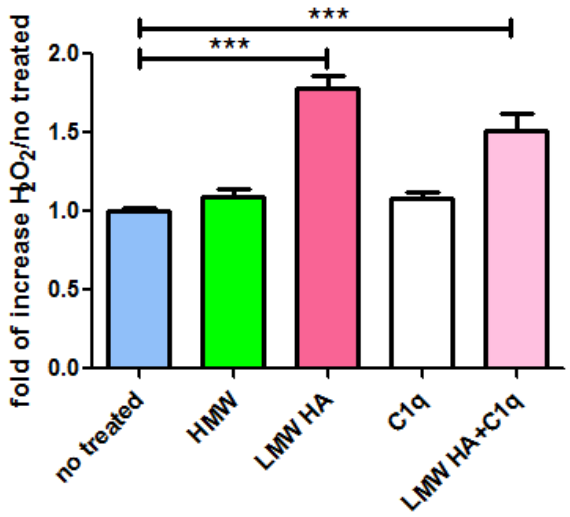

Figure 22. Extracellular production of ROS increased by LMW HA in MES cells. H_2O_2 production by LMW HA-stimulated MES cells has been shown to be higher comparable with the MES stimulated with HMW HA or C1q alone. The fluorescence (F.U.) was measured on Tecan (E/I 535nm/595nm). The means of three to five experiments performed in triplicate are reported ± SEM. ***<0,0001

We therefore aimed to test whether MES cells are able to synhtesise ROS and, most importantly, whether C1q would be able to affect their production. To this aim MES cells were stimulated with C1q, HA, LMW-HA, and LMW-HA in the presence of C1q and H_2O_2 released into the medium was measured 5 min after stimulation using Ampiflu Red reagent. ROS production was enhaced by LMW-HA treatment regardeless of the presence or absence of C1q, thus suggesting that the complement component is uneffective as shown on **Figure 22**.

DISCUSSION

Malignant pleural mesothelioma (MPM) is an highly aggressive cancer, which arises from the mesothelium lining the pleura and it is associated with a massive exposure to asbestos fibres. In USA, MPM accounts for 10 cases/million since the incidence in UK and Australia increases up on 30 cases per million (Robinson, 2012). In Europe the peak is expected around 2020 due to the long latency period between asbestos exposure and diagnosis (30–50 years) and, due to the fact that exposure to asbestos fibers had just started in 1970 (Peto et al., 1999). A lot of efforts have been made to find out efficient therapies to cure the disease, being the standard frontline treatment, namely cisplatin plus pemetrexed chemotherapy, of quite insufficient efficacy, and no additional validated treatments beyond this first-line therapy are available nowadays (Scherpereel et al., 2018). The development of new therapeutic strategies has been hampered by the poor understandings of the pathobiology of the disease and the molecular mechanisms underlying the formation and progression of MPM.

The establishment of primary cell lines represents an important tool in the study of mesothelioma at cellular, molecular and genetic levels as well as to test the efficacy of new therapeutic approaches. We established 17 primary mesothelioma cell lines derived from 16 males and only 1 female diagnosed for MPM. Based on the histological characterization 11 cases belonged to the epithelioid histotype, 2 cases were sarcomatoid, 2 biphasic and only for 2 of them it was not possible to achieve a clear determination of the histotype.

Mesothelioma cells have been isolated from pleural biopsy speciments following the protocol previously described (Agostinis et al., 2017b). All MES cells were morphologically and immunophenotypically characterized for the expression of several markers known to be expressed by this type of cancer such as mesothelin, epithelial cytokeratin 8/18 (CK8/18), cell surface HA-binding glycoprotein CD44, Epithelial-Membrane Antigen (EMA), mesenchymal CD9 and vimentin. MES were negative for the common lymphocyte antigen CD45, the monocyte differentiation antigen CD14 and the endothelial marker von Willebrand Factor (vWF). All MES cells were also tested for CD68, a standard macrophages marker, predominantly localized in late endosomal and lysosomal compartments (Ramprasad et al., 1995). Surprisingly we observed that MES cells express, on their surface, the macrophage CD68, as already reported by Philippeaux and colleagues (Philippeaux et al., 2004a). Moreover, high positivity for CD68 was shown on primary human fibroblast, thus clearly demonstrating that the expression of CD68 is not restricted to the macrophage lineage (Kunz-

Schughart et al., 2003). CD68 may provide an additional antigenic marker for the diagnosis of mesothelioma, as already suggested by Philippeaux (Philippeaux et al., 2004b).

In the present study it was clearly demonstrated that MES cells are actively involved in HA synthesis, and this HA is not only deposited in the extracellular space to build up the so-called pericellular coat but also a consistent amount of it is sequestered inside the cell.
The intracellular HA was visualized using specific hyaluronan-binding proteins conjugated to biotin and detected by fluorescently labeled Strepavidin. Hyaluronan staining appeared to fill the entire cell, as round vesicular/globular structures, but also as a diffuse pattern often particularly prominent in the perinuclear region. FA-HA up-take as well as double-labeling experiments performed with EE1A and Lamp1, well-established markers of the endocytic system (data not shown), seem to exclude the possibility that this intracellular HA derives from the internalization of an extracellular pool. The first reports attesting the presence of HA in the cytoplasm were published in the 1970s. Since then intracellular HA has been identified in the rough endoplasmic reticulum (Londoño and Bendayan, 1988), in the nucleus, mostly associated with the nuclear periphery and/or nucleoli (Evanko and Wight, 1999), and in the caveolated portions of the plasma membrane (Eggli and Graber, 1995). This phenomenon was observed in a variety of cells, including smooth muscle cells, endothelial cells, fibroblasts, normal mammary epithelial cells, mammary tumor cells and epidermal keratinocytes, but the functional consequences of this distribution are still poorly understood.
From studies available in the literature, intracellular hyaluronan may be involved in growth regulation and mitosis. An increase in intracellular hyaluronan was in fact detected in 3T3 cells that have been growth-arrested by serum deprivation and subsequently stimulated by serum or platelet-derived growth factor (PDGF). Under these conditions, intracellular hyaluronan appeared to be maximal in the rounded mitotic cells. A similar increase in intracellular HA was also seen in association with migration of keratinocytes following *in vitro* wounding assays (Rilla et al., 2002).
Only limited studies tried to address the source of intracellular hyaluronan, and up to now the mechanisms involved in its cytosplamic/nuclear synthesis/translocation are still not completely known. The recognition that hyaluronan is present intracellularly at key times during cell proliferation and migration suggests that it may have an intracellular mode of action in the regulation of these processes. MESs are actively dividing cancer cells, therefore the high abundance of intracellular HA is in line with what was observed in other types of proliferating cells. One emerging possibility is that the processes of synthesis, uptake,

translocation, and degradation of HA may be integral to the signalling and regulatory mechanisms associated with the intracellular hyaluronan-binding molecules (IHABPs), or hyaladherins. However, most of the functional aspects of intracellular hyaluronan are still quite speculative and will require further work to be fully elucidated.

Better known is the role played by the extracellular/pericellular HA that cancer cells produce autonomously and this production has emerged to represent an indicator of their aggressiveness. These HA pericellular matrices, in fact, seem to facilitate tumour growth and progression via several mechanisms. They organize and cluster HA receptors on the plasma membrane and sequester growth factors and cytokines near the cell membrane. Receptor clustering, in turn, induces the formation of plasma membrane microdomains, such as lipid rafts, which, in the presence of trapped growth factors and cytokines, can couple and sustain activation of driver oncogenic anti-apoptotic, and proinvasion/migration signal transduction cascades. Pericellular coats were also identified as favouring the adhesion of tumour cells to microvessel endothelium, as it has been shown for metastatic prostate carcinoma cells in culture (Simpson MA et al., 2002), and breast tumour cells (Veiseh M et al., 2014). It has been additionally proposed that pericellular HA matrices produce a cancer friendly microenvironment by stimulating the release of microvesicles from HA-rich cell microvilli (Koistinen et al., 2015).

Malignant pleural mesotheliomas is in most cases associated with an elevated synthesis of hyaluronan (Cortes-Dericks and Schmid, 2017; Fujimoto et al., 2013). HA, in fact, is normally secreted by mesothelial cells, being required for the proper lubrification of the pleural membrane. The amount of HA produced either by the tumour cells themselves or by adjacent noncancerous stromal cells has been directly correlated with the invasive and metastatic behaviour of mesothelioma.

Our studies allowed the identification of C1q as a key component of the mesothelioma microenvironment. By immunohistochemistry, C1q resulted abundantly expressed in all mesothelioma histological variants, being particularly high in the epithelioid histotype. We believe that the tumour-infiltrating myeloid elements, and possibly the endothelial cells of the small vessels, are the cell types responsible for its local synthesis and deposition. Indeed macrophages, together with other antigen presenting cells, are well-known producers of C1q molecules (Faust and Loos, 2002; Loos et al., 1989; Lubbers et al., 2017); endothelial cells can express several components of both classical and alternative pathways as well as C

regulatory proteins and C1q production was proven only for the endothelial cells of the decidua (Bulla et al., 2008).

Interestingly we demonstrated that C1q is able to interact with hyaluronan and this interaction is not accompanied by complement activation (Agostinis et al., 2017b; Bulla et al., 2016). These results prompted us to hypothesize that C1q bound HA can modify the signalling properties of the ECM rendering it even more permissive for the development and progression of the tumor (Agostinis et al., 2017b). Indeed we discovered that C1q bound to HA is more efficient, than C1q or HA alone, in enhancing adhesion, spreading and proliferation of MES cells. Moreover C1q-HA complex was able to activate more efficiently several cancer-related signalling pathways, as shown by the enhanced phosphorylation status of members of the MAPK family, ERK1/2, SAPK/JNK, and p38 (Agostinis et al., 2017b) and the mammalian target of rapamycin (mTOR) measured by PathScan approach.
It is interesting to note that the autocrine pericellular HA coats produced by cancer cells are not sufficient to achieve full metastatic features. It seems of critical importance that tumour cells acquire the ability to fragment and metabolize HA. Accumulating evidences support the notion that the so-called low molecular weight HA (LMW-HA) possesses biologic activites that are pretty diverse from high molecular mass form of HA. LMW-HAs are efficient inducer of angiogenesis and lymphangiogenesis, activities fundamental for the metastatic process; they can enhance adhesion and cell motility necessary for cancer cell invasion (Wu et al., 2015, 2014); moreover LMW-HAs were shown to induce the expression of several metalloproteinases which are involved in matrix degradation, thus contributing to cancer cells evasion and dissemination (Fieber, 2004).

HA can be fragmented by at least two mechansisms: it can undergo an enzymatic attack from one or more of several hyaluronidases (e.g. Hyal 1, 2 or 3) and/or it can be cleaved by oxygen (and nitrogen) free radicals that are usually elevated in the tumor microenvironment (Stern et al., 2007). Based on quantitative Reverse Transcription-PCR performed on several MES populations we consistently detected an increase in the mRNA expression of hyaluronidase HYAL2 upon seeding the cells on C1q-bound HA matrix. The upregulation of HYAL2 mRNA was associated with an increase in the expression of the corresponding protein, as detected by Western blot analysis. HYAL2 is a GPI anchored protein and this post-translational modification was shown to aid HYAL2 association with lipid rafts at the cell surface (Andre et al., 2011). HYAL2 can also exist in a soluble intracellular form lacking the

GPI anchor, in certain cell types (Chow et al., 2006). The presence of HYAL2 at the plasma membrane was long questioned due to the fact that the optimal pH for HYAL2 activity was supposed to be acidic since initial studies pointed to a lysosomal localization (Lepperdinger et al., 1998). In these experiments, the GFP-tag was attached to the C-terminus of HYAL2 and the tag was later found to prevent the addition of the GPI anchor to the hyaluronidase, thus hampering its correct targeting. Subsequent studies suggested HYAL2 to be localized to the cell surface, mitochondria and nucleus, leaving the localization of HYAL2 quite enigmatic (Chang, 2002; Chow et al., 2006).

Moreover, further *in vitro* characterizations demonstrated that HYAL2 has an intrinsically very weak enzymatic activity that can be fuelled upon its interaction with CD44, the main receptor for HA, which is also associated to lipid rafts (Harada and Takahashi, 2007). Based on recent findings the following model for HYAL2 functioning has been proposed: first of all, the main site of action of HYAL2 is considered to be the plasma membrane; second, HYAL2 strictly relies on CD44 interaction to actively degrade HA of the pericellular coat; third, CD44, localized in membrane microdomains enriched in cholesterol and gangliosides, is able to recruit a specific Na^+-H^+ exchanger whose activity leads to a local acidification with a concomitant upregulation of HYAL2 catalytic activity (Bourguignon et al., 2004; Harada and Takahashi, 2007). Recent observations also pointed to an additional role of HYAL2 that is independent from its hyaluronidase activity: upon association, it is able to decluster CD44, thus hampering CD44 ability to bind surface HA and making the pericellual coat even more accessible to HYAL-2 mediated break-up (Duterme et al., 2009). This phenomenon has been described mostly in cancer cells, where it can be induced by HA oligosaccharides, and it seems to play a critical role in tumour cell migration (Duterme et al., 2009). Based on our flow citometry assays and surface biotinylation experiments we were able to detect HYAL2 on the cell surface of MES cells and we estimate that about 30% of the total HYAL2 is indeed exposed to the extracellular space ready to degrade HA.

Although HYAL2 was accessible to biotin labeling at the cell surface, a large proportion of it was present within the cell. We therefore performed co-immunolabelling experiments with several markers of the endocytic-endosomal compartments as well as of the secretory pathway, and we analyzed them at the confocal microscope. As expected for a GPI-anchored molecule, HYAL2 co-localization with the ER resident protein Calnexin was pretty much intense, in agreement with the results obtained by Bourguignon and colleagues (Bourguignon and Flamion, 2016; Rai et al., 2001).

Interestingly, the highest overlap was observed when gC1q receptor (gC1qR) was investigated in HYAL2 co-labeling experiments. gC1qR is a multifunctional and ubiquitously expressed cellular protein, maily present on the mitochondria matrix (Dedio et al., 1998; Muta et al., 1997) but also found in several other intracellular compartments, such as the endoplasmic reticulum, the nucleus, and the cell surface, possibly associated with lipid rafts (Braun et al., 2000; Ghebrehiwet et al., 2001; Kittlesen et al., 2000). Three laboratories have discovered almost simultaneously gC1qR and named this protein differently. In 1994 Ghebrehiwet and colleagues identified this protein as the receptor for the globular head of the C1q complement component (Ghebrehiwet et al., 1994), but almost a decade before the same molecule was named hyaluronan-binding protein 1 (HABP1) based on its ability to interact with high affinity to HA and referred to as hyaluronectin (D'Souza and Datta, 1985). Finally gC1q was also cloned as the p32 subunit of the human pre-mRNA splicing factor SF2 (Honoré et al., 1993). Over several decades from its identification, myriad of proteins have been reported to bind to gC1qR/HABP1/p32, underlying the complex role this protein can play in different cellular processes and at different subcellular districts (Saha and Datta, 2018).

The data collected in our MES populations showed that HYAL2 and gC1qR are following overlapping trafficking pathways inside the cell, suggesting that they could form a "functional complex" at the plasma membrane, being both proteins able to associate with lipid rafts. As a consequence, HYAL2/gC1qR may be found in close proximity to CD44, which is known to interact directly with HYAL2, and whose interaction is essential to upregulate HYAL2 catalytic activity. Taking into account that CD44 and gC1qR are both hyalaldherins, their proximity may create high affinity anchorage spots for pericellular HA, thus making it more available for HYAL2 mediated degradation. It is tempting to speculate that gC1qR, while recruited by HYAL2/CD44, could undergo conformational changes, thus exposing its binding sites for the C1q globular heads. In this way C1q present in the tumor microenvironment could be enrolled into such macromolecular signalling complex, where it will be able to promote signalling events *via* CD44 and/or gC1qR itself. Even though highly speculative, this proposed working model herein illustrated takes into account the different binding affinities gC1qR shows toward its ligands. In fact the affinity of gC1qR for hyaluronan is 100 time higher than that for C1q globular heads (Kd 1×10^{-9}M for HA and Kd 1×10^{-7}M for gC1q), at least under physilogical conditions (collected in review Saha and Datta 2018). Being HA highly packed in the pericellular matrix, it seems more plausible that gC1qR may select HA,

instead of C1q, as the preferential binding partner. An additional, but not mutually exclusive, possibility is that C1q, by interacting with HA as an hyalalderin, could affect the three-dimensional conformation of HA bound to it, making HA more available for CD44 and/or gC1qR interaction. Based on the pull-down experiments performed upon surface biotinylation we did not detect significant differences in the surface expression of HYAL2 upon HA or HA-bound C1q stimulation, while, at the protein level, total HYAL2 appeared to be upregulated on HA-C1q matrix. On one hand, an increase in HYAL2 surface abundance could have explained a higher rate of HA degradation, which is connected with the aggressiveness of the tumour, and therefore expected to occur during mesothelioma progression. On the other hand, it could be plausible that the catalytic activity of HYAL2, in complex with CD44 and possibly with gC1qR, both engaged in HA interaction, is further enhaced by C1q, whithout the need of significant changes in its surface recruitment. Further studies will be needed to dissect all the mechanistic steps involved in this complex network of interactions and to carefully monitor changes in the catalytic activity of HYAL2.

LMW-HA production in the tumor microenvironment could also be supplied by reactive oxygen species (ROS) (Grishko et al., 2009)-mediated breakage of pericellular/extracellular HA. MES cells stimulated with LMW-HA were found to increase their ROS production as compared to HMW-HA but the concomitant presence of C1q was totally uneffective. Therefore we can conclude that C1q, together with HA, can be seen as the initial driver of HA enzymatic degradation *via* HYAL2, leading to LMW-HA deposition in the tumour microenvironment which in turn favours ROS production and further HA degradation.

In our analysis of HYAL2 intracellular distribution we often observed bright spots of HYAL2 immunoreactivity specifically localized within the nucleus of MES. Even though we still neglet what are the functional consequences of this nuclear translocation, it is worth mentioning that very recently the group of Meran and colleagues (Midgley et al., 2017) identified HYAL2 as a key regulator of pre-mRNA splicing, dictating the production of CD44 variants at the cell surface. The genomic organization of CD44 relies indeed on twenty exons. The first five and the last five exons are constant whereas the ten exons located between these regions undergo to alternative splicing (Naor et al., 1997). The smallest molecule (85–95 kDa), which lacks the whole variable region, is the standard CD44 (CD44s) whereas CD44v6 (CD44 variant exon 6) is the major CD44 isoform that regulates tumour invasion, progression and metastasis (Salmi et al., 1993). Several MPM cell lines were shown to be positive for CD44v9 (variable exon 9), including the CD44v8-10, the former being statistically associated

with NF2 (neurofibromatosis type 2), a common feature of MPM. In this context, it will be important to establish which CD44 splice variants are expressed by our primary mesothelioma cell populations.

CONCLUSION

In conclusion, we provided evidences that C1q is highly abundant in malignant pleural mesothelioma tissues of all hystotype variants (epithelioid, sarcomatoid and biphasic), it interacts with HA, another key player in tumour growth and progression, whose increased synthesis has been clearly attested in several MPM patients, and it interferes with adhesion, migration and proliferation of MES cells. Interestingly, we demonstrated that C1q, in concert with HA, can alter the signalling properties of the tumour microenvironment, rendering it even more permissive to cancer survival, growth and migration, through the promotion of HA catabolism and the activation of several cancer-related signalling pathways.

BIBLIOGRAPHY

Adamia, S., Pilarski, P.M., Belch, A.R., Pilarski, L.M., 2013. Aberrant Splicing, Hyaluronan Synthases and Intracellular Hyaluronan as Drivers of Oncogenesis and Potential Drug Targets. Current Cancer Drug Targets 13, 347–361. https://doi.org/10.2174/1568009611313040001

Afify, A.M., Stern, R., Michael, C.W., 2005. Differentiation of mesothelioma from adenocarcinoma in serous effusions: the role of hyaluronic acid and CD44 localization. Diagn. Cytopathol. 32, 145–150. https://doi.org/10.1002/dc.20201

Agostinis, C., Bulla, R., Tripodo, C., Gismondi, A., Stabile, H., Bossi, F., Guarnotta, C., Garlanda, C., De Seta, F., Spessotto, P., Santoni, A., Ghebrehiwet, B., Girardi, G., Tedesco, F., 2010. An Alternative Role of C1q in Cell Migration and Tissue Remodeling: Contribution to Trophoblast Invasion and Placental Development. The Journal of Immunology 185, 4420–4429. https://doi.org/10.4049/jimmunol.0903215

Agostinis, C., Tedesco, F., Bulla, R., 2017a. Alternative functions of the complement protein C1q at embryo implantation site. Journal of Reproductive Immunology 119, 74–80. https://doi.org/10.1016/j.jri.2016.09.001

Agostinis, C., Vidergar, R., Belmonte, B., Mangogna, A., Amadio, L., Geri, P., Borelli, V., Zanconati, F., Tedesco, F., Confalonieri, M., Tripodo, C., Kishore, U., Bulla, R., 2017b. Complement Protein C1q Binds to Hyaluronic Acid in the Malignant Pleural Mesothelioma Microenvironment and Promotes Tumor Growth. Front Immunol 8, 1559. https://doi.org/10.3389/fimmu.2017.01559

Alawieh, A., Tomlinson, S., 2016. Injury site-specific targeting of complement inhibitors for treating stroke. Immunological Reviews 274, 270–280. https://doi.org/10.1111/imr.12470

Albrecht, E.A., Chinnaiyan, A.M., Varambally, S., Kumar-Sinha, C., Barrette, T.R., Sarma, J.V., Ward, P.A., 2004. C5a-induced gene expression in human umbilical vein endothelial cells. Am. J. Pathol. 164, 849–859. https://doi.org/10.1016/S0002-9440(10)63173-2

Amara, U., Rittirsch, D., Flierl, M., Bruckner, U., Klos, A., Gebhard, F., Lambris, J.D., Huber-Lang, M., 2008. Interaction between the coagulation and complement system. Adv. Exp. Med. Biol. 632, 71–79.

Andre, B., Duterme, C., Van Moer, K., Mertens-Strijthagen, J., Jadot, M., Flamion, B., 2011. Hyal2 is a glycosylphosphatidylinositol-anchored, lipid raft-associated hyaluronidase. Biochem. Biophys. Res. Commun. 411, 175–179. https://doi.org/10.1016/j.bbrc.2011.06.125

Anttila, M.A., Tammi, R.H., Tammi, M.I., Syrjänen, K.J., Saarikoski, S.V., Kosma, V.M., 2000. High levels of stromal hyaluronan predict poor disease outcome in epithelial ovarian cancer. Cancer Res. 60, 150–155.

Aruffo, A., Stamenkovic, I., Melnick, M., Underhill, C.B., Seed, B., 1990. CD44 is the principal cell surface receptor for hyaluronate. Cell 61, 1303–1313.

Attanoos, R.L., Gibbs, A.R., 1997. Pathology of malignant mesothelioma. Histopathology 30, 403–418.

Auvinen, P., Tammi, R., Parkkinen, J., Tammi, M., Agren, U., Johansson, R., Hirvikoski, P., Eskelinen, M., Kosma, V.M., 2000. Hyaluronan in peritumoral stroma and malignant cells associates with breast cancer spreading and predicts survival. Am. J. Pathol. 156, 529–536. https://doi.org/10.1016/S0002-9440(10)64757-8

Barrallo-Gimeno, A., 2005. The Snail genes as inducers of cell movement and survival: implications in development and cancer. Development 132, 3151–3161. https://doi.org/10.1242/dev.01907

Bexborn, F., Andersson, P.O., Chen, H., Nilsson, B., Ekdahl, K.N., 2008. The tick-over theory revisited: formation and regulation of the soluble alternative complement C3 convertase (C3(H2O)Bb). Mol. Immunol. 45, 2370–2379. https://doi.org/10.1016/j.molimm.2007.11.003

Bianchi, A.B., Mitsunaga, S.I., Cheng, J.Q., Klein, W.M., Jhanwar, S.C., Seizinger, B., Kley, N., Klein-Szanto, A.J., Testa, J.R., 1995. High frequency of inactivating mutations in the neurofibromatosis type 2 gene (NF2) in primary malignant mesotheliomas. Proc. Natl. Acad. Sci. U.S.A. 92, 10854–10858.

Biró, A., Thielens, N.M., Cervenák, L., Prohászka, Z., Füst, G., Arlaud, G.J., 2007. Modified low density lipoproteins differentially bind and activate the C1 complex of complement. Molecular Immunology 44, 1169–1177. https://doi.org/10.1016/j.molimm.2006.06.013

Bjørge, L., Hakulinen, J., Vintermyr, O.K., Jarva, H., Jensen, T.S., Iversen, O.E., Meri, S., 2005. Ascitic complement system in ovarian cancer. Br. J. Cancer 92, 895–905. https://doi.org/10.1038/sj.bjc.6602334

Bleckmann, A., Siam, L., Klemm, F., Rietkötter, E., Wegner, C., Kramer, F., Beissbarth, T., Binder, C., Stadelmann, C., Pukrop, T., 2013. Nuclear LEF1/TCF4 correlate with poor prognosis but not with nuclear β-catenin in cerebral metastasis of lung adenocarcinomas. Clinical & Experimental Metastasis 30, 471–482. https://doi.org/10.1007/s10585-012-9552-7

Bonifati, D.M., Kishore, U., 2007. Role of complement in neurodegeneration and neuroinflammation. Mol. Immunol. 44, 999–1010. https://doi.org/10.1016/j.molimm.2006.03.007

Bora, P.S., Sohn, J.-H., Cruz, J.M.C., Jha, P., Nishihori, H., Wang, Y., Kaliappan, S., Kaplan, H.J., Bora, N.S., 2005. Role of complement and complement membrane attack complex in laser-induced choroidal neovascularization. J. Immunol. 174, 491–497.

Bossi, F., Tripodo, C., Rizzi, L., Bulla, R., Agostinis, C., Guarnotta, C., Munaut, C., Baldassarre, G., Papa, G., Zorzet, S., Ghebrehiwet, B., Ling, G.S., Botto, M., Tedesco, F., 2014. C1q as a unique player in angiogenesis with therapeutic implication in wound healing. Proc. Natl. Acad. Sci. U.S.A. 111, 4209–4214. https://doi.org/10.1073/pnas.1311968111

Bott, M., Brevet, M., Taylor, B.S., Shimizu, S., Ito, T., Wang, L., Creaney, J., Lake, R.A., Zakowski, M.F., Reva, B., Sander, C., Delsite, R., Powell, S., Zhou, Q., Shen, R., Olshen, A., Rusch, V., Ladanyi, M., 2011. The nuclear deubiquitinase BAP1 is commonly inactivated by somatic mutations and 3p21.1 losses in malignant pleural mesothelioma. Nat. Genet. 43, 668–672. https://doi.org/10.1038/ng.855

Bourguignon, L.Y.W., Singleton, P.A., Diedrich, F., Stern, R., Gilad, E., 2004. CD44 interaction with Na+-H+ exchanger (NHE1) creates acidic microenvironments leading to hyaluronidase-2 and

cathepsin B activation and breast tumor cell invasion. J. Biol. Chem. 279, 26991–27007. https://doi.org/10.1074/jbc.M311838200

Bourguignon, V., Flamion, B., 2016. Respective roles of hyaluronidases 1 and 2 in endogenous hyaluronan turnover. FASEB J. 30, 2108–2114. https://doi.org/10.1096/fj.201500178R

Boutin, C., Dumortier, P., Rey, F., Viallat, J.R., De Vuyst, P., 1996. Black spots concentrate oncogenic asbestos fibers in the parietal pleura. Thoracoscopic and mineralogic study. Am. J. Respir. Crit. Care Med. 153, 444–449. https://doi.org/10.1164/ajrccm.153.1.8542156

Braun, L., Ghebrehiwet, B., Cossart, P., 2000. gC1q-R/p32, a C1q-binding protein, is a receptor for the InlB invasion protein of Listeria monocytogenes. EMBO J. 19, 1458–1466. https://doi.org/10.1093/emboj/19.7.1458

Brodsky-Doyle, B., Leonard, K.R., Reid, K.B., 1976. Circular-dichroism and electron-microscopy studies of human subcomponent C1q before and after limited proteolysis by pepsin. Biochem. J. 159, 279–286.

Brown, D.M., Beswick, P.H., Donaldson, K., 1999. Induction of nuclear translocation of NF-kappaB in epithelial cells by respirable mineral fibres. J. Pathol. 189, 258–264. https://doi.org/10.1002/(SICI)1096-9896(199910)189:2<258::AID-PATH410>3.0.CO;2-E

Bu, X., Zheng, Z., Wang, C., Yu, Y., 2007. Significance of C4d deposition in the follicular lymphoma and MALT lymphoma and their relationship with follicular dendritic cells. Pathol. Res. Pract. 203, 163–167. https://doi.org/10.1016/j.prp.2006.11.004

Budzko, D.B., Lachmann, P.J., McConnell, I., 1976. Activation of the alternative complement pathway by lymphoblastoid cell lines derived from patients with Burkitt's lymphoma and infectious mononucleosis. Cell. Immunol. 22, 98–109.

Bulla, R., Agostinis, C., Bossi, F., Rizzi, L., Debeus, A., Tripodo, C., Radillo, O., De Seta, F., Ghebrehiwet, B., Tedesco, F., 2008. Decidual endothelial cells express surface-bound C1q as a molecular bridge between endovascular trophoblast and decidual endothelium. Mol. Immunol. 45, 2629–2640. https://doi.org/10.1016/j.molimm.2007.12.025

Bulla, R., Tripodo, C., Rami, D., Ling, G.S., Agostinis, C., Guarnotta, C., Zorzet, S., Durigutto, P., Botto, M., Tedesco, F., 2016. C1q acts in the tumour microenvironment as a cancer-promoting factor independently of complement activation. Nature Communications 7, 10346. https://doi.org/10.1038/ncomms10346

Busacca, S., Germano, S., De Cecco, L., Rinaldi, M., Comoglio, F., Favero, F., Murer, B., Mutti, L., Pierotti, M., Gaudino, G., 2010. MicroRNA signature of malignant mesothelioma with potential diagnostic and prognostic implications. Am. J. Respir. Cell Mol. Biol. 42, 312–319. https://doi.org/10.1165/rcmb.2009-0060OC

Carli, M., Bucolo, C., Pannunzio, M.T., Ongaro, G., Businaro, R., Revoltella, R., 1979. Fluctuation of serum complement levels in children with neuroblastoma. Cancer 43, 2399–2404.

Carmeliet, P., 2003. Angiogenesis in health and disease. Nat. Med. 9, 653–660. https://doi.org/10.1038/nm0603-653

Carroll, M.C., Isenman, D.E., 2012. Regulation of Humoral Immunity by Complement. Immunity 37, 199–207. https://doi.org/10.1016/j.immuni.2012.08.002

Chang, N.-S., 2002. Transforming growth factor-beta1 blocks the enhancement of tumor necrosis factor cytotoxicity by hyaluronidase Hyal-2 in L929 fibroblasts. BMC Cell Biol. 3, 8.

Chen, W.Y., Abatangelo, G., 1999. Functions of hyaluronan in wound repair. Wound Repair Regen 7, 79–89.

Chew, S.H., Toyokuni, S., 2015. Malignant mesothelioma as an oxidative stress-induced cancer: An update. Free Radic. Biol. Med. 86, 166–178. https://doi.org/10.1016/j.freeradbiomed.2015.05.002

Chow, G., Knudson, C.B., Knudson, W., 2006. Human hyaluronidase-2 is localized intracellularly in articular chondrocytes and other cultured cell lines. Osteoarthritis and Cartilage 14, 1312–1314. https://doi.org/10.1016/j.joca.2006.08.005

Chowdhury, B., Hemming, R., Faiyaz, S., Triggs-Raine, B., 2016. Hyaluronidase 2 (HYAL2) is expressed in endothelial cells, as well as some specialized epithelial cells, and is required for normal hyaluronan catabolism. Histochemistry and Cell Biology 145, 53–66. https://doi.org/10.1007/s00418-015-1373-8

Corrales, L., Ajona, D., Rafail, S., Lasarte, J.J., Riezu-Boj, J.I., Lambris, J.D., Rouzaut, A., Pajares, M.J., Montuenga, L.M., Pio, R., 2012. Anaphylatoxin C5a creates a favorable microenvironment for lung cancer progression. J. Immunol. 189, 4674–4683. https://doi.org/10.4049/jimmunol.1201654

Cortes-Dericks, L., Schmid, R.A., 2017. CD44 and its ligand hyaluronan as potential biomarkers in malignant pleural mesothelioma: evidence and perspectives. Respir. Res. 18, 58. https://doi.org/10.1186/s12931-017-0546-5

Costello, L.C., Franklin, R.B., 2005. “Why do tumour cells glycolyse?”: from glycolysis through citrate to lipogenesis. Mol. Cell. Biochem. 280, 1–8.

Coussens, L.M., Werb, Z., 2002. Inflammation and cancer. Nature 420, 860–867. https://doi.org/10.1038/nature01322

Cyphert, J.M., Trempus, C.S., Garantziotis, S., 2015. Size Matters: Molecular Weight Specificity of Hyaluronan Effects in Cell Biology. Int J Cell Biol 2015, 563818. https://doi.org/10.1155/2015/563818

Danesh, J., Wheeler, J.G., Hirschfield, G.M., Eda, S., Eiriksdottir, G., Rumley, A., Lowe, G.D.O., Pepys, M.B., Gudnason, V., 2004. C-reactive protein and other circulating markers of inflammation in the prediction of coronary heart disease. N. Engl. J. Med. 350, 1387–1397. https://doi.org/10.1056/NEJMoa032804

de Klerk, N., Reid, A., 2017. Hazards of residential exposure to household asbestos. Lancet Public Health 2, e490–e491. https://doi.org/10.1016/S2468-2667(17)30200-1

de la Motte, C., Nigro, J., Vasanji, A., Rho, H., Kessler, S., Bandyopadhyay, S., Danese, S., Fiocchi, C., Stern, R., 2009. Platelet-derived hyaluronidase 2 cleaves hyaluronan into fragments that trigger

monocyte-mediated production of proinflammatory cytokines. Am. J. Pathol. 174, 2254–2264. https://doi.org/10.2353/ajpath.2009.080831

Dechert, T.A., Ducale, A.E., Ward, S.I., Yager, D.R., 2006. Hyaluronan in human acute and chronic dermal wounds. Wound Repair Regen 14, 252–258. https://doi.org/10.1111/j.1743-6109.2006.00119.x

Dedio, J., Jahnen-Dechent, W., Bachmann, M., Müller-Esterl, W., 1998. The multiligand-binding protein gC1qR, putative C1q receptor, is a mitochondrial protein. J. Immunol. 160, 3534–3542.

Dicker, K.T., Gurski, L.A., Pradhan-Bhatt, S., Witt, R.L., Farach-Carson, M.C., Jia, X., 2014. Hyaluronan: a simple polysaccharide with diverse biological functions. Acta Biomater 10, 1558–1570. https://doi.org/10.1016/j.actbio.2013.12.019

Donaldson, K., Murphy, F.A., Duffin, R., Poland, C.A., 2010. Asbestos, carbon nanotubes and the pleural mesothelium: a review of the hypothesis regarding the role of long fibre retention in the parietal pleura, inflammation and mesothelioma. Part Fibre Toxicol 7, 5. https://doi.org/10.1186/1743-8977-7-5

Dostert, C., Pétrilli, V., Van Bruggen, R., Steele, C., Mossman, B.T., Tschopp, J., 2008. Innate immune activation through Nalp3 inflammasome sensing of asbestos and silica. Science 320, 674–677. https://doi.org/10.1126/science.1156995

D'Souza, M., Datta, K., 1985. Evidence for naturally occurring hyaluronic acid binding protein in rat liver. Biochem. Int. 10, 43–51.

Duterme, C., Mertens-Strijthagen, J., Tammi, M., Flamion, B., 2009. Two Novel Functions of Hyaluronidase-2 (Hyal2) Are Formation of the Glycocalyx and Control of CD44-ERM Interactions. Journal of Biological Chemistry 284, 33495–33508. https://doi.org/10.1074/jbc.M109.044362

Eggli, P.S., Graber, W., 1995. Association of hyaluronan with rat vascular endothelial and smooth muscle cells. J. Histochem. Cytochem. 43, 689–697.

Ettinger, D.S., Akerley, W., Borghaei, H., Chang, A., Cheney, R.T., Chirieac, L.R., D'Amico, T.A., Demmy, T.L., Ganti, A.K.P., Govindan, R., Grannis, F.W., Horn, L., Jahan, T.M., Jahanzeb, M., Kessinger, A., Komaki, R., Kong, F.-M.S., Kris, M.G., Krug, L.M., Lennes, I.T., Loo, B.W., Martins, R., O'Malley, J., Osarogiagbon, R.U., Otterson, G.A., Patel, J.D., Schenck, M.P., Pisters, K.M., Reckamp, K., Riely, G.J., Rohren, E., Swanson, S.J., Wood, D.E., Yang, S.C., National Comprehensive Cancer Network, 2012. Malignant pleural mesothelioma. J Natl Compr Canc Netw 10, 26–41.

Evanko, S.P., Wight, T.N., 1999. Intracellular Localization of Hyaluronan in Proliferating Cells. Journal of Histochemistry & Cytochemistry 47, 1331–1341. https://doi.org/10.1177/002215549904701013

Faust, D., Loos, M., 2002. In vitro modulation of C1q mRNA expression and secretion by interleukin-1, interleukin-6, and interferon-gamma in resident and stimulated murine peritoneal macrophages. Immunobiology 206, 368–376.

Feng, X., Tonnesen, M.G., Peerschke, E.I.B., Ghebrehiwet, B., 2002. Cooperation of C1q receptors and integrins in C1q-mediated endothelial cell adhesion and spreading. J. Immunol. 168, 2441–2448.

Fieber, C., 2004. Hyaluronan-oligosaccharide-induced transcription of metalloproteases. Journal of Cell Science 117, 359–367. https://doi.org/10.1242/jcs.00831

Frade, R., Rodrigues-Lima, F., Huang, S., Xie, K., Guillaume, N., Bar-Eli, M., 1998. Procathepsin-L, a proteinase that cleaves human C3 (the third component of complement), confers high tumorigenic and metastatic properties to human melanoma cells. Cancer Res. 58, 2733–2736.

Fraser, D.A., Pisalyaput, K., Tenner, A.J., 2010. C1q enhances microglial clearance of apoptotic neurons and neuronal blebs, and modulates subsequent inflammatory cytokine production. J. Neurochem. 112, 733–743. https://doi.org/10.1111/j.1471-4159.2009.06494.x

Fraser, J.R., Laurent, T.C., Laurent, U.B., 1997. Hyaluronan: its nature, distribution, functions and turnover. J. Intern. Med. 242, 27–33.

Frost, G.I., Csóka, A.B., Wong, T., Stern, R., Csóka, T.B., 1997. Purification, cloning, and expression of human plasma hyaluronidase. Biochem. Biophys. Res. Commun. 236, 10–15.

Fujimoto, N., Gemba, K., Asano, M., Fuchimoto, Y., Wada, S., Ono, K., Ozaki, S., Kishimoto, T., 2013. Hyaluronic acid in the pleural fluid of patients with malignant pleural mesothelioma. Respiratory Investigation 51, 92–97. https://doi.org/10.1016/j.resinv.2013.02.002

Füst, G., Miszlay, Z., Czink, E., Varga, L., Pálóczi, K., Szegedi, G., Hollán, S.R., 1987. C1 and C4 abnormalities in chronic lymphocytic leukaemia and their significance. Immunol. Lett. 14, 255–259.

Galateau-Salle, F., Churg, A., Roggli, V., Travis, W.D., World Health Organization Committee for Tumors of the Pleura, 2016. The 2015 World Health Organization Classification of Tumors of the Pleura: Advances since the 2004 Classification. J Thorac Oncol 11, 142–154. https://doi.org/10.1016/j.jtho.2015.11.005

Ghebrehiwet, B., CebadaMora, C., Tantral, L., Jesty, J., Peerschke, E.I.B., 2006. gC1qR/p33 serves as a molecular bridge between the complement and contact activation systems and is an important catalyst in inflammation. Adv. Exp. Med. Biol. 586, 95–105. https://doi.org/10.1007/0-387-34134-X_7

Ghebrehiwet, B., Hosszu, K.H., Peerschke, E.I.B., 2017. C1q as an autocrine and paracrine regulator of cellular functions. Molecular Immunology 84, 26–33. https://doi.org/10.1016/j.molimm.2016.11.003

Ghebrehiwet, B., Kandov, E., Kishore, U., Peerschke, E.I.B., 2018. Is the A-Chain the Engine That Drives the Diversity of C1q Functions? Revisiting Its Unique Structure. Frontiers in Immunology 9. https://doi.org/10.3389/fimmu.2018.00162

Ghebrehiwet, B., Lim, B.L., Kumar, R., Feng, X., Peerschke, E.I., 2001. gC1q-R/p33, a member of a new class of multifunctional and multicompartmental cellular proteins, is involved in inflammation and infection. Immunol. Rev. 180, 65–77.

Ghebrehiwet, B., Lim, B.L., Peerschke, E.I., Willis, A.C., Reid, K.B., 1994. Isolation, cDNA cloning, and overexpression of a 33-kD cell surface glycoprotein that binds to the globular “heads” of C1q. J. Exp. Med. 179, 1809–1821.

Girardi, G., Yarilin, D., Thurman, J.M., Holers, V.M., Salmon, J.E., 2006. Complement activation induces dysregulation of angiogenic factors and causes fetal rejection and growth restriction. The Journal of Experimental Medicine 203, 2165–2175. https://doi.org/10.1084/jem.20061022

Gmiński, J., Mykała-Cieśla, J., Machalski, M., Drózdz, M., Najda, J., 1992. Immunoglobulins and complement components levels in patients with lung cancer. Rom J Intern Med 30, 39–44.

Goldberg, M., Luce, D., 2009. The health impact of nonoccupational exposure to asbestos: what do we know? Eur. J. Cancer Prev. 18, 489–503. https://doi.org/10.1097/CEJ.0b013e32832f9bee

Gonzalez, J.M., Franzke, C.-W., Yang, F., Romero, R., Girardi, G., 2011. Complement activation triggers metalloproteinases release inducing cervical remodeling and preterm birth in mice. Am. J. Pathol. 179, 838–849. https://doi.org/10.1016/j.ajpath.2011.04.024

Goswami, C.P., Nakshatri, H., 2014. PROGgeneV2: enhancements on the existing database. BMC Cancer 14, 970. https://doi.org/10.1186/1471-2407-14-970

Griffin, J.L., Kauppinen, R.A., 2007. Tumour metabolomics in animal models of human cancer. J. Proteome Res. 6, 498–505. https://doi.org/10.1021/pr060464h

Grishko, V., Xu, M., Ho, R., Mates, A., Watson, S., Kim, J.T., Wilson, G.L., Pearsall, A.W., 2009. Effects of hyaluronic acid on mitochondrial function and mitochondria-driven apoptosis following oxidative stress in human chondrocytes. J. Biol. Chem. 284, 9132–9139. https://doi.org/10.1074/jbc.M804178200

Gunn, L., Ding, C., Liu, M., Ma, Y., Qi, C., Cai, Y., Hu, X., Aggarwal, D., Zhang, H.-G., Yan, J., 2012. Opposing roles for complement component C5a in tumor progression and the tumor microenvironment. J. Immunol. 189, 2985–2994. https://doi.org/10.4049/jimmunol.1200846

Hair, P.S., Gronemus, J.Q., Crawford, K.B., Salvi, V.P., Cunnion, K.M., Thielens, N.M., Arlaud, G.J., Rawal, N., Krishna, N.K., 2010. Human astrovirus coat protein binds C1q and MBL and inhibits the classical and lectin pathways of complement activation. Mol. Immunol. 47, 792–798. https://doi.org/10.1016/j.molimm.2009.10.006

Hakomori, S., 2002. Glycosylation defining cancer malignancy: new wine in an old bottle. Proc. Natl. Acad. Sci. U.S.A. 99, 10231–10233. https://doi.org/10.1073/pnas.172380699

Harada, H., Takahashi, M., 2007. CD44-dependent Intracellular and Extracellular Catabolism of Hyaluronic Acid by Hyaluronidase-1 and -2. Journal of Biological Chemistry 282, 5597–5607. https://doi.org/10.1074/jbc.M608358200

Hardingham, T.E., Adams, P., 1976. A method for the determination of hyaluronate in the presence of other glycosaminoglycans and its application to human intervertebral disc. Biochem. J. 159, 143–147.

Hardingham, T.E., Muir, H., 1972. The specific interaction of hyaluronic acid with cartillage proteoglycans. Biochim. Biophys. Acta 279, 401–405.

Hardwick, C., Hoare, K., Owens, R., Hohn, H.P., Hook, M., Moore, D., Cripps, V., Austen, L., Nance, D.M., Turley, E.A., 1992. Molecular cloning of a novel hyaluronan receptor that mediates tumor cell motility. J. Cell Biol. 117, 1343–1350.

Harington, J.S., Miller, K., Macnab, G., 1971. Hemolysis by asbestos. Environmental Research 4, 95–117. https://doi.org/10.1016/0013-9351(71)90038-7

Hascall, V.C., Majors, A.K., De La Motte, C.A., Evanko, S.P., Wang, A., Drazba, J.A., Strong, S.A., Wight, T.N., 2004. Intracellular hyaluronan: a new frontier for inflammation? Biochim. Biophys. Acta 1673, 3–12. https://doi.org/10.1016/j.bbagen.2004.02.013

Heintz, N.H., Janssen, Y.M., Mossman, B.T., 1993. Persistent induction of c-fos and c-jun expression by asbestos. Proceedings of the National Academy of Sciences 90, 3299–3303. https://doi.org/10.1073/pnas.90.8.3299

Heintz, N.H., Janssen-Heininger, Y.M.W., Mossman, B.T., 2010. Asbestos, lung cancers, and mesotheliomas: from molecular approaches to targeting tumor survival pathways. Am. J. Respir. Cell Mol. Biol. 42, 133–139. https://doi.org/10.1165/rcmb.2009-0206TR

Honoré, B., Madsen, P., Rasmussen, H.H., Vandekerckhove, J., Celisb, J.E., Leffers, H., 1993. Cloning and expression of a cDNA covering the complete coding region of the P32 subunit of human pre-m RNA splicing factor SF2. Gene 134, 283–287. https://doi.org/10.1016/0378-1119(93)90108-F

Hourcade, D.E., 2008. Properdin and complement activation: a fresh perspective. Curr Drug Targets 9, 158–164.

Hsu, L.-J., Schultz, L., Hong, Q., Van Moer, K., Heath, J., Li, M.-Y., Lai, F.-J., Lin, S.-R., Lee, M.-H., Lo, C.-P., Lin, Y.-S., Chen, S.-T., Chang, N.-S., 2009. Transforming growth factor beta1 signaling via interaction with cell surface Hyal-2 and recruitment of WWOX/WOX1. J. Biol. Chem. 284, 16049–16059. https://doi.org/10.1074/jbc.M806688200

Huarte, M., 2015. The emerging role of lncRNAs in cancer. Nat. Med. 21, 1253–1261. https://doi.org/10.1038/nm.3981

Huen, M.S.Y., Sy, S.M.H., Chen, J., 2010. BRCA1 and its toolbox for the maintenance of genome integrity. Nat. Rev. Mol. Cell Biol. 11, 138–148. https://doi.org/10.1038/nrm2831

Husain, A.N., Colby, T., Ordonez, N., Krausz, T., Attanoos, R., Beasley, M.B., Borczuk, A.C., Butnor, K., Cagle, P.T., Chirieac, L.R., Churg, A., Dacic, S., Fraire, A., Galateau-Salle, F., Gibbs, A., Gown, A., Hammar, S., Litzky, L., Marchevsky, A.M., Nicholson, A.G., Roggli, V., Travis, W.D., Wick, M., International Mesothelioma Interest Group, 2013. Guidelines for pathologic diagnosis of malignant mesothelioma: 2012 update of the consensus statement from the International Mesothelioma Interest Group. Arch. Pathol. Lab. Med. 137, 647–667. https://doi.org/10.5858/arpa.2012-0214-OA

Itano, N., Kimata, K., 2008. Altered hyaluronan biosynthesis in cancer progression. Seminars in Cancer Biology 18, 268–274. https://doi.org/10.1016/j.semcancer.2008.03.006

Itano, N., Sawai, T., Yoshida, M., Lenas, P., Yamada, Y., Imagawa, M., Shinomura, T., Hamaguchi, M., Yoshida, Y., Ohnuki, Y., Miyauchi, S., Spicer, A.P., McDonald, J.A., Kimata, K., 1999. Three isoforms of

mammalian hyaluronan synthases have distinct enzymatic properties. J. Biol. Chem. 274, 25085–25092.

Jagadeeswaran, R., Ma, P.C., Seiwert, T.Y., Jagadeeswaran, S., Zumba, O., Nallasura, V., Ahmed, S., Filiberti, R., Paganuzzi, M., Puntoni, R., Kratzke, R.A., Gordon, G.J., Sugarbaker, D.J., Bueno, R., Janamanchi, V., Bindokas, V.P., Kindler, H.L., Salgia, R., 2006. Functional analysis of c-Met/hepatocyte growth factor pathway in malignant pleural mesothelioma. Cancer Res. 66, 352–361. https://doi.org/10.1158/0008-5472.CAN-04-4567

Jiang, L., Nagai, H., Ohara, H., Hara, S., Tachibana, M., Hirano, S., Shinohara, Y., Kohyama, N., Akatsuka, S., Toyokuni, S., 2008. Characteristics and modifying factors of asbestos-induced oxidative DNA damage. Cancer Science 99, 2142–2151. https://doi.org/10.1111/j.1349-7006.2008.00934.x

Jiang, L., Yamashita, Y., Chew, S.-H., Akatsuka, S., Ukai, S., Wang, S., Nagai, H., Okazaki, Y., Takahashi, T., Toyokuni, S., 2014. Connective tissue growth factor and β-catenin constitute an autocrine loop for activation in rat sarcomatoid mesothelioma. J. Pathol. 233, 402–414. https://doi.org/10.1002/path.4377

Jube, S., Rivera, Z.S., Bianchi, M.E., Powers, A., Wang, E., Pagano, I., Pass, H.I., Gaudino, G., Carbone, M., Yang, H., 2012. Cancer cell secretion of the DAMP protein HMGB1 supports progression in malignant mesothelioma. Cancer Res. 72, 3290–3301. https://doi.org/10.1158/0008-5472.CAN-11-3481

Kamp, D.W., Graceffa, P., Pryor, W.A., Weitzman, S.A., 1992. The role of free radicals in asbestos-induced diseases. Free Radic. Biol. Med. 12, 293–315.

Karjalainen, J.M., Tammi, R.H., Tammi, M.I., Eskelinen, M.J., Agren, U.M., Parkkinen, J.J., Alhava, E.M., Kosma, V.M., 2000. Reduced level of CD44 and hyaluronan associated with unfavorable prognosis in clinical stage I cutaneous melanoma. Am. J. Pathol. 157, 957–965. https://doi.org/10.1016/S0002-9440(10)64608-1

Kaufman, A.J., Pass, H.I., 2008. Current concepts in malignant pleural mesothelioma. Expert Review of Anticancer Therapy 8, 293–303. https://doi.org/10.1586/14737140.8.2.293

Kaur, A., Sultan, S.H.A., Murugaiah, V., Pathan, A.A., Alhamlan, F.S., Karteris, E., Kishore, U., 2016. Human C1q Induces Apoptosis in an Ovarian Cancer Cell Line via Tumor Necrosis Factor Pathway. Frontiers in Immunology 7. https://doi.org/10.3389/fimmu.2016.00599

Kim, R., Emi, M., Tanabe, K., Arihiro, K., 2006. Tumor-driven evolution of immunosuppressive networks during malignant progression. Cancer Res. 66, 5527–5536. https://doi.org/10.1158/0008-5472.CAN-05-4128

Kishore, U., Ghai, R., Greenhough, T.J., Shrive, A.K., Bonifati, D.M., Gadjeva, M.G., Waters, P., Kojouharova, M.S., Chakraborty, T., Agrawal, A., 2004. Structural and functional anatomy of the globular domain of complement protein C1q. Immunol. Lett. 95, 113–128. https://doi.org/10.1016/j.imlet.2004.06.015

Kishore, U., Thielens, N.M., Gaboriaud, C., 2016. Editorial: State-of-the-Art Research on C1q and the Classical Complement Pathway. Front Immunol 7, 398. https://doi.org/10.3389/fimmu.2016.00398

Kittlesen, D.J., Chianese-Bullock, K.A., Yao, Z.Q., Braciale, T.J., Hahn, Y.S., 2000. Interaction between complement receptor gC1qR and hepatitis C virus core protein inhibits T-lymphocyte proliferation. Journal of Clinical Investigation 106, 1239–1249. https://doi.org/10.1172/JCI10323

Knobel, H.R., Villiger, W., Isliker, H., 1975. Chemical analysis and electron microscopy studies of human C1q prepared by different methods. Eur. J. Immunol. 5, 78–82. https://doi.org/10.1002/eji.1830050119

Kobayashi, W., Ozawa, M., 2013. The transcription factor LEF-1 induces an epithelial–mesenchymal transition in MDCK cells independent of β-catenin. Biochemical and Biophysical Research Communications 442, 133–138. https://doi.org/10.1016/j.bbrc.2013.11.031

Koistinen, V., Kärnä, R., Koistinen, A., Arjonen, A., Tammi, M., Rilla, K., 2015. Cell protrusions induced by hyaluronan synthase 3 (HAS3) resemble mesothelial microvilli and share cytoskeletal features of filopodia. Experimental Cell Research 337, 179–191. https://doi.org/10.1016/j.yexcr.2015.06.016

Kojouharova, M., Reid, K., Gadjeva, M., 2010. New insights into the molecular mechanisms of classical complement activation. Mol. Immunol. 47, 2154–2160. https://doi.org/10.1016/j.molimm.2010.05.011

Kouser, L., Madhukaran, S.P., Shastri, A., Saraon, A., Ferluga, J., Al-Mozaini, M., Kishore, U., 2015. Emerging and Novel Functions of Complement Protein C1q. Front Immunol 6, 317. https://doi.org/10.3389/fimmu.2015.00317

Koyama, H., Hibi, T., Isogai, Z., Yoneda, M., Fujimori, M., Amano, J., Kawakubo, M., Kannagi, R., Kimata, K., Taniguchi, S., Itano, N., 2007. Hyperproduction of hyaluronan in neu-induced mammary tumor accelerates angiogenesis through stromal cell recruitment: possible involvement of versican/PG-M. Am. J. Pathol. 170, 1086–1099. https://doi.org/10.2353/ajpath.2007.060793

Kraut, E.H., Sagone, A.L., 1981. Alternative pathway of complement in multiple myeloma. Am. J. Hematol. 11, 335–345.

Krumdieck, R., Höök, M., Rosenberg, L.C., Volanakis, J.E., 1992. The proteoglycan decorin binds C1q and inhibits the activity of the C1 complex. J. Immunol. 149, 3695–3701.

Kunz-Schughart, L.A., Weber, A., Rehli, M., Gottfried, E., Brockhoff, G., Krause, S.W., Andreesen, R., Kreutz, M., 2003. [The “classical” macrophage marker CD68 is strongly expressed in primary human fibroblasts]. Verh Dtsch Ges Pathol 87, 215–223.

Laurent, T.C., Fraser, J.R., 1992. Hyaluronan. FASEB J. 6, 2397–2404.

Lee, J.Y., Spicer, A.P., 2000. Hyaluronan: a multifunctional, megaDalton, stealth molecule. Curr. Opin. Cell Biol. 12, 581–586.

Lepperdinger, G., Strobl, B., Kreil, G., 1998. HYAL2, a human gene expressed in many cells, encodes a lysosomal hyaluronidase with a novel type of specificity. J. Biol. Chem. 273, 22466–22470.

Lesley, J., He, Q., Miyake, K., Hamann, A., Hyman, R., Kincade, P.W., 1992. Requirements for hyaluronic acid binding by CD44: a role for the cytoplasmic domain and activation by antibody. J. Exp. Med. 175, 257–266.

Leung, A.K.L., Sharp, P.A., 2010. MicroRNA functions in stress responses. Mol. Cell 40, 205–215. https://doi.org/10.1016/j.molcel.2010.09.027

Li, C.-L., Yang, D., Cao, X., Wang, F., Hong, D.-Y., Wang, J., Shen, X.-C., Chen, Y., 2017. Fibronectin induces epithelial-mesenchymal transition in human breast cancer MCF-7 cells via activation of calpain. Oncology Letters 13, 3889–3895. https://doi.org/10.3892/ol.2017.5896

Londoño, I., Bendayan, M., 1988. High-resolution cytochemistry of neuraminic and hexuronic acid-containing macromolecules applying the enzyme-gold approach. Journal of Histochemistry & Cytochemistry 36, 1005–1014. https://doi.org/10.1177/36.8.3392391

Loos, M., Martin, H., Petry, F., 1989. The biosynthesis of C1q, the collagen-like and Fc-recognizing molecule of the complement system. Behring Inst. Mitt. 32–41.

Lorusso, G., Rüegg, C., 2008. The tumor microenvironment and its contribution to tumor evolution toward metastasis. Histochem. Cell Biol. 130, 1091–1103. https://doi.org/10.1007/s00418-008-0530-8

Lubbers, R., van Essen, M.F., van Kooten, C., Trouw, L.A., 2017. Production of complement components by cells of the immune system. Clin. Exp. Immunol. 188, 183–194. https://doi.org/10.1111/cei.12952

Lucas, S.D., Karlsson-Parra, A., Nilsson, B., Grimelius, L., Akerström, G., Rastad, J., Juhlin, C., 1996. Tumor-specific deposition of immunoglobulin G and complement in papillary thyroid carcinoma. Hum. Pathol. 27, 1329–1335.

MacCorkle, R.A., Slattery, S.D., Nash, D.R., Brinkley, B.R., 2006. Intracellular protein binding to asbestos induces aneuploidy in human lung fibroblasts. Cell Motil. Cytoskeleton 63, 646–657. https://doi.org/10.1002/cm.20151

Macor, P., Capolla, S., Tedesco, F., 2018. Complement as a Biological Tool to Control Tumor Growth. Frontiers in Immunology 9. https://doi.org/10.3389/fimmu.2018.02203

Markiewski, M.M., DeAngelis, R.A., Benencia, F., Ricklin-Lichtsteiner, S.K., Koutoulaki, A., Gerard, C., Coukos, G., Lambris, J.D., 2008. Modulation of the antitumor immune response by complement. Nat. Immunol. 9, 1225–1235. https://doi.org/10.1038/ni.1655

Martin, D.C., Atmuri, V., Hemming, R.J., Farley, J., Mort, J.S., Byers, S., Hombach-Klonisch, S., Stern, R., Triggs-Raine, B.L., 2008. A mouse model of human mucopolysaccharidosis IX exhibits osteoarthritis. Human Molecular Genetics 17, 1904–1915. https://doi.org/10.1093/hmg/ddn088

Matsushita, M., Thiel, S., Jensenius, J.C., Terai, I., Fujita, T., 2000. Proteolytic activities of two types of mannose-binding lectin-associated serine protease. J. Immunol. 165, 2637–2642.

Mattheolabakis, G., Milane, L., Singh, A., Amiji, M.M., 2015. Hyaluronic acid targeting of CD44 for cancer therapy: from receptor biology to nanomedicine. Journal of Drug Targeting 23, 605–618. https://doi.org/10.3109/1061186X.2015.1052072

McClatchey, A.I., Giovannini, M., 2005. Membrane organization and tumorigenesis--the NF2 tumor suppressor, Merlin. Genes Dev. 19, 2265–2277. https://doi.org/10.1101/gad.1335605

McGrath, F.D.G., Brouwer, M.C., Arlaud, G.J., Daha, M.R., Hack, C.E., Roos, A., 2006. Evidence that complement protein C1q interacts with C-reactive protein through its globular head region. J. Immunol. 176, 2950–2957.

Meyer, K., Palmer, J., 1934. The polysaccharide of the vitreous humor. Journal of Biological Chemistry, 107, 629-634.

Midgley, A.C., Oltean, S., Hascall, V., Woods, E.L., Steadman, R., Phillips, A.O., Meran, S., 2017. Nuclear hyaluronidase 2 drives alternative splicing of CD44 pre-mRNA to determine profibrotic or antifibrotic cell phenotype. Sci Signal 10. https://doi.org/10.1126/scisignal.aao1822

Miserocchi, G., Sancini, G., Mantegazza, F., Chiappino, G., 2008. Translocation pathways for inhaled asbestos fibers. Environ Health 7, 4. https://doi.org/10.1186/1476-069X-7-4

Misra, S., Hascall, V.C., Markwald, R.R., Ghatak, S., 2015. Interactions between Hyaluronan and Its Receptors (CD44, RHAMM) Regulate the Activities of Inflammation and Cancer. Front Immunol 6, 201. https://doi.org/10.3389/fimmu.2015.00201

Mitchell, D.A., Kirby, L., Paulin, S.M., Villiers, C.L., Sim, R.B., 2007. Prion protein activates and fixes complement directly via the classical pathway: implications for the mechanism of scrapie agent propagation in lymphoid tissue. Mol. Immunol. 44, 2997–3004. https://doi.org/10.1016/j.molimm.2006.12.027

Muta, T., Kang, D., Kitajima, S., Fujiwara, T., Hamasaki, N., 1997. p32 protein, a splicing factor 2-associated protein, is localized in mitochondrial matrix and is functionally important in maintaining oxidative phosphorylation. J. Biol. Chem. 272, 24363–24370.

Naor, D., Sionov, R.V., Ish-Shalom, D., 1997. CD44: structure, function, and association with the malignant process. Adv. Cancer Res. 71, 241–319.

Nauta, A.J., Trouw, L.A., Daha, M.R., Tijsma, O., Nieuwland, R., Schwaeble, W.J., Gingras, A.R., Mantovani, A., Hack, E.C., Roos, A., 2002. Direct binding of C1q to apoptotic cells and cell blebs induces complement activation. Eur. J. Immunol. 32, 1726–1736. https://doi.org/10.1002/1521-4141(200206)32:6<1726::AID-IMMU1726>3.0.CO;2-R

Nayak, A., Ferluga, J., Tsolaki, A.G., Kishore, U., 2010a. The non-classical functions of the classical complement pathway recognition subcomponent C1q. Immunology letters 131, 139–50. https://doi.org/10.1016/j.imlet.2010.03.012

Nayak, A., Ferluga, J., Tsolaki, A.G., Kishore, U., 2010b. The non-classical functions of the classical complement pathway recognition subcomponent C1q. Immunology Letters 131, 139–150. https://doi.org/10.1016/j.imlet.2010.03.012

Nayak, A., Pednekar, L., Reid, K.B., Kishore, U., 2012. Complement and non-complement activating functions of C1q: A prototypical innate immune molecule. Innate Immunity 18, 350–363. https://doi.org/10.1177/1753425910396252

Necas, J., Bartosikova, L., Brauner, P., Kolar, J., 2008. Hyaluronic acid (hyaluronan): a review. Veterinární Medicína 53, 397–411. https://doi.org/10.17221/1930-VETMED

Niehans, G.A., Cherwitz, D.L., Staley, N.A., Knapp, D.J., Dalmasso, A.P., 1996. Human carcinomas variably express the complement inhibitory proteins CD46 (membrane cofactor protein), CD55 (decay-accelerating factor), and CD59 (protectin). Am. J. Pathol. 149, 129–142.

Nonaka, M., 2014. Evolution of the Complement System, in: Anderluh, G., Gilbert, R. (Eds.), MACPF/CDC Proteins - Agents of Defence, Attack and Invasion. Springer Netherlands, Dordrecht, pp. 31–43. https://doi.org/10.1007/978-94-017-8881-6_3

Nozaki, M., Raisler, B.J., Sakurai, E., Sarma, J.V., Barnum, S.R., Lambris, J.D., Chen, Y., Zhang, K., Ambati, B.K., Baffi, J.Z., Ambati, J., 2006. Drusen complement components C3a and C5a promote choroidal neovascularization. Proc. Natl. Acad. Sci. U.S.A. 103, 2328–2333. https://doi.org/10.1073/pnas.0408835103

Nunez-Cruz, S., Gimotty, P.A., Guerra, M.W., Connolly, D.C., Wu, Y.-Q., DeAngelis, R.A., Lambris, J.D., Coukos, G., Scholler, N., 2012. Genetic and pharmacologic inhibition of complement impairs endothelial cell function and ablates ovarian cancer neovascularization. Neoplasia 14, 994–1004.

Nurminen, M., Karjalainen, A., Takahashi, K., 2003. Estimating the induction period of pleural mesothelioma from aggregate data on asbestos consumption. J. Occup. Environ. Med. 45, 1107–1115. https://doi.org/10.1097/01.jom.0000091682.95314.01

Oberkersch, R., Attorresi, A.I., Calabrese, G.C., 2010. Low-molecular-weight heparin inhibition in classical complement activation pathway during pregnancy. Thromb. Res. 125, e240-245. https://doi.org/10.1016/j.thromres.2009.11.030

Ogden, C.A., deCathelineau, A., Hoffmann, P.R., Bratton, D., Ghebrehiwet, B., Fadok, V.A., Henson, P.M., 2001. C1q and mannose binding lectin engagement of cell surface calreticulin and CD91 initiates macropinocytosis and uptake of apoptotic cells. J. Exp. Med. 194, 781–795.

Paiva, P., Van Damme, M.-P., Tellbach, M., Jones, R.L., Jobling, T., Salamonsen, L.A., 2005. Expression patterns of hyaluronan, hyaluronan synthases and hyaluronidases indicate a role for hyaluronan in the progression of endometrial cancer. Gynecol. Oncol. 98, 193–202. https://doi.org/10.1016/j.ygyno.2005.02.031

Pangburn, M.K., Rawal, N., 2002. Structure and function of complement C5 convertase enzymes. Biochem. Soc. Trans. 30, 1006–1010. https://doi.org/10.1042/

Pangburn, M.K., Schreiber, R.D., Müller-Eberhard, H.J., 1981. Formation of the initial C3 convertase of the alternative complement pathway. Acquisition of C3b-like activities by spontaneous hydrolysis of the putative thioester in native C3. J. Exp. Med. 154, 856–867.

Peto, J., Decarli, A., La Vecchia, C., Levi, F., Negri, E., 1999. The European mesothelioma epidemic. Br. J. Cancer 79, 666–672. https://doi.org/10.1038/sj.bjc.6690105

Philippeaux, M.-M., Pache, J.-C., Dahoun, S., Barnet, M., Robert, J.-H., Mauël, J., Spiliopoulos, A., 2004a. Establishment of permanent cell lines purified from human mesothelioma: morphological aspects, new marker expression and karyotypic analysis. Histochemistry and cell biology 122, 249–60. https://doi.org/10.1007/s00418-004-0701-1

Philippeaux, M.-M., Pache, J.-C., Dahoun, S., Barnet, M., Robert, J.-H., Mau�l, J., Spiliopoulos, A., 2004b. Establishment of permanent cell lines purified from human mesothelioma: morphological aspects, new marker expression and karyotypic analysis. Histochemistry and Cell Biology 122, 249–260. https://doi.org/10.1007/s00418-004-0701-1

Philipson, L.H., Westley, J., Schwartz, N.B., 1985. Effect of hyaluronidase treatment of intact cells on hyaluronate synthetase activity. Biochemistry 24, 7899–7906.

Pio, R., Corrales, L., Lambris, J.D., 2014. The role of complement in tumor growth. Adv. Exp. Med. Biol. 772, 229–262. https://doi.org/10.1007/978-1-4614-5915-6_11

Pondman, K.M., Salvador-Morales, C., Paudyal, B., Sim, R.B., Kishore, U., 2017. Interactions of the innate immune system with carbon nanotubes. Nanoscale Horizons 2, 174–186. https://doi.org/10.1039/C6NH00227G

Ponta, H., Sherman, L., Herrlich, P.A., 2003. CD44: from adhesion molecules to signalling regulators. Nat. Rev. Mol. Cell Biol. 4, 33–45. https://doi.org/10.1038/nrm1004

Puissant, E., Gilis, F., Dogné, S., Flamion, B., Jadot, M., Boonen, M., 2014. Subcellular Trafficking and Activity of Hyal-1 and Its Processed Forms in Murine Macrophages: Trafficking of Hyal-1 in Mouse Macrophages. Traffic 15, 500–515. https://doi.org/10.1111/tra.12162

Qi, F., Okimoto, G., Jube, S., Napolitano, A., Pass, H.I., Laczko, R., Demay, R.M., Khan, G., Tiirikainen, M., Rinaudo, C., Croce, A., Yang, H., Gaudino, G., Carbone, M., 2013. Continuous exposure to chrysotile asbestos can cause transformation of human mesothelial cells via HMGB1 and TNF-α signaling. Am. J. Pathol. 183, 1654–1666. https://doi.org/10.1016/j.ajpath.2013.07.029

Quinn, L., Finn, S.P., Cuffe, S., Gray, S.G., 2015. Non-coding RNA repertoires in malignant pleural mesothelioma. Lung Cancer 90, 417–426. https://doi.org/10.1016/j.lungcan.2015.11.002

Rai, S.K., Duh, F.-M., Vigdorovich, V., Danilkovitch-Miagkova, A., Lerman, M.I., Miller, A.D., 2001. Candidate tumor suppressor HYAL2 is a glycosylphosphatidylinositol (GPI)-anchored cell-surface receptor for jaagsiekte sheep retrovirus, the envelope protein of which mediates oncogenic transformation. Proceedings of the National Academy of Sciences 98, 4443–4448. https://doi.org/10.1073/pnas.071572898

Ramprasad, M.P., Fischer, W., Witztum, J.L., Sambrano, G.R., Quehenberger, O., Steinberg, D., 1995. The 94- to 97-kDa mouse macrophage membrane protein that recognizes oxidized low density lipoprotein and phosphatidylserine-rich liposomes is identical to macrosialin, the mouse homologue of human CD68. Proc. Natl. Acad. Sci. U.S.A. 92, 9580–9584.

Raynaud, C., Greillier, L., Mazieres, J., Monnet, I., Mastroianni, B., Robinet, G., Fraboulet, G., Dixmier, A., Berard, H., Lamy, R., Letreut, J., Lena, H., Oliviero, G., Botta, S., Vergnenegre, A., Borget, I., Chouaid, C., 2015. Management of malignant pleural mesothelioma: a French multicenter retrospective study (GFPC 0802 study). BMC Cancer 15, 857. https://doi.org/10.1186/s12885-015-1881-x

Ricklin, D., Hajishengallis, G., Yang, K., Lambris, J.D., 2010. Complement: a key system for immune surveillance and homeostasis. Nat. Immunol. 11, 785–797. https://doi.org/10.1038/ni.1923

Rilla, K., Lammi, M.J., Sironen, R., Törrönen, K., Luukkonen, M., Hascall, V.C., Midura, R.J., Hyttinen, M., Pelkonen, J., Tammi, M., Tammi, R., 2002. Changed lamellipodial extension, adhesion plaques and migration in epidermal keratinocytes containing constitutively expressed sense and antisense hyaluronan synthase 2 (Has2) genes. J. Cell. Sci. 115, 3633–3643.

Robinson, B.M., 2012. Malignant pleural mesothelioma: an epidemiological perspective. Ann Cardiothorac Surg 1, 491–496. https://doi.org/10.3978/j.issn.2225-319X.2012.11.04

Ropponen, K., Tammi, M., Parkkinen, J., Eskelinen, M., Tammi, R., Lipponen, P., Agren, U., Alhava, E., Kosma, V.M., 1998. Tumor cell-associated hyaluronan as an unfavorable prognostic factor in colorectal cancer. Cancer Res. 58, 342–347.

Rosenzweig, K.E., 2017. Malignant pleural mesothelioma: adjuvant therapy with radiation therapy. Annals of Translational Medicine 5, 242–242. https://doi.org/10.21037/atm.2017.06.25

Roumenina, L.T., Popov, K.T., Bureeva, S.V., Kojouharova, M., Gadjeva, M., Rabheru, S., Thakrar, R., Kaplun, A., Kishore, U., 2008. Interaction of the globular domain of human C1q with Salmonella typhimurium lipopolysaccharide. Biochim. Biophys. Acta 1784, 1271–1276. https://doi.org/10.1016/j.bbapap.2008.04.029

Rozanov, D.V., Savinov, A.Y., Golubkov, V.S., Tomlinson, S., Strongin, A.Y., 2006. Interference with the complement system by tumor cell membrane type-1 matrix metalloproteinase plays a significant role in promoting metastasis in mice. Cancer Res. 66, 6258–6263. https://doi.org/10.1158/0008-5472.CAN-06-0539

Rutkowski, M.J., Sughrue, M.E., Kane, A.J., Mills, S.A., Parsa, A.T., 2010. Cancer and the Complement Cascade. Molecular Cancer Research 8, 1453–1465. https://doi.org/10.1158/1541-7786.MCR-10-0225

Sage, A.P., Martinez, V.D., Minatel, B.C., Pewarchuk, M.E., Marshall, E.A., MacAulay, G.M., Hubaux, R., Pearson, D.D., Goodarzi, A.A., Dellaire, G., Lam, W.L., 2018. Genomics and Epigenetics of Malignant Mesothelioma. High Throughput 7. https://doi.org/10.3390/ht7030020

Saha, P., Datta, K., 2018. Multi-functional, multicompartmental hyaluronan-binding protein 1 (HABP1/p32/gC1qR): implication in cancer progression and metastasis. Oncotarget 9, 10784–10807. https://doi.org/10.18632/oncotarget.24082

Salmi, M., Grön-Virta, K., Sointu, P., Grenman, R., Kalimo, H., Jalkanen, S., 1993. Regulated expression of exon v6 containing isoforms of CD44 in man: downregulation during malignant transformation of tumors of squamocellular origin. J. Cell Biol. 122, 431–442.

Salwowska, N.M., Bebenek, K.A., Żądło, D.A., Wcisło-Dziadecka, D.L., 2016. Physiochemical properties and application of hyaluronic acid: a systematic review. Journal of Cosmetic Dermatology 15, 520–526. https://doi.org/10.1111/jocd.12237

Santarelli, L., Strafella, E., Staffolani, S., Amati, M., Emanuelli, M., Sartini, D., Pozzi, V., Carbonari, D., Bracci, M., Pignotti, E., Mazzanti, P., Sabbatini, A., Ranaldi, R., Gasparini, S., Neuzil, J., Tomasetti, M., 2011. Association of MiR-126 with soluble mesothelin-related peptides, a marker for malignant mesothelioma. PLoS ONE 6, e18232. https://doi.org/10.1371/journal.pone.0018232

Scherpereel, A., Wallyn, F., Albelda, S.M., Munck, C., 2018. Novel therapies for malignant pleural mesothelioma. Lancet Oncol. 19, e161–e172. https://doi.org/10.1016/S1470-2045(18)30100-1

Schraufstatter, I.U., Trieu, K., Sikora, L., Sriramarao, P., DiScipio, R., 2002. Complement c3a and c5a induce different signal transduction cascades in endothelial cells. J. Immunol. 169, 2102–2110.

Sellar, G.C., Blake, D.J., Reid, K.B., 1991. Characterization and organization of the genes encoding the A-, B- and C-chains of human complement subcomponent C1q. The complete derived amino acid sequence of human C1q. Biochem. J. 274 (Pt 2), 481–490.

Shuttleworth, T.L., Wilson, M.D., Wicklow, B.A., Wilkins, J.A., Triggs-Raine, B.L., 2002. Characterization of the murine hyaluronidase gene region reveals complex organization and cotranscription of Hyal1 with downstream genes, Fus2 and Hyal3. J. Biol. Chem. 277, 23008–23018. https://doi.org/10.1074/jbc.M108991200

Sim, R.B., Schwaeble, W., Fujita, T., 2016. Complement research in the 18th–21st centuries: Progress comes with new technology. Immunobiology 221, 1037–1045. https://doi.org/10.1016/j.imbio.2016.06.011

Sjöberg, A.P., Manderson, G.A., Mörgelin, M., Day, A.J., Heinegård, D., Blom, A.M., 2009. Short leucine-rich glycoproteins of the extracellular matrix display diverse patterns of complement interaction and activation. Mol. Immunol. 46, 830–839. https://doi.org/10.1016/j.molimm.2008.09.018

Sleeman, J.P., Thiery, J.P., 2011. SnapShot: The epithelial-mesenchymal transition. Cell 145, 162.e1. https://doi.org/10.1016/j.cell.2011.03.029

Stern, R., Jedrzejas, M.J., 2006. Hyaluronidases: Their Genomics, Structures, and Mechanisms of Action. Chemical Reviews 106, 818–839. https://doi.org/10.1021/cr050247k

Stern, R., Kogan, G., Jedrzejas, M.J., Šoltés, L., 2007. The many ways to cleave hyaluronan. Biotechnology Advances 25, 537–557. https://doi.org/10.1016/j.biotechadv.2007.07.001

Stone, S., Jiang, P., Dayananth, P., Tavtigian, S.V., Katcher, H., Parry, D., Peters, G., Kamb, A., 1995. Complex structure and regulation of the P16 (MTS1) locus. Cancer Res. 55, 2988–2994.

Stott, F.J., 1998. The alternative product from the human CDKN2A locus, p14ARF, participates in a regulatory feedback loop with p53 and MDM2. The EMBO Journal 17, 5001–5014. https://doi.org/10.1093/emboj/17.17.5001

Strobl, B., Wechselberger, C., Beier, D.R., Lepperdinger, G., 1998. Structural Organization and Chromosomal Localization ofHyal2,a Gene Encoding a Lysosomal Hyaluronidase. Genomics 53, 214–219. https://doi.org/10.1006/geno.1998.5472

Tang, Z., Lu, B., Hatch, E., Sacks, S.H., Sheerin, N.S., 2009. C3a mediates epithelial-to-mesenchymal transition in proteinuric nephropathy. J. Am. Soc. Nephrol. 20, 593–603. https://doi.org/10.1681/ASN.2008040434

Thiel, S., 2007. Complement activating soluble pattern recognition molecules with collagen-like regions, mannan-binding lectin, ficolins and associated proteins. Mol. Immunol. 44, 3875–3888. https://doi.org/10.1016/j.molimm.2007.06.005

Tomasetti, M., Nocchi, L., Staffolani, S., Manzella, N., Amati, M., Goodwin, J., Kluckova, K., Nguyen, M., Strafella, E., Bajzikova, M., Peterka, M., Lettlova, S., Truksa, J., Lee, W., Dong, L.-F., Santarelli, L., Neuzil, J., 2014. MicroRNA-126 suppresses mesothelioma malignancy by targeting IRS1 and interfering with the mitochondrial function. Antioxid. Redox Signal. 21, 2109–2125. https://doi.org/10.1089/ars.2013.5215

Toole, B.P., 2002. Hyaluronan promotes the malignant phenotype. Glycobiology 12, 37R-42R.

Toole, B.P., 1997. Hyaluronan in morphogenesis. J. Intern. Med. 242, 35–40.

Toole, B.P., Wight, T.N., Tammi, M.I., 2002. Hyaluronan-cell interactions in cancer and vascular disease. J. Biol. Chem. 277, 4593–4596. https://doi.org/10.1074/jbc.R100039200

Törrönen, K., Nikunen, K., Kärnä, R., Tammi, M., Tammi, R., Rilla, K., 2014. Tissue distribution and subcellular localization of hyaluronan synthase isoenzymes. Histochem. Cell Biol. 141, 17–31. https://doi.org/10.1007/s00418-013-1143-4

Törrönen, K., Soini, Y., Pääkkö, P., Parkkinen, J., Sironen, R., Rilla, K., 2016. Mesotheliomas show higher hyaluronan positivity around tumor cells than metastatic pulmonary adenocarcinomas. Histol. Histopathol. 31, 1113–1122. https://doi.org/10.14670/HH-11-740

Toyokuni, S., Sagripanti, J.-L., 1992. Iron-mediated DNA damage: Sensitive detection of DNA strand breakage catalyzed by iron. Journal of Inorganic Biochemistry 47, 241–248. https://doi.org/10.1016/0162-0134(92)84069-Y

Triggs-Raine, B., 2015. Biology of hyaluronan: Insights from genetic disorders of hyaluronan metabolism. World Journal of Biological Chemistry 6, 110. https://doi.org/10.4331/wjbc.v6.i3.110

Triggs-Raine, B., Salo, T.J., Zhang, H., Wicklow, B.A., Natowicz, M.R., 1999. Mutations in HYAL1, a member of a tandemly distributed multigene family encoding disparate hyaluronidase activities, cause a newly described lysosomal disorder, mucopolysaccharidosis IX. Proc. Natl. Acad. Sci. U.S.A. 96, 6296–6300.

Tsao, A.S., Wistuba, I., Roth, J.A., Kindler, H.L., 2009. Malignant Pleural Mesothelioma. Journal of Clinical Oncology 27, 2081–2090. https://doi.org/10.1200/JCO.2008.19.8523

Tsepilov, R.N., Beloded, A.V., 2015. Hyaluronic acid — an “old” molecule with “new” functions: biosynthesis and depolymerization of hyaluronic acid in bacteria and vertebrate tissues including during carcinogenesis. Biochemistry (Moscow) 80, 1093–1108. https://doi.org/10.1134/S0006297915090011

Walport, M.J., 2001. Complement. First of two parts. N. Engl. J. Med. 344, 1058–1066. https://doi.org/10.1056/NEJM200104053441406

Weigel, P.H., Hascall, V.C., Tammi, M., 1997. Hyaluronan synthases. J. Biol. Chem. 272, 13997–14000.

Weissmann, B., Meyer, K., 1954. The Structure of Hyalobiuronic Acid and of Hyaluronic Acid from Umbilical Cord [1,2]. Journal of the American Chemical Society 76, 1753–1757. https://doi.org/10.1021/ja01636a010

Wu, M., Cao, M., He, Y., Liu, Y., Yang, C., Du, Y., Wang, W., Gao, F., 2015. A novel role of low molecular weight hyaluronan in breast cancer metastasis. The FASEB Journal 29, 1290–1298. https://doi.org/10.1096/fj.14-259978

Wu, M., Du, Y., Liu, Y., He, Y., Yang, C., Wang, W., Gao, F., 2014. Low molecular weight hyaluronan induces lymphangiogenesis through LYVE-1-mediated signaling pathways. PLoS ONE 9, e92857. https://doi.org/10.1371/journal.pone.0092857

Yang, H., Bocchetta, M., Kroczynska, B., Elmishad, A.G., Chen, Y., Liu, Z., Bubici, C., Mossman, B.T., Pass, H.I., Testa, J.R., Franzoso, G., Carbone, M., 2006. TNF-alpha inhibits asbestos-induced cytotoxicity via a NF-kappaB-dependent pathway, a possible mechanism for asbestos-induced oncogenesis. Proc. Natl. Acad. Sci. U.S.A. 103, 10397–10402. https://doi.org/10.1073/pnas.0604008103

Yin, W., Ghebrehiwet, B., Weksler, B., Peerschke, E.I., 2007. Classical pathway complement activation on human endothelial cells. Mol. Immunol. 44, 2228–2234. https://doi.org/10.1016/j.molimm.2006.11.012

Ying, S.C., Gewurz, A.T., Jiang, H., Gewurz, H., 1993. Human serum amyloid P component oligomers bind and activate the classical complement pathway via residues 14-26 and 76-92 of the A chain collagen-like region of C1q. J. Immunol. 150, 169–176.

Yokoyama, T., Osada, H., Murakami, H., Tatematsu, Y., Taniguchi, T., Kondo, Y., Yatabe, Y., Hasegawa, Y., Shimokata, K., Horio, Y., Hida, T., Sekido, Y., 2008. YAP1 is involved in mesothelioma development and negatively regulated by Merlin through phosphorylation. Carcinogenesis 29, 2139–2146. https://doi.org/10.1093/carcin/bgn200

Ytting, H., Jensenius, J.C., Christensen, I.J., Thiel, S., Nielsen, H.J., 2004. Increased activity of the mannan-binding lectin complement activation pathway in patients with colorectal cancer. Scand. J. Gastroenterol. 39, 674–679. https://doi.org/10.1080/00365520410005603

Yuan, Y., Jiang, Y.-C., Sun, C.-K., Chen, Q.-M., 2016. Role of the tumor microenvironment in tumor progression and the clinical applications (Review). Oncology Reports 35, 2499–2515. https://doi.org/10.3892/or.2016.4660

Zanella, C.L., Posada, J., Tritton, T.R., Mossman, B.T., 1996. Asbestos causes stimulation of the extracellular signal-regulated kinase 1 mitogen-activated protein kinase cascade after phosphorylation of the epidermal growth factor receptor. Cancer Res. 56, 5334–5338.

Zhou, S., Liu, L., Li, H., Eilers, G., Kuang, Y., Shi, S., Yan, Z., Li, X., Corson, J.M., Meng, F., Zhou, H., Sheng, Q., Fletcher, J.A., Ou, W.-B., 2014. Multipoint targeting of the PI3K/mTOR pathway in mesothelioma. British Journal of Cancer 110, 2479–2488. https://doi.org/10.1038/bjc.2014.220

Zoltan-Jones, A., Huang, L., Ghatak, S., Toole, B.P., 2003. Elevated hyaluronan production induces mesenchymal and transformed properties in epithelial cells. J. Biol. Chem. 278, 45801–45810. https://doi.org/10.1074/jbc.M308168200

Zou, W., 2005. Immunosuppressive networks in the tumour environment and their therapeutic relevance. Nat. Rev. Cancer 5, 263–274. https://doi.org/10.1038/nrc1586